Title
Aspects of Gauge-Gravity Duality and Holography

Author
Samani, Joshua

Publication Date
2014

Peer reviewed|Thesis/dissertation

UNIVERSITY OF CALIFORNIA

Los Angeles

Aspects of Gauge-Gravity Duality and Holography

A dissertation submitted in partial satisfaction of the

requirements for the degree of Doctor of Philosophy

in Physics

by

Joshua Fred Samani

2014

ABSTRACT OF THE DISSERTATION

Aspects of Gauge-Gravity Duality and Holography

by

Joshua Fred Samani

Doctor of Philosophy in Physics

University of California, Los Angeles, 2014

Professor Michael Gutperle, Chair

We study three aspects of gauge-gravity duality. First, we explore holographic models of conformal field theories with boundary by way of holographic renormalization group flows. Second, we propose an extension and application of the covariant holographic entangelement entropy proposal to warped anti-de-Sitter spacetimes. Third, we exhibit the existence of higher-spin black holes with Lifshitz asymptotics in the Chern-Simons formulation of higher spin gravity.

The dissertation of Joshua Fred Samani is approved.

Eric D'Hoker

Terence Tao

Michael Gutperle, Committee Chair

University of California, Los Angeles

2014

DEDICATION

I dedicate this dissertation to my father, Aziz Samani

who imbued me with his curiosity and sense of wonder.

I could not have traveled this far without either.

Contents

LIST OF FIGURES

ACKNOWLEDGEMENTS

This work would not have been possible without the help and contributions of many people.

First, and foremost, I must express my deep gratitude to my advisor, Michael Gutperle. I have been fortunate to have such a supportive, encouraging advisor and co-author. His patience, positivity, and humor have made research enjoyable, and his insights formed the basis for all of our work together, especially chapters 2 and 4 of this dissertation which are versions of [121] and [119] respectively.

Second, I'd like to thank my other co-authors Edgar Shaghoulian, Dionysios Anninos, and Eliot Hijano. Without Edgar's perseverance and vision coupled with Dionysios's physical insights and intuition, chapter 3, a version of [17], would not have been possible. The quality and breadth of results of chapter 4 are, in large part, due to Eliot Hijano's dedication and computational acumen.

Third, a special thanks to Eric D'Hoker and Per Kraus. Eric taught me quantum mechanics, and I served as his teaching assistant for many graduate courses. Our interactions have contributed a great deal to the depth of my understanding of physics. Per has always been willing and available to interact and clarify concepts, and his consistent involvement and leadership in the string theory journal club have improved the breadth of my understanding of the field.

Finally, thank you to my committee for their time and consideration.

VITA

B.A. Physics, 2008, University of California, Berkeley

B.S. Mathematics, 2008, University of California, Berkeley

Chapter 1

Introduction

1.1 What is holography?

The holographic principle asserts that a gravitational theory in a region of spacetime can be described by degrees of freedom on its boundary. For some decades, physicists have been constructing concrete mathematical realizations of this principle. In particular, they have made unambiguous specifications of the terms "gravitational theory" and "degrees of freedom," in a number of contexts, and there is now a whole industry in the theoretical physics community consisting of exploring these mathematical constructions and their physical consequences.

The earliest hints at the formalization of the holographic principle arose from the work of Bekenstein and others on black holes and information. Motivated by the work of Christodoulou, Ruffini, and Hawking on black hole thermodynamics and gravitational radiation [64, 65, 123], Bekenstein initiated a program of exploring the relationship between black holes and information by asserting that the entropy of a black hole is proportional to the area of its event

horizon [33];

$$S_{\rm BH} = \eta k_B L_p^{-2} A. \tag{1.1}$$

Here A is the area of the black hole horizon, $L_p = (\hbar G/c^3)^{1/2}$ is the Planck length, k_B is Boltzmann's constant, and η is a dimensionless number of order unity. Bekenstein was originally motivated to write down this formula by noticing that black hole horizon area exhibits behaviors that are strongly reminiscent of the behavior of thermodynamic entropy. Perhaps most striking among these behaviors is that black hole [horizon] area never decreases, and that it increases for all but a very special class of black-hole transformation. [33] This property of horizon area is much like the behavior of thermodynamic entropy in the Second Law of Thermodynamics which states that the entropy of an isolated thermodynamic system never decreases.

Soon after introducing the notion that black hole entropy is proportional to horizon area, Bekenstein used information-theoretic arguments to strengthen this connection by showing that if black hole entropy is defined as "the measure of information about a black hole interior which is inaccessible to an exterior observer," [34], then it must be proportional to the area of the black hole horizon. Moreover, he determined that the dimensionless constant η in formula (1.1) has value 1/4.

Roughly a decade later, Bekenstein further proposed the following universal upper-bound

on the entropy for bounded systems of effective radius R:

$$S \leq \frac{2\pi kRE}{\hbar c}, \tag{1.2}$$

where E is the total energy of the system and c is the speed of light. One can easily check, for example, that black holes obey this bound. If we consider the Schwarzschild black hole and identify R as the horizon radius, then we obtain $A = 4\pi R^2$, and if we recall that the horizon radius is given by $R = 2GM/c^2$, then the expression on the right of the bound (1.2) exactly reproduces the black hole entropy. In other words, the black hole entropy saturates Bekenstein's bound. Further investigation following Bekenstein's demonstrated that for certain gravitational systems, such as those undergoing gravitational collapse, the bound (1.2) can be violated. However, the bound has since been generalized by Bousso to the so-called covariant entropy bound which applies to any spacetime admitted by Einstein's equation which satisfies the dominant energy condition for matter [43].

This and other work on black hole information and on the entropy of gravitating systems hinted at a holographic principle. Entropy, which is the logarithm of the number of quantum states accessible to a system, "counts" the number of degrees of freedom in a gravitational system. Therefore, the entropy bounds described above show that the number of degrees of freedom in a certain region is bounded by a quantity proportional to the area of that region. This has led some to believe that there is a deep connection between theories that describe the quantum physics of gravitating systems and theories that describe the degrees of freedom on their boundaries. In fact, 't Hooft and Susskind [180, 178] ultimately suggested that when

one combines quantum mechanics and gravity, one is inevitably led to the conclusion that our three-dimensional universe can be described as an image of information on a two-dimensional projection in much the same way that a hologram encodes three dimensional information on a two-dimensional surface. In fact, this idea is the origin of the the term "holography" in the present context.

1.2 Toward holographic gauge-gravity duality

Although black holes and information motivate the general notion of holography, they do not give a precise, mathematical framework in which a correspondence between gravitational degrees of freedom and boundary degrees of freedom is made explicit. This has led physicists to desire a concrete realization of holography that lends itself to calculation. A natural, systematic, and by now widely adopted procedure to produce such a realization proceeds according to the following recipe: (i) construct a quantum theory of gravity on an asymptotically AdS spacetime, (ii) identify a theory describing the degrees of freedom on its boundary, and (iii) exhibit a one-to-one correspondence between objects that characterize the theory of quantum gravity and those that characterize theory living on its boundary.

We don't yet have a complete quantum theory of gravity, but we do have a good candidate: string theory, so it's natural to attempt to find a correspondence between string theory defined on some spacetime and another theory defined on its boundary. A first step in this direction is to note that in the large N limit, the perturbative expansion of a diagram in an

SU(N) gauge theory can be written in the form

$$\sum_{g=0}^{\infty} N^{2-2g} f_g(\lambda) \tag{1.3}$$

where g is the genus of an associated surface and $f_g(\lambda)$ is a polynomial in the 't Hooft coupling λ. In the large-N limit, we see that large-genus terms will be subdominant. Moreover, the form of this expansion is the same as one finds in a perturbative theory of closed, oriented strings if one identifies $1/N$ with the string coupling. In this sense, the large-N limit of gauge theories are similar to free string theories [6]. These observations motivate us to look for a correspondence between a string theory and a qauntum field theory exhibiting gauge invariance.

A next step in this direction is to note that there is a compelling relationship between the symmetries of certain gauge theories, and the symmetries of certain spacetime backgrounds on which string theories can be defined. On the gauge theory side, four-dimensional $\mathcal{N} = 4$ Super Yang-Mills (SYM) exhibits full SO$(4,2)$ conformal invariance and possesses an SU$(4) \cong$ SO(6) R-symmetry. On the spacetime side, the SO$(4,2)$ conformal invariance of $\mathcal{N} = 4$ SYM is precisely the local isometry group of AdS_5, the maximally-symmetry solution to the source-free Einstein equation with negative cosmological constant. Moreover, the group SO(6) is precisely the isometry group of the five-sphere S^5. Therefore, at least at the level of spacetime geometry, we obtain a match between the symmetries of $\mathcal{N} = 4$ SYM, and those of a string theory defined on $\mathrm{AdS}_5 \times S^5$ [157].

However, the argument for a relationship between gauge theories and string theory on

AdS is much richer than the basic symmetry analysis just outlined. Such a correspondence is also well-motivated by the study of D-branes in string theory. In string perturbation theory, D3-branes are surfaces on which the endpoints of open strings live. To see the relationship between branes and gauge-gravity duality, one considers a stack of N parallel, coincident D3-branes in flat 10-dimensional spacetime. The theory contains open strings, which can be thought of as brane excitations, and closed strings which are excitations of the bulk space. In the low-energy limit, the closed string excitations decouple from the open string excitations. Furthermore, in the weak coupling regime $gN \ll 1$, where here g denotes the string coupling constant, the open string excitations describe $\mathcal{N} = 4$ SYM with gauge group $\mathrm{SU}(N)$, while in the strong coupling regime $gN \gg 1$ they describe type IIB string theory on $\mathrm{AdS}_5 \times S^5$. On the other hand, the type IIB string theory itself makes sense whether or not the coupling is weak, so one might conjecture that the open string excitations at weak coupling also describe type IIB string theory. A natural way to explain this is that the gauge theory and string theory descriptions that describe the weak coupling dynamics are just two ways of describing the same thing. Namely, they are equivalent physical theories [117, 157].

Thus far, we have made heuristic arguments for a correspondence between a quantum theory of gravity on $\mathrm{AdS}_5 \times S^5$ and a gauge theory without gravity living on 4-dimensional Minkowski space $\mathbb{R}^{3,1}$. We haven't, however, argued how this relates to holography in the sense that the gravity theory is being described by a theory living on its *boundary*. Strictly speaking, (global) AdS_5 is not a manifold with boundary; it contains no points with a neighborhood homeomorphic to a neighborhood of a point on the boundary of the upper-

half space $\mathbb{H}^n \subseteq \mathbb{R}^n$. However, AdS_5 *does* have a *conformal* boundary after conformal compactification, and its conformal boundary is precisely a conformal compactification of $\mathbb{R}^{3,1}$. In other words, there is a conformal transformation that maps AdS_5 onto the interior of a manifold with boundary, and the boundary of this manifold is precisely a conformal compactification of $\mathbb{R}^{3,1}$. Moreover, it is possible to view the string theory on $\mathrm{AdS}_5 \times S^5$ as a theory on only the AdS factor by performing a Kaluza-Klein reduction on S^5. In this sense, the correspondence is viewed as being "holographic;" one has a correspondence between a quantum theory of gravity that effectively lives on AdS_5 and a gauge theory that lives on its conformal boundary $\mathbb{R}^{3,1}$.

1.3 The AdS/CFT conjecture

In the last section, we argued the plausibility of an equivalence between $\mathcal{N} = 4$ SYM and string theory on $\mathrm{AdS}_5 \times S^5$ which was first proposed by Maldacena [157]. We now describe a formal conjecture stating the details of this equivalence. The conjecture provides a full specification of the theories on each side of the equivalence, and it gives the explicit mapping between quantities that characterize each theory. The details of the mapping between the theories were clarified by Witten [190].

On the "AdS side" of the equivalence is Type IIB string theory on $\mathrm{AdS}_5 \times S^5$ where the type IIB 5-form flux through S^5 is an integer N and the AdS_5 and S^5 factors have equal radii satisfying $L^4 = 4\pi g_s N \alpha'$. Here, g_s is the string coupling constant, and α' is related to the string tension as $T_s = 1/(2\pi\alpha')$. On the "CFT side" of the equivalence is four-dimensional

$\mathcal{N} = 4$ SYM in its conformal phase with gauge group SU(N) and Yang-Mills coupling g_{YM} that is related to the string coupling as $g_{YM}^2 = g_s$. The conjecture is that these two theories are equivalent to one another; there is a one-to-one correspondence between the observables and dynamics of each theory.

On the AdS side of the correspondence, we decompose fields into Kaluza-Klein towers on S^5. The result is effectively a theory of fields ϕ_Δ on AdS_5 where Δ is the conformal dimension of the operator on the CFT side to which the field is dual. We suppress other quantum numbers in the notation. Near the boundary, one assumes that these bulk fields satisfy the equation for a free, massive field with mass m_Δ. If we write euclidean AdS_5 in Poincare coordinates $(z_0, \mathbf{z})$, where the boundary is located at $z_0 = 0$, then the field will have one of the following asymptotic behaviors near the boundary:

$$\phi_\Delta(z_0, \mathbf{z}) \sim \begin{cases} z_0^\Delta \\ z_0^{4-\Delta} \end{cases} . \tag{1.4}$$

The normalizable mode z_0^Δ determines the vacuum expectation values of operators in the CFT with corresponding conformal dimensions Δ. The non-normalizable mode $z_0^{4-\Delta}$ corresponds to coupling to sources. In particular, given a bulk field ϕ_Δ, we can define an associated boundary field as follows:

$$\bar{\phi}_\Delta(\mathbf{z}) = \lim_{z_0 \to 0} z_0^{4-\Delta} \phi_\Delta(z_0, \mathbf{z}). \tag{1.5}$$

Now let $S[\phi_\Delta]$ denote the string action that gives the bulk dynamics, then the conjecture

states that [190]

$$\exp(-S_{\rm os}[\phi_\Delta]) = \left\langle \exp\left(\int \bar{\phi}_\Delta \mathcal{O}_\Delta\right)\right\rangle \tag{1.6}$$

where the left hand side is the bulk action evaluated on shell on bulk fields having associated boundary fields ϕ_Δ, and the right hand side is the generating functional for correlators of the operators $\mathcal{O}_\Delta$ in the CFT having conformal dimension Δ.

The strong version of the correspondence is conjectured to hold for all values of N and for all values of the string coupling g_s. Indirect but strong evidence for the conjecture exists in certain limits. In terms of the 't Hooft coupling $\lambda = g^2_{\rm YM}N$ on the SYM side of the conjecture, the limit $N \to \infty$ while keeping λ fixed corresponds to classical string theory on the $\mathrm{AdS}_5 \times S^5$ side. If one takes the further limit $\lambda \to \infty$, then classical string theory reduces to Type IIB supergravity on $\mathrm{AdS}_5 \times S^5$, and it is in this regime that the conjecture has been checked extensively [150, 92, 167].

1.4 A glimpse at generalizing Maldacena's conjecture

Although the AdS/CFT conjecture is one of the first concrete, detailed realizations of holography, it is not the only realization. Since the statement of the conjecture, there has been an explosion of work indicating that gauge-gravity duality and holography can be realized on bulk dimensions other than 5 and that the boundary theory need not even be conformal. In

fact, their is now a large body of computations supporting a whole sea of dualities between gravity theories in the bulk and quantum field theories on their boundaries. There are a number of reasons for which one might expect that gauge-gravity duality and its connection to holography is much more general than the conjecture detailed in the last section; c.f. [132, 173] for reviews.

The first such reason derives from symmetry considerations. Recall that one of the main plausibility arguments for the duality between a gravitational theory on AdS_5 and a conformal field theory on $\mathbb{R}^{3,1}$ involved matching bulk and boundary symmetries. The bulk has isometry group $\mathrm{SO}(4,2)$, and this is precisely the symmetry enjoyed by the boundary theory since $\mathrm{SO}(4,2)$ is the conformal group on $\mathbb{R}^{3,1}$. One may wonder if this symmetry matching extends to higher dimensions, and its does. In fact, the isometry group of AdS_{d+1} is $\mathrm{SO}(d,2)$, and this is precisely the conformal group of $\mathbb{R}^{d-1,1}$ for all $d \geq 3$.

For $d = 2$, the situation is more subtle. On $\mathbb{R}^{1,1}$, there is no longer a finite-dimensional group describing conformal transformations. Instead, conformal transformations are described by an infinite-dimensional Lie algebra called the Witt algebra, and the conformal symmetry algebra of a euclidean CFT in two dimensions turns out to be the direct sum $\mathrm{Vir} \oplus \mathrm{Vir}$ where Vir is a central extension of the Witt algebra called the Virasoro algebra. As a result, one might speculate that the plausibility argument for a correspondence between theories of gravity on AdS_3 and conformal field theories on $\mathbb{R}^{1,1}$ breaks down. Incredibly, however, this is not the case. Brown and Henneaux [44] demonstrated that given appropriate boundary conditions at spatial infinity, the asymptotic symmetry algebra of

three-dimensional Einstein gravity with negative cosmological constant is the conformal algebra of two-dimensional, Euclidean conformal field theory. Since two-dimensional CFT is very well-studied, the result of Brown and Henneaux motivates a lot of current work on gauge-gravity duality.

Recall that the original conjecture between string theory on AdS_5 and $\mathcal{N} = 4$ SYM on $\mathbb{R}^{3,1}$ is considered holographic because the conformal boundary of AdS_5 equals the conformal compactification of $\mathbb{R}^{3,1}$, so the duality is between a gravitating theory on a spacetime, and a different theory on its boundary which encodes all of the information about the bulk theory. Just as with the analysis of symmetries, the conformal boundary analysis also extends to general dimensions; the conformal boundary of AdS_{d+1} equals the conformal compactification of $\mathbb{R}^{d-1,1}$.

We've thus far shown that arguments about symmetry and conformal boundaries that lend plausibility to Maldacena's $\mathrm{AdS}_5/\mathrm{CFT}_4$ conjecture can be generalized to any non-trivial dimension. One can go even further than this to argue for the existence of a gauge-gravity duality that is more general than $\mathrm{AdS}_5/\mathrm{CFT}_4$. For example, if one considers a gauge theory with gauge group $\mathrm{SU}(N)$ and coupling g, then in the so-called 't Hooft limit where one takes $N \to \infty$ while keeping the combination g^2N fixed, one can show that in perturbation theory, the gauge theory looks the same as a theory of oriented, closed strings with string coupling constant $1/N$. Of course, without further investigation, this argument is itself merely suggestive since an exact correspondence between gauge and string theory would require one to go beyond perturbation theory. Nonetheless, in hindsight, such arguments

are clearly more than just suggestive since, as we review in the next section, gauge-gravity duality does indeed have concrete realizations beyond the original conjecture.

1.5 Holography since the conjecture

In the last section, we argued that certain aspects of the AdS/CFT correspondence can be easily generalized to dimensions other than $d = 4$ and to SU(N) gauge theories other than $\mathcal{N} = 4$ SYM. Since the original Maldacena conjecture, the prospect of constructing other concrete examples of holographic dualities has been taken seriously, and enormous progress has been made in demonstrating that gauge-gravity duality and holography can be concretely realized in quite varied circumstances. Since this is a broad area of active research, we list only a few of the notable areas of study that are especially relevant to this dissertation.

One of the most important objects studied in quantum field theories is reonormalization group (RG) flow which determines how a theory behaves at different scales. Shortly after Maldacena's original conjecture, much work was done to demonstrate how renormalization group flows can be understood holographically. Namely, if one knows that a certain quantum field theory is holographically dual to a theory of gravity, then one can extract information about the RG flow of the boundary theory directly from doing calculations in the bulk. Henningson and Skenderis [127] showed that by regularizing the gravitational part of the supergravity action, one can compute the Weyl anomaly for CFTs described through AdS/CFT. Balasubramanian and Kraus [25] proposed a method for computing the boundary stress tensor associated with a gravitating system in any spacetime that is asymptotically

AdS and used their result to determine a nonzero ground state energy for global AdS_5 and show that it matched the Casimir energy of $\mathcal{N} = 4$ SYM on $S^3 \times \mathbb{R}$. They then also showed [26] that AdS can be foliated by a family of surfaces homeomorphic to its boundary and that there is a holographic correspondence between the theories living on each surface in the foliation and quantum field theory enclosed in its volume. Moreover, the flow of observables on successive surfaces can be described by a renormalization group equation, so that flowing from the boundary theory into the bulk geometry can be interpreted as flowing from the UV to the IR in the boundary theory. Jan de Boer, Verlinde, and Verlinde [78] used Hamilton-Jacobi theory to show that the first order flow equations for the classical action of five-dimensional supergravity take the same form as the Callan-Symanzik RG equations of four-dimensional large N gauge theory. By regularizing the bulk on-shell supergravity action and adding counterterms to remove divergences, de Haro, Skenderis, and Solodukhin [79] developed the systematics of computing correlation functions using holographic renormalization. For a nice review of holographic renormalization see the lecture notes by Skenderis [175].

Another active area of research involves determining how one can holographically compute various quantum field theoretic observables. In particular, Ryu and Takayangi [172] proposed that by computing the areas of certain minimal surfaces in the bulk gravitational theory that satisfy appropriate boundary conditions, one can compute the entangelement entropy between two regions in the dual CFT when it is in the ground state. Their work was extended by Hubeny, Rangamani, and Takayanagi [134] who proposed that for time-

dependent states on the boundary, a similar prescription can be used in which one computes the areas of extremal surfaces in the bulk. Although the original proposal of Ryu and Takayanagi was a conjecture, a large amount of work has since been done to demonstrate its validity and utility in a wide-variety of contexts. Casini, Huerta, and Myers [51] derived the Ryu-Takayanagi proposal for a general class of situations in which the so-called entangling surface dividing the regions on the boundary is spherical. More recently, Lewkowycz and Maldacena [152] exhibited a generalization of the black hole entropy formula to Euclidean bulk solutions and in the process effectively proved the proposal of Ryu and Takayanagi for Einstein gravity.

The last area of research pertinent to this dissertation is so-called higher-spin holography. Gravitational theories in AdS containing a guage field for each spin $s > 2$ were first constructed by Vasiliev in AdS_4 [184]. Such theories are now referred to as "higher-spin" theories. Vasiliev later extended his results to dimensions other than four, including to AdS_3 [185, 186]. In three dimensions, higher-spin theories are characterized by a real parameter λ which specifies their gauge algebra denoted $\mathrm{hs}[\lambda]$. Klebanov and Polyakov showed that the singlet sector of the critical $O(N)$ vector model is dual, in the large N limit, to the minimal bosonic theory in AdS_4 containing massless gauge fields of even spin [141]. In the large central charge limit, the asymptotic symmetry algebra of such theories was shown [126] to coincide with $\mathcal{W}_\infty[\lambda]$. This motivated the proposal of Gaberdiel and Gopakumar [103] that $\mathrm{hs}[\lambda]$ higher spin theories are dual to a 't Hooft-like, large N limit of W_N minimal models.

More recently, Campoleoni, Fredenhagen, Pfenniger, and Theisen [49] demonstrated that when a three-dimensional higher-spin theory is described as a $\mathrm{SL}(3,\mathbb{R}) \times \mathrm{SL}(3,\mathbb{R})$ Chern-Simons theory, then its asymptotic symmetry algebra can be computed and is given by two copies of the classical $\mathcal{W}_3$ algebra. Motivated by this discovery, much work has been done in understanding $\mathrm{SL}(N,\mathbb{R}) \times \mathrm{SL}(N,\mathbb{R})$ Chern-Simons theory as a theory of higher spin gravity, especially for $N = 3$, with the hope that these investigations will yield a large class of computationally tractable examples with which higher spin AdS/CFT can be explored. A particularly exciting development was the discovery of higher spin black holes by Gutperle, and Kraus [120] who constructed solutions to three-dimensional, higher spin gravity in the Chern-Simons formulation that generalize the BTZ black hole in the sense that they share its holonomies, but that also carry spin-3 charge. Their work is particularly relevant in this dissertation as it forms the basis for further investigations of higher spin black holes in chapter 4.

1.6 What's in this dissertation?

This dissertation is broken into three chapters, each of which explores a different aspect of holography and gauge-gravity duality.

In chapter 2, we discuss a simple model for realizing holographic duals of conformal field theories with boundaries (BCTFs) and interfaces (ICFTs). As we describe in detail, BCFTs and ICFTs have less symmetry than their boundaryless counterparts. We show that by using a three-dimensional Janus ansatz in the bulk, one can holographically reproduce important

aspects of BCFTs and ICFTs including their symmetries. We discuss the holographic dictionary in these models, and we show how one applies the holographic entanglement entropy proposal of Ryu and Takayanagi to determine both the entanglement entropy and so-called boundary entropy.

In chapter 3, we apply the covariant holographic entanglement entropy proposal of Hubeny, Rangamani, and Takayanagi to AdS in fibered coordinates and to Warped AdS with small warping. We holographically compute the entanglement entropy of a single interval and show that in certain limits, our result reproduces the value for the left and right central charges computed independently by demanding consistency with the Cardy formula for two-dimensional CFTs.

In chapter 4, we construct a three-dimensional higher-spin Lifshitz black hole. We begin by showing that asymptotically Lifshitz spacetimes can be realized in $\mathrm{SL}(3,\mathbb{R}) \times \mathrm{SL}(3,\mathbb{R})$ Chern-Simons theory, and we show that the algebra generating Lifshitz isometries can be realized in this context. We then show that this class of Chern-Simons solutions admits non-rotating black hole solutions with sensible thermodynamics and a gauge in which the corresponding metric is a black hole with a regular horizon.

Chapter 2

Holographic RG flows and AdS/BCFT

The AdS/CFT correspondence relates string theory or M-theory on $\mathrm{AdS}_{d+1} \times M$ to a conformal field theory in d-dimensions [157, 117, 190]. The best-known example is given by the duality between Type IIB string theory on $\mathrm{AdS}_5 \times S^5$ and 4-dimensional $\mathcal{N} = 4$ super Yang-Mills theory.

It is possible to deform d-dimensional conformal field theories by the introduction of boundaries or defects/interfaces such that a subgroup of their (super)conformal symmetries is unbroken. The classification and construction of such interface and boundary CFTs is an important problem that enjoys several physical applications (see e.g. [50] for a discussion of the two-dimensional case).

In the context of the AdS/CFT correspondence, it is often possible to find a holographic solution corresponding to the deformation of the CFT. A well-known example consists of putting a black hole in the bulk of the AdS space which corresponds to a CFT at finite temperature [191].

There have been several constructions in the literature of holographic duals to interface

CFTs. In the probe approximation, holographic defects can be described by placing branes with an AdS_d world-volume inside the bulk of AdS_{d+1} [138]. The Janus solution utilizes an ansatz where AdS_{d+1} is sliced using AdS_d factors. The solution found in [21] (see also [67, 163]) is dual to an interface of $\mathcal{N} = 4$ super Yang-Mills theory where the Yang-Mills coupling constant jumps across the interface. The original solution breaks all supersymmetries, but many generalizations have been found which realize superconformal interface theories [83, 84, 85, 86, 87, 60, 63]. For related work by other authors see [66, 113, 154, 155, 192, 112, 148, 149, 156].

Recently a proposal for the holographic description of boundary CFT has been made in [181, 101] (building on the original proposal of [138]), where an additional boundary Q in the bulk of AdS_{d+1} cuts off the the bulk spacetime. The intersection of Q with the boundary of AdS_{d+1} constitutes the location of the boundary of the CFT.

The half-BPS interface solutions can also be used to obtain holographic duals of BCFTs by taking limits of the regular interface solutions. These solutions were constructed for four dimensional BCFTs [18, 5, 36] and for two dimensional BCFTs [62]. Note that these solutions are necessarily singular. Recently a completely regular holographic BCFT in two dimensions was constructed using the higher genus half-BPS interface solutions of six dimensional supergravity [61].

Renormalization group flows of CFTs are obtained by deforming the theory by a relevant operator in the UV. The endpoint of the flow in the IR can be another CFT or a massive theory. In the context of AdS/CFT, a simple realization of renormalization group flows is given by turning on a scalar field dual to a relevant operator deformation and solving the coupled equations of motion in the bulk. Examples of flows between two conformal fixed points and flows to massive theories can be found in [99, 82, 111]. Note that on the gravity side, the RG solutions corresponding to the flow to massive theories are generically singular.

The goal of the present paper is to use the techniques of holographic RG flows with the

Janus ansatz to find new realizations of boundary and interface CFTs. We turn on scalar field dual to a relevant operator using a Janus-like AdS_d slicing of AdS_{d+1}. An new feature of our paper is that on the CFT side such an ansatz corresponds to turning on a relevant operator with a source that depends on the coordinate transverse to the interface/boundary.

We obtain numerical solutions of the $(d+1)$-dimensional equations of motion which realize interfaces, and we find that the solutions interpolate between different values of the source and expectation value of the operator on either side of the interface. Furthermore, we realize boundary CFTs where the solution becomes singular in the bulk. We interpret this as a flow where the source of the operator becomes infinite and the theory on one side of the interface becomes massive leaving only a boundary CFT on the other side of the interface. We illustrate this with example in $d = 2$ and $d = 4$ dimensions.

The organization of the paper is as follows: In section 4.1 we set up the equations of motion for a scalar coupled to gravity in $d+1$ dimensions for a Janus ansatz, and we discuss the boundary conditions which correspond to a spatially dependent source for a relevant operator. In section 4.2 the equations of motion are solved numerically, and examples of interface CFTs as well as boundary CFTs are presented. In section 4.3 we evaluate the entanglement entropy following the prescription of [172, 171] for the solutions found in section 4.2. We discuss our results and possible directions for further research in section 4.4.

2.1 AdS-slicing and BCFT

The action for a scalar minimally coupled to $d+1$ dimensional gravity is

$$S = \int_M d^{d+1}x\sqrt{|g|}\Big(-\frac{1}{4}R + \frac{1}{2}g^{\mu\nu}\partial_\mu\phi\partial_\nu\phi + V(\phi)\Big) \tag{2.1}$$

where we have set Newton's constant equal to one. The stress tensor takes the following form

$$T_{\mu\nu} = \partial_\mu\phi\partial_\nu\phi - \frac{1}{2}g_{\mu\nu}g^{\rho\sigma}\partial_\rho\phi\partial_\sigma\phi - g_{\mu\nu}V(\phi). \tag{2.2}$$

The equations of motion for the coupled scalar-gravity system are

$$0 = \Delta\phi - V'(\phi) \tag{2.3}$$

$$0 = R_{\mu\nu} - \frac{1}{2}g_{\mu\nu}R - 2T_{\mu\nu}. \tag{2.4}$$

We normalize the potential by extracting the cosmological constant

$$V(\phi) = -\frac{d(d-1)}{4} + \widehat{V}(\phi). \tag{2.5}$$

We take $\widehat{V}(0) = 0$, so for $\phi = 0$ the equations of motion are solved by AdS_{d+1} with unit curvature radius, where the metric in Poincaré coordinates is given by

$$ds^2 = \frac{1}{z^2}\Big(dz^2 + dx_\perp^2 - dt^2 + \sum_{i=2}^{d-1} dx_i^2\Big). \tag{2.6}$$

In contrast, The Janus ansatz uses a deformation of the AdS_d slicing of AdS_{d+1}. The Poincaré slicing (2.6) can be mapped to the AdS_d slicing by[1]

$$x_\perp = y\cos\mu, \qquad z = y\sin\mu, \tag{2.7}$$

[1]The AdS slicing is related to the one of [21] by a shift in μ by $\pi/2$. The present coordinates are more convenient for the description of BCFT.

which gives the metric

$$ds^2 = \frac{1}{\sin^2\mu}\left(d\mu^2 + \frac{dy^2 - dt^2 + \sum_{i=2}^{d-1} dx_i^2}{y^2}\right). \tag{2.8}$$

Here the slicing coordinate $\mu \in [0, \pi]$. The boundary of the Poincaré slicing metric (2.6) is located at $z = 0$. In the AdS slicing, the boundary is mapped into three connected components that we conceptually distinguish from one-another, namely $\mu = 0, \pi$ corresponding to two d-dimensional half spaces and $y = 0$ corresponding to a $(d-1)$-dimensional interface where the two half-spaces are glued together.

2.2 Janus ansatz and symmetries

In constructing a holographic dual to an ICFT or BCFT, we look for a bulk spacetime whose group of isometries is the conformal group of the BCFT. For dimensions $d > 2$ the conformal group of $\mathbb{R}^{1,d-1}$ is $\mathrm{SO}(2,d)$, hence a CFT_d is expected to exhibit $\mathrm{SO}(2,d)$ invariance.

In this paper we consider an interface or boundary which is the $\mathbb{R}^{1,d-2}$ subspace localized at $x^\perp = 0$. By definition we demand that the field theories are invariant under only those elements of $\mathrm{SO}(2,d)$ which preserve the boundary. The subgroup of conformal transformations that preserve this boundary is precisely the conformal group $\mathrm{SO}(2,d-1)$ of the boundary. This, in turn, is precisely the isometry group of AdS_d. Therefore in searching for a candidate holographic dual to BCFT_d, we look for a spacetime whose bulk exhibits invariance under the full isometry group of AdS_d.

The BCFT symmetries are realized by a Janus ansatz which is based on an AdS_d sliced metric. All other fields have nontrivial dependence only on the slicing coordinate μ. The

bulk therefore has manifest $\mathrm{SO}(2, d-1)$ symmetry as desired.

$$ds^2 = f(\mu)\left(d\mu^2 + \frac{dy^2 - dt^2 + \sum_{i=2}^{d-1} dx_i^2}{y^2}\right), \qquad \phi = \phi(\mu). \tag{2.9}$$

With this ansatz, the scalar equation (2.3) becomes

$$0 = \phi'' - f\widehat{V}'(\phi) + \frac{d-1}{2}\frac{f'}{f}\phi', \tag{2.10}$$

and the gravitational equations become

$$0 = \frac{f''}{f} - \frac{3}{2}\frac{f'f'}{f^2} + \frac{4}{d-1}\phi'\phi' - 2 \tag{2.11}$$

$$0 = \frac{1}{4}\phi'\phi' - \frac{d(d-1)}{32}\frac{f'f'}{f^2} - \frac{d(d-1)}{8} + \frac{d(d-1)}{8}f - \frac{1}{2}f\widehat{V}. \tag{2.12}$$

Note that only two of the three equations (2.10)-(2.12) are independent. Also note that equation (2.12) contains only first order derivatives and can be viewed as a constraint of the evolution with respect to the coordinate μ.

2.2.1 Perturbative solution

Let us assume that the potential $\widehat{V}$ has the form

$$\widehat{V}(\phi) = \frac{1}{2}m^2\phi^2 + \sum_{k=3}^{\infty}\frac{\widehat{V}^{(k)}(0)}{k!}\phi^k. \tag{2.13}$$

We find a perturbative solution to the scalar-gravity equations. Consider an ansatz for f and ϕ that takes the form of a formal power series in a parameter ε;

$$f(\varepsilon, \mu) = \sum_{k=0}^{\infty} f_{2k}(\mu)\varepsilon^{2k}, \qquad \phi(\varepsilon, \mu) = \sum_{k=0}^{\infty}\phi_{2k+1}(\mu)\varepsilon^{2k+1}. \tag{2.14}$$

Notice that to zeroth order in ε the solution corresponds to the vacuum solution with no scalar present. The first order solution corresponds to a small scalar living in the vacuum, the second order solution gives backreaction of the scalar on the gravity solution, and so on. Plugging this ansatz into the scalar and constraint equations, and setting the coefficients of ε to zero order-by-order, we obtain a sequence of equations that can, in principle, be solved recursively for the coefficient functions f_{2k} and ϕ_{2k+1} in the expansions (2.14). To zeroth order in ε, we obtain the following equation:

$$0 = (f_0')^2 + 4f_0^2 - 4f_0^3. \tag{2.15}$$

The solution to this equation gives the AdS vacuum. The higher order functions f_2, f_4, f_6 and so on give modifications to f due to back-reaction. The solution to (2.15) with initial condition $f_0(\pi/2) = 1$ is

$$f_0(\mu) = \frac{1}{\sin^2 \mu} \tag{2.16}$$

which, as expected, is precisely the appropriate f for the AdS_d slicing of AdS_{d+1}; see (2.8). To first order in ε, one obtains the following equation:

$$0 = 2f_0\phi_1'' + (d-1)f_0'\phi_1' - 2f_0^2 V''(0)\phi_1. \tag{2.17}$$

Plugging in $f_0 = 1/\sin^2 \mu$ and $V''(0) = m^2$ (see (2.13)), we obtain

$$0 = \phi_1'' - (d-1)\cot\mu\,\phi_1' - m^2 \csc^2\mu\,\phi_1 \tag{2.18}$$

whose general solution is a linear combination of the following form

$$\phi(\mu) = C_1 \; P^{\frac{1}{2}\sqrt{d^2+4m^2}}_{\frac{d-2}{2}}(\cos\mu)\sin^{d/2}+C_2 \; Q^{\frac{1}{2}\sqrt{d^2+4m^2}}_{\frac{d-2}{2}}(\cos\mu)\sin^{d/2}\mu. \tag{2.19}$$

In the following we will not go to higher than first order in ε since we will solve the equations numerically.

2.3 Holographic dictionary

The standard holographic dictionary relates the mass m of the scalar field to the conformal dimension Δ of the dual operator O_Δ;

$$m^2 = \Delta(\Delta - d), \qquad \Delta = \frac{1}{2}\Big(d + \sqrt{d^2 + 4m^2}\Big). \tag{2.20}$$

The second relation holds for the so-called "standard quantization." We will consider operators which are IR relevant. This is equivalent to considering scalar fields with squared mass m^2 satisfying

$$-\frac{d^2}{4} < m^2 < 0, \qquad \frac{d}{2} < \Delta < d. \tag{2.21}$$

Near the AdS boundary in Poincaré slicing the the scalar field behaves as follows

$$\phi \sim \phi_1(x) z^{d-\Delta} + \phi_2(x) z^{\Delta} + \cdots . \tag{2.22}$$

The standard holographic dictionary identifies ϕ_1 with the (linearized) source added to the action and ϕ_2 with the expectation value for the operator O_Δ [190].

The solution of the linearized scalar equation in the AdS slicing (2.19) behaves as follows near the boundary $\mu = 0$:

$$\phi(\mu) \sim \alpha \; \mu^{\Delta} + \beta \; \mu^{d-\Delta} + \cdots . \tag{2.23}$$

The constants α, β determine the initial conditions for the evolution equations (2.10) and (2.11). One might conclude, by following the holographic prescription outlined above that β corresponds to a constant source and α to a constant expectation value of the dual operator on the half space located at $\mu = 0$. However, inverting the relations (2.7) for $\mu \to 0$ and $y > 0$ we obtain

$$\mu = \frac{z}{x_\perp}, \quad y = x_\perp \tag{2.24}$$

which is valid as long as $y >> \mu$. Hence by mapping coordinates from AdS slicing to Poincaré slicing, one obtains the behavior near $z = 0$ but with $x_\perp > 0$ which corresponds to the points away from the interface;

$$\lim_{z\to 0} \phi(z, x_\perp) \sim \frac{\alpha}{(x_\perp)^\Delta} z^\Delta + \frac{\beta}{(x_\perp)^{d-\Delta}} z^{d-\Delta} + \cdots . \tag{2.25}$$

In the Poincaré slicing realization of RG flows, the surfaces of constant z correspond to a fixed energy scale in the dual CFT. It follows from (2.25) that the scalar behavior near the boundary corresponds to sources and expectation values for the dual operator which are dependent on the transverse coordinate $x_\perp$. In a recent paper [89] spacetime dependent couplings in RG-flows were discussed and it was noted that the space time dependence can change the relevance of the operator perturbation. This is a new feature of the Janus ansatz and is not the case for holographic RG flows with Poincaré symmetry which are translation invariant along all directions in $\mathbb{R}^d$. The extra $x_\perp$ dependence of the coupling in (2.25) seems to make the perturbation marginal, we will still call the evolution RG-flow as the coupled scalar-gravity evolution shares many features of the holographic Poincaré RG-flow.

2.4 Holographic ICFT and BCFT via RG flow

Turning on a relevant operator in a d-dimensional CFT generates a renormalization group flow. In the IR, the theory can flow either to a new conformal fixed point, or become massive. The holographic realization of RG flows in the Poincaré slicing has been studied many papers (see e.g. [99, 82]). In the following we will instead study RG flows using the Janus ansatz described in the previous section.

The main difference between the Poincaré slicing and AdS_d slicing lies in the fact that for the AdS_d slicing, as discussed in section 4.1, the UV boundary of AdS_{d+1} has three components, corresponding to the two d-dimensional half spaces glued together at a $d-1$-dimensional interface.

For a holographic interface we choose the two boundary components associated with the two half spaces to be located at μ_+ and μ_-. Since the metric becomes asymptotically AdS at $\mu = \mu_\pm$, the metric and scalar field behave as follows:

$$\begin{aligned} &\lim_{\mu\to\mu_\pm} f(\mu) \sim \frac{1}{(\mu-\mu_\pm)^2} + \cdots \\ &\lim_{\mu\to\mu_\pm} \phi(\mu) \sim \alpha_\pm(\mu-\mu_\pm)^\Delta + \beta_\pm(\mu-\mu_\pm)^{d-\Delta} + \cdots . \end{aligned} \tag{2.1}$$

It follows from (2.25) that $\alpha_\pm$ correspond to position-dependent expectation values for O_Δ at on the two half spaces and $\beta_\pm$ correspond to the position-dependent sources for O_Δ at on the two half spaces. Note that for a smooth solution of the equations of motion (2.10) and (2.11) only two of the four constants $\alpha_\pm, \beta_\pm$ are independent. In particular for the linearized solution given in (2.19), one neglects the gravitational back reaction and hence the value of $\mu_\pm$ is unchanged from the undeformed AdS values, i.e. $\mu_- = 0$ and $\mu_+ = \pi$. From (2.19) one can read off a linear relation between a_+, β_+ and a_-, β_-. For simplicity and in order to compare with the boundary conditions that we impose on numerical solutions in later

sections, we choose to set the expectation value to zero at μ_-, namely we choose $\alpha_- = 0$. The resulting linear relations between α_+, β_+, and β_- are

$$\alpha_+ = \frac{\pi 2^{d-2\Delta} \csc\left(\frac{1}{2}\pi(d-2\Delta)\right) \Gamma\left(\frac{d}{2}-\Delta+1\right)}{\Gamma(1-\Delta)\Gamma(d-\Delta)\Gamma\left(-\frac{d}{2}+\Delta+1\right)} \beta_- + \mathcal{O}(\beta_-^2), \tag{2.2}$$

$$\beta_+ = -\sin\left(\frac{\pi d}{2}\right) \csc\left(\frac{1}{2}\pi(d-2\Delta\right) \beta_- + \mathcal{O}(\beta_-^2). \tag{2.3}$$

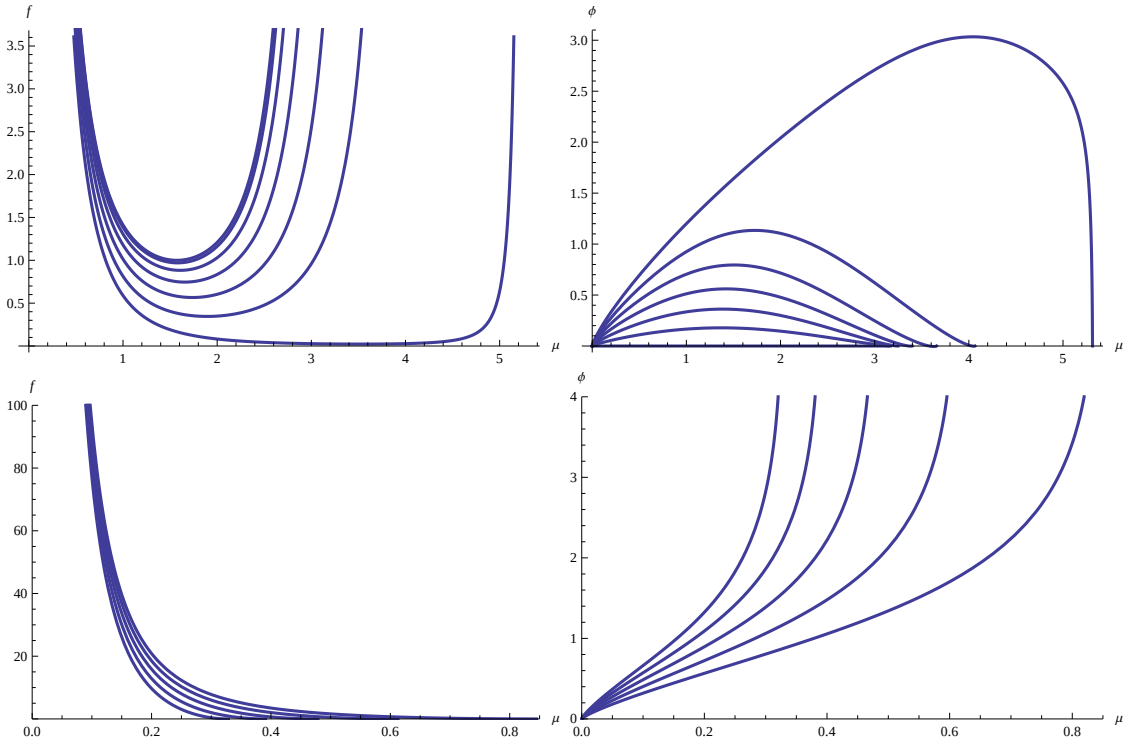

Figure 2.1: Plots of $f(\mu)$ and $\phi(\mu)$ in the ICFT (top row) and BCFT (bottom row) cases with $\Delta = 1.202$ and $\lambda_4 = -4.8$. We have used $d = 2$ with potential given by (2.4). The family of curves in each plot is generated by varying the value of the source β_-. The ICFT curves correspond to $\beta_- = 0, 0.2, 0.4, \ldots, 1.2$ while the BCFT curves correspond to $\beta_- = 2, 2.5, 3, 3.5, 4$.

2.5 ICFT and BCFT in $d = 2$

In order to go beyond the linearized approximation, we numerically solve the equations of motion (2.10) and (2.11) subject to the constraint (2.12). We choose to locate one boundary at $\mu_- = 0$, and we impose boundary conditions on the scalar field there corresponding to a vanishing expectation value with only a source turned on, i.e. $a_- = 0$. In the following we study the case $d = 2$ which corresponds to a deformation of a 2-dimensional CFT. We consider a toy model with a potential

$$\hat{V}(\phi) = \frac{1}{2}\Delta(\Delta - 2)\phi^2 + \frac{1}{4!}\lambda_4\phi^4. \tag{2.4}$$

As an example we choose the the operator O_Δ to be relevant and have dimension $\Delta = 1.2$ and consider a potential with a small negative quartic coupling $\lambda_4 = -4.8$. Note that for these values, $\phi = 0$ is the only extremum of the potential $\hat{V}$. The behavior of the resulting solution depicted in the following is generic for any relevant operator deformation.

As a function of the source β_-, the numerical solution displays the following properties: For very small β_-, the values of α_+, β_+, which are obtained by a numerical fit, approach their linearized values given by (2.2) and (2.3). The values of the source β_+ and expectation value α_+ on the second half space grow for increasing values of the source. Following the discussion above, we can interpret these solutions as Janus-like interfaces, where the two CFTs defined on the half spaces at $\mu = \mu_\pm$ have different $x_\perp$-dependent sources and expectation values on either side.

At a critical value of β_-, both μ_+ and α_+, β_+ diverge, the metric function f approaches a zero, and the solution becomes singular. We interpret this in the following way: The operator deformation on the half-space at $\mu = \mu_+$ becomes so large that the theory is becoming massive, and the second asymptotic region disappears. Consequently for values of the source β_- larger than the critical value, the solution becomes singular in the bulk and

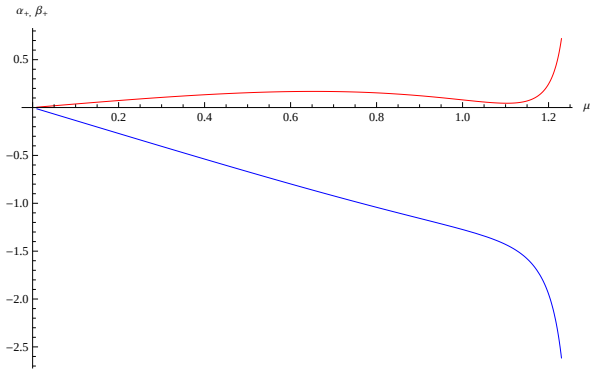

Figure 2.2: Plot of expectation value α_+ (red) and source β_+ (blue) as a function of the source β_-

corresponds to a BCFT since there is only one asymptotically AdS boundary corresponding to a single half-space.

We will use these numerical solutions to study the entanglement entropy for the ICFT and BCFT solutions in section 2.10.

2.6 Interface and BCFT in $d = 4$

In this section we consider specific examples of $d = 4$ ICFT and BCFT RG-flows. Qualitatively the solutions behave in the same way as in the 2-dimensional case presented in section 2.5. We consider a truncation of $\mathcal{N} = 8$ supergravity introduced in [111] called the GPPZ solution. The potential V can be expressed in terms of a pre-potential

$$W(\phi) = -\frac{3}{4}\left[1 + \cosh\left(\frac{2\phi}{\sqrt{3}}\right)\right] \tag{2.5}$$

which determines the potential as follows:

$$\begin{aligned} V(\phi) &= \frac{1}{2}\left(\partial_\phi W\right)^2 - \frac{4}{3}W^2 \\ &= -3 - \frac{3}{2}\phi^2 - \frac{1}{3}\phi^4 + o(\phi^6). \end{aligned} \tag{2.6}$$

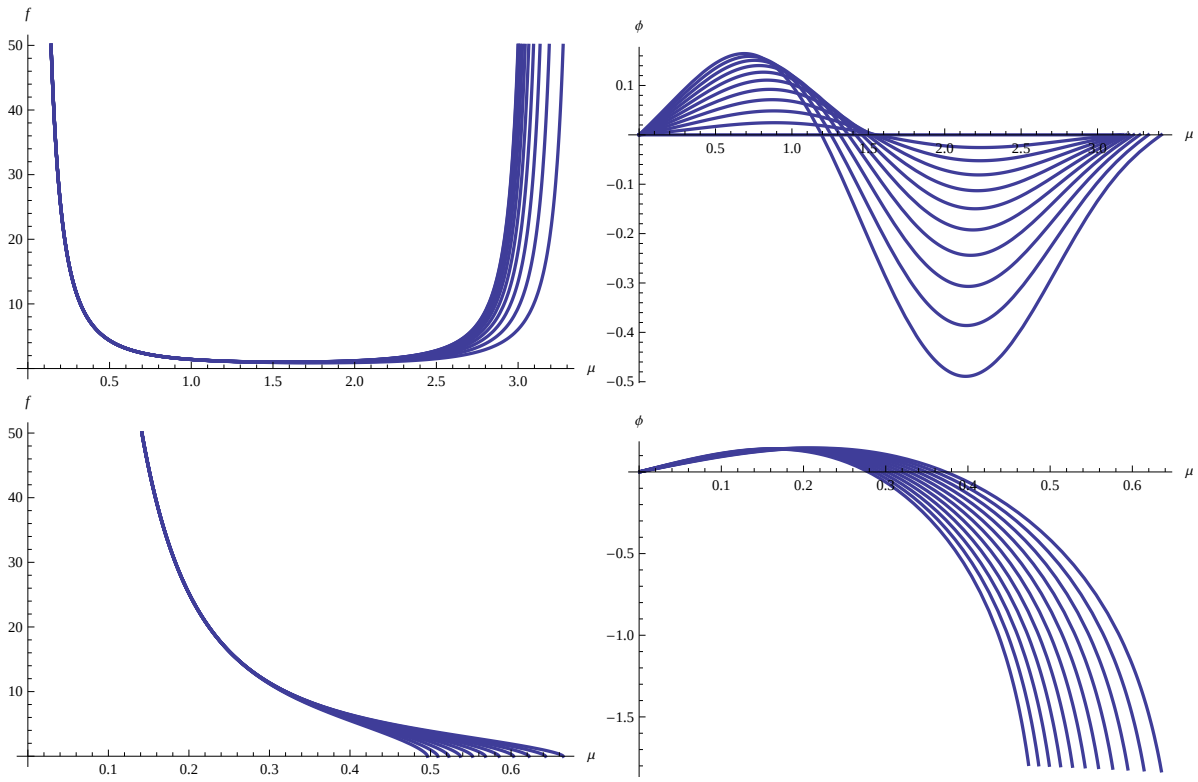

Figure 2.3: Plots of $f(\mu)$ and $\phi(\mu)$ in the ICFT (top row) and BCFT (bottom row) cases. We have used $d = 4$ with GPPZ potential given by (2.5). The family of curves in each plot is generated by varying the value of the source β_-. The ICFT curves correspond to $\beta_- = 0, 0.03, 0.06, \ldots, 0.3$ while the BCFT curves correspond to $\beta_- = 1, 1.03, 1.06, \ldots, 1.3$.

Expanding the potential around the maximum $\phi = 0$ indicates that the scalar field is dual to a relevant operator with dimension $\Delta = 3$. In [111] it was argued that a Poincaré slicing RG flow solution becomes singular and the singularity represents the flow of $\mathcal{N} = 4$ SYM to a massive fixed point with $\mathcal{N} = 1$ supersymmetry[2]. In the following, we numerically solve the equations of motion for an AdS-sliced RG-flow in $d = 4$ with the potential given in eq. (2.6).

As with the 2-dimensional solutions, we set the expectation value α_- of the dual operator at $\mu_- = 0$ to zero, and we plot the corresponding solutions for a few values of the operator source β_-. Qualitatively, the behavior of the solutions is very similar to that of the solutions

[2]See [153, 7] for a recent discussion of Poincaré RG flows for the GPPZ flow and the evaluation of entanglement entropy for such flows.

found in section 2.5. For small values of β_-, we have a holographic ICFT where at the $\mu = \mu_+$ boundary the scalar generally has a nonzero source and expectation value. A set of representative plots is given in figure 2.3. For a critical value of the source β_-, the solution becomes singular, and we have a holographic BCFT. The location of the singularity is a function of β_-. A set of representative plots is given in figure 2.3.

2.7 Entanglement entropy and minimal surfaces

Consider a QFT defined on a d-dimensional spacetime, and let A be a subregion of a constant time slice of that spacetime. The entanglement entropy (see e.g. [46] for a review) for A is defined as follows. Let B be the complement of A in the time slice. The Hilbert space of the system can be expressed as a tensor product of degrees of freedom localized in either A or B, namely $\mathcal{H} = \mathcal{H}_A \otimes \mathcal{H}_B$. The general state of the system can be described by a density operator ρ on $\mathcal{H}$, and the state of a subsystem A is described by a reduced density operator $\rho_A = \mathrm{tr}_B\, \rho$. One then defines the entanglement entropy of system A with system B as the von Neumann entropy associated with the reduced density operator ρ_A;

$$S_A = -\,\mathrm{tr}\, \rho_A \ln \rho_A. \tag{2.1}$$

A proposal to holographically calculate the entanglement entropy of d-dimensional CFT was discussed in [172, 171]. Working in Poincaré coordinates, the CFT is defined on Minkowski space $\mathbb{R}^{1,d-1}$ which can be thought of as the boundary of AdS_{d+1}. The subsystem A is a d-dimensional sub-region in the constant-time slice. The boundary of A will be denoted by ∂A (see figure 2.4). One finds the static minimal surface γ_A that extends into the AdS_{d+1} bulk and ends on ∂A as one approaches the boundary of AdS_{d+1}. The holographic entanglement

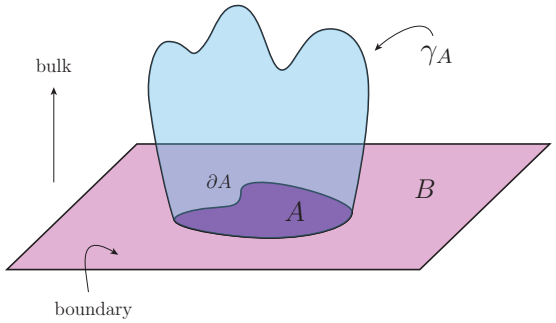

Figure 2.4: Minimal surface γ_A used for the calculation of holographic entanglement entropy.

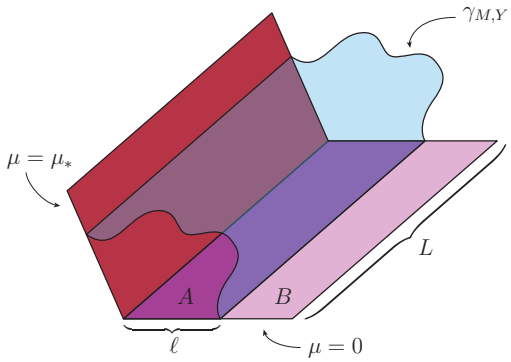

Figure 2.5: Minimal surface for calculation of the holographic entanglement entropy in the strip geometry in the case of a flow to a BCFT.

entropy can then be calculated as follows [172, 171]:

$$S_A = \frac{\text{Area}(\gamma_A)}{4G_N^{(d+1)}}, \tag{2.2}$$

where $\text{Area}(\gamma_A)$ denotes the area of the minimal surface γ_A, and $G_N^{(d+1)}$ is the Newton constant of the $(d+1)$-dimensional gravity.

2.8 Janus minimal surfaces

We first adapt the holographic entanglement entropy formula (2.2) to the Janus geometry in the BCFT case. Given $\ell > 0$, we divide a time slice of the BCFT living on the boundary $\mu = 0$ into two regions: region A consisting of all points satisfying $y < \ell$, and region B consisting of all points satisfying $y > 0$. We want to compute the entanglement entropy between these two regions. Taking a time slice of the Janus metric, we compute the minimal surfaces that intersects ∂A which consists of those points with $\mu = 0$ and $y = \ell$. This setup

is called the strip geometry. A time slice of the Janus metric has the following metric:

$$ds^2 = f(\mu)\left(d\mu^2 + \frac{dy^2 + \sum_{i=1}^{d-2} dx_i^2}{y^2}\right). \tag{2.3}$$

In the strip geometry, we expect minimal surfaces to be invariant under translations in the transverse directions $\vec{x} = (x_1, \ldots, x_{d-2})$, so we look for minimal surfaces with embedding coordinates of the following form:

$$\mu(s, \vec{x}) = M(s), \qquad y(s, \vec{x}) = Y(s), \qquad \vec{x}(s, \vec{x}) = \vec{x}. \tag{2.4}$$

The induced metric $h_{ij}(s, \vec{x})$ on a manifold described by these embedding coordinates is diagonal with entries

$$h_{ss}(s, \vec{x}) = f(M(s))\left(M'(s)^2 + \frac{Y'(s)^2}{Y(s)^2}\right) \tag{2.5}$$

$$h_{ii}(s, \vec{x}) = \frac{f(M(s))}{Y(s)^2}; \qquad i = 1, \ldots, d-2. \tag{2.6}$$

In the transverse directions, we take the strip to be a cube $[0, L]^{d-2}$ of side length L. The area of a surface $\gamma_{M,Y}$ parameterized in this way is

$$\text{Area}[d, f; \gamma_{M,Y}] = L^{d-2} \int ds\, \mathcal{L}_{d,f;M,Y}(s), \tag{2.7}$$

where

$$\mathcal{L}_{d,f;M,Y}(s) = \sqrt{\frac{f(M(s))^{d-1}}{Y(s)^{2d-4}}\left(M'(s)^2 + \frac{Y'(s)^2}{Y(s)^2}\right)} \tag{2.8}$$

can be viewed as the "Lagrangian" for the area functional. The problem of finding minimal surfaces is equivalent to determining solutions to the Euler equations for the functions M

and Y obtained by minimizing this area functional. The solution will be characterized by a parameterized curve $(M(s), Y(s))$ in the μ-y plane which gives the constant $\vec{x}$ profile of the surface. The minimal surface Euler equation obeyed by the component functions M and Y is given by

$$0 = 2Yf(M)\left[(d-2)Y^2\left(M'\right)^3 + (d-3)M'\left(Y'\right)^2 + Y\left(M'Y'' - Y'M''\right)\right] + (d-1)Y'f'(M)\left[Y^2\left(M'\right)^2 + \left(Y'\right)^2\right]. \tag{2.9}$$

2.9 Asymptotic Expansion and initial data

In a sufficiently small neighborhood of the boundary $\mu = 0$, any minimal surface intersecting the point $(\mu, y) = (0, \ell)$ can be parameterized as follows $(M(s), Y(s)) = (s, Y(s))$. In other words, the parameter s is simply the angular coordinate μ. The minimal surface equation (2.9) then reduces to the following equation for the function Y:

$$0 = (d-1)f'Y'\left(Y^2 + \left(Y'\right)^2\right) + 2fY\left((d-2)Y^2 + (d-3)\left(Y'\right)^2 + YY''\right). \tag{2.10}$$

In this description, the boundary data are $(0, \ell) = (0, Y(0))$, so in particular, we require the initial datum $Y(0) = \ell$ on the function Y. On the other hand, for the boundary conditions which we are considering, i.e. setting the expectation value of the dual operator to zero, f has the following asymptotic expansion near $\mu = 0$ We display the expansion for the two cases we are discussing in the paper. First, for $d = 2$ and generic $1 < \Delta < 2$

$$\begin{aligned} d = 2, \Delta: \qquad \phi(\mu) &= \beta_-\mu^{2-\Delta} - \frac{1}{12}\beta_-(\Delta-1)\mu^{4-\Delta} + \cdots \\ f(\mu) &= \frac{1}{\mu^2} + \frac{1}{3} + \frac{1}{15}\mu^2 - 2\beta_-^2\frac{\Delta-2}{2\Delta-5}\mu^{2-2\Delta}, \end{aligned} \tag{2.11}$$

and second for $d = 4, \Delta = 3$ and the GPPZ potential.

$$\begin{aligned} d = 4, \Delta = 3 : \qquad \phi(\mu) &= \beta_- \mu - \beta_- \mu^3 \log(\mu) + \cdots \\ f(\mu) &= \frac{1}{\mu^2} + \frac{(3 - 2\beta_-^2)}{9} + \frac{2\beta_-^2}{5}\mu^2 \log \mu + \cdots . \end{aligned} \tag{2.12}$$

In both cases β_- is the source of the dual operator and we have set the expectation value to zero. The behavior of the minimal surface function Y near $\mu = 0$ can then be obtained by plugging the expansion of f into (2.10), yields the following expansions

$$d = 2, \Delta : \qquad Y(\mu) = \ell + \hat{y}\ \mu^2 + \frac{\beta_-^2\ \hat{y}(\Delta - 2)}{(\Delta - 3)(2\Delta - 5)}\mu^{6-2\Delta} + \cdots \tag{2.13}$$

$$d = 4, \Delta = 3 : \qquad Y(\mu) = \ell + \frac{\ell}{2}\mu^2 + \hat{y}\ \mu^4 + \frac{\beta_-^2\ \ell}{6}\mu^4 \log \mu + \cdots . \tag{2.14}$$

For both cases the expansion depends on two arbitrary integration constants $\ell, \hat{y}$, as is expected for a second order differential equation. The constant ℓ determines the location where Y intersects the AdS boundary at $\mu = 0$, the second constant y determines (roughly) how the minimal surface curves.

2.10 Holographic entanglement entropy in $d = 2$

Setting $d = 2$ in the metric (2.3) yields

$$ds^2 = f(\mu)\left(d\mu^2 + \frac{dy^2}{y^2}\right). \tag{2.15}$$

In order to compute the engtanglement entropy for a strip of width $\ell > 0$, we need to compute minimal surfaces that intersect the point $(\mu, y) = (0, \ell)$. In this low-dimensional case, the surfaces in question are really just geodesics in the geometry (2.15). For the AdS vacuum, one has $f(\mu) = \csc^2 \mu$ with $\mu \in [0, \pi]$, and the calculation is easy since (2.15) is the

metric on the Poincaré upper-half plane in polar coordinates with angular coordinate μ and radial coordinate y. In this case, geodesics come in two classes: semicircles centered on the axis $\mu = 0$ and straight lines perpendicular to this axis. Given a strip of width ℓ, there is a family of geodesics consisting of the straight line and semicircles with different radii which intersect the point $(0, \ell)$.

We are most interested in going beyond the AdS vacuum and examining those functions f that fall into one of the following two families: those that correspond to a holographic realization of an ICFT, and those that correspond to a holographic realization of a BCFT. In both cases, f behaves like $\csc^2 \mu$ as $\mu \to 0$ since the spacetime is asymptotically AdS. In the ICFT case, the geometry flows to another AdS region at some $\mu = \mu_*$ while in the BCFT case, the geometry becomes singular at some $\mu = \mu_*$. For such functions f, geodesics in the geometry (2.15) with initial data imposed near $\mu = 0$ behave like geodesics on the Poincaré upper-half plane, but they are deformed away from these vacuum solutions as flow move into the bulk. Interestingly, for $d = 2$ one of the vacuum solutions survives for general f. For any $\ell > 0$ and any f, the geodesic equation (2.9) is solved by $Y(s) = \ell$, the circular solution centered at the origin. To determine all other relevant geodesics in the ICFT and BCFT cases, we turn to numerical methods. We find that with the exception of the circular solution $Y(s) = \ell$, geodesics in the ICFT and BCFT cases exhibit distinct qualitative behaviors in the bulk.

2.10.1 ICFT geodesics in $d = 2$

For a given $\ell > 0$, there is an infinite family of geodesics intersecting the point $(\mu, y) = (0, \ell)$ on the boundary. In the parameterization $Y = Y(\mu)$, members of this family are distinguished by the value of the parameter $\hat{y}$ in the asymptotic expansion (2.13). In figure 2.6, curves colored orange have negative values of $\hat{y}$, while curves colored blue have positive

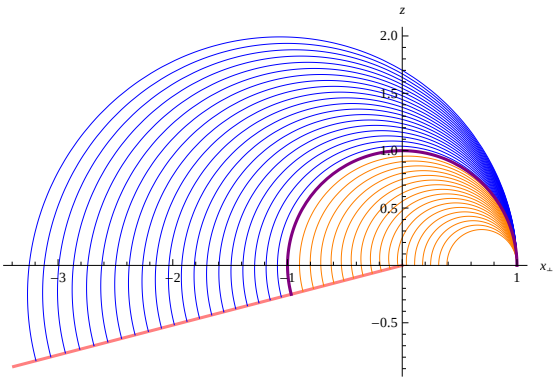

Figure 2.6: Geodesics for $d = 2$ holographic ICFT geometries with $\Delta = 1.212$, $\lambda_4 = -4.8$, $\beta_- = 0.6$, and $\ell = 1$. The pink radial line indicates the $\mu = \mu_*$ ray where the geometry is asymptotically AdS_3.

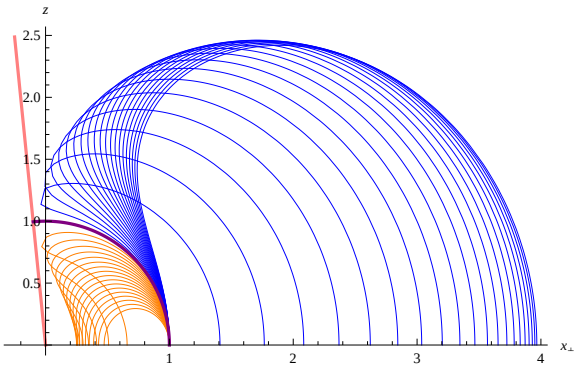

Figure 2.7: Geodesics for $d = 2$ holographic BCFT geometries for $\Delta = 1.212$, $\lambda_4 = -4.8$, $\beta_- = 1.4$, and $\ell = 1$. The red line indicates the $\mu = \mu_*$ ray where the geometry develops a curvature singularity.

values of $\hat{y}$. The purple curve has $y = 0$ and is the semicircular solution $Y(\mu) = \ell$. Those curves with a larger value of y intersect the $z = 0$ axis at lower values of $x_\perp$. Solutions that flow all the way to the second AdS region at $\mu = \mu_*$ correspond to entangling surfaces that stretch across the interface. Those orange solutions that flow back to the first asymptotic region at $\mu = 0$ correspond to entangling surfaces that remain on one side of the interface.

2.10.2 BCFT geodesics in $d = 2$

As in the ICFT case, for a given $\ell > 0$, there is an infinite family of geodesics intersecting the point $(\mu, y) = (0, \ell)$, and they are differentiated by the parameter $\hat{y}$ in (2.13). Unlike in the ICFT case, the geometry exhibits a curvature singularity at $\mu = \mu_*$, and this affects the geodesics. In particular, there is exactly one geodesic that reaches the singularity: the circular solution $Y(\mu) = \ell$. Every other geodesic is repelled by the singularity, turns around, returns to the asymptotic AdS region $\mu = 0$, and intersects the $\mu = 0$ axis. This behavior can be seen in figure 2.7. As in the ICFT plot, orange curves have $\hat{y} < 0$ while blue curves have $\hat{y} > 0$, and the purple curve is the circular solution.

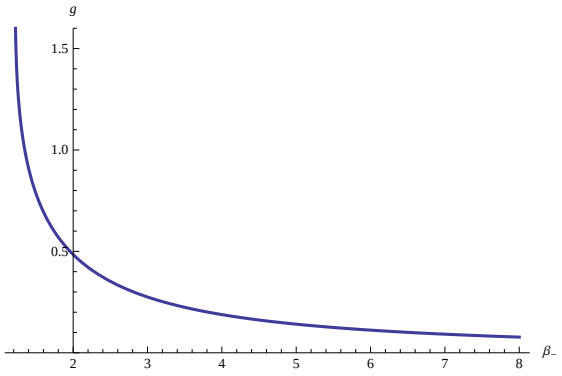

Figure 2.8: Boundary entropy "g-factor" g as a function of the source strength β_- for a potential with $\Delta = 1.212$ and $\lambda_4 = -4.8$.

2.10.3 BCFT holographic entanglement and boundary entropy

Given a two-dimensional BCFT, it is a well-known result [46] that the entanglement entropy of the strip geometry is

$$S = \frac{c}{6} \ln \frac{\ell}{\varepsilon} + \ln g \tag{2.16}$$

where c is the central charge of the BCFT, ℓ is the width of the strip, ε is the UV cutoff, g is the so-called g-factor introduced in [2], and $\ln g$ is called the boundary entropy. Since the symmetric semi-circular geodesic is the only one that reaches the singularity at $\mu = \mu_*$ and therefore the unique one to enclose the boundary of the CFT at the origin, we use it to compute the holographic entanglement entropy, and from this, we can extract the boundary entropy. The area of a minimal surface is computed via (2.7) and (2.8). For the circular solution, we can use the $(\mu, Y(\mu))$ parameterization for the whole curve with $Y(\mu) = \ell$. The function $f \sim 1/\mu^2$ as $\mu \to 0$ signaling a UV divergence that must be regulated. In the Poincaré slicing (2.6), the UV regulator can be taken as a hard cutoff at some small $z = \varepsilon$. The coordinate transformation (2.7) shows that the appropriate corresponding μ used to cutoff the area integral is $\mu_\varepsilon = \varepsilon/\ell$ for small ε. The minimal surface therefore ranges over values of μ satisfying $\mu_\varepsilon < \mu < \mu_*$, and we obtain the following expression for the holographic

entanglement entropy in the strip geometry:

$$S = \frac{1}{4G_N^{(3)}} \int_{\mu_\varepsilon}^{\mu_*} d\mu \, \sqrt{f(\mu)}. \tag{2.17}$$

The series expansion of f about $\mu = 0$ shows that after performing the integral, the only divergent piece is that coming from the leading behavior $f \sim 1/\mu^2$ in the AdS region. In fact, the divergent part is precisely $\log(\ell/\varepsilon)$ as expected from the formula (2.16). Therefore, the boundary entropy can be identified as

$$\ln g = \lim_{\varepsilon \to 0} \left[\frac{1}{4G_N^{(3)}} \left(\int_{\mu_\varepsilon}^{\mu_*} d\mu \, \sqrt{f(\mu)} - \ln \frac{\ell}{\varepsilon} \right) \right]. \tag{2.18}$$

For the BCFT solution presented in section 2.5 the boundary g factor given in (2.18) can be evaluated numerically. For the $d = 2$ RG flow BCFT found in section 2.5, the solution depends on the strength β_- of the operator source. In figure 2.8 we plot the g factor as a function of β_- for the numerical example given in section 2.5.

2.11 Holographic Entanglement entropy in $d = 4$

The qualitative features of the AdS sliced RG flow solutions in two and four dimensions are very similar. In this section we solve the minimal surface equations in the GPPZ flow solutions presented in section 2.6, and we calculate the holographic entanglement entropy for the strip geometry.

Inspection of the minimal surface equation (2.10) shows that, as the term proportional to $(M')^3$ is non-vanishing in $d = 4$, the circular solution $Y(\mu) = \ell$ does not describe a minimal surface. However in $d = 4$, the BCFT background admits a solution which serves as the analog of the $d = 2$ circular solution; it is the unique solution that satisfies the desired initial condition $Y(0) = \ell$, and it also reaches the singularity. This solution can be determined

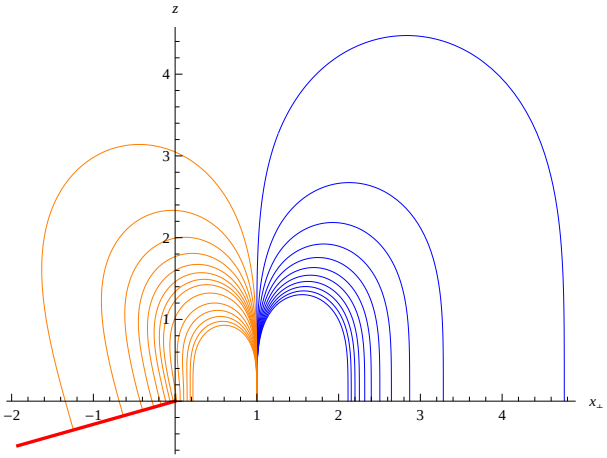

Figure 2.9: Critical surface profiles for $d = 4$ holographic ICFT geometries with $\Delta = 3$, $\beta_- = 0.3$, and $\ell = 1$. The red line indicates the $\mu = \mu_*$ ray where the geometry is asymptotically AdS_5.

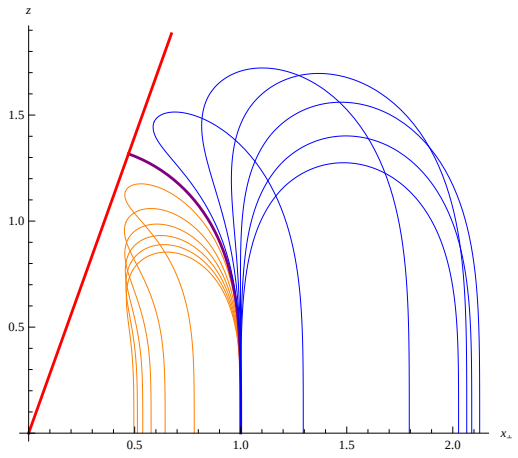

Figure 2.10: Critical surface profiles for $d = 4$ holographic BCFT geometries with $\Delta = 3$, $\beta_- = 0.6$, and $\ell = 1$. The red line indicates the $\mu = \mu_*$ ray where the geometry develops a curvature singularity.

numerically by shooting for the appropriate value of the second undetermined parameter y in the asymptotic expansion (2.14) with $d = 4$.

2.11.1 ICFT minimal surfaces in $d = 4$

For each $\ell > 0$, there is a family of minimal surfaces satisfying the initial condition $Y(0) = \ell$. We have plotted this family for the case $\ell = 1$ in figure 2.9. We have identified two subfamilies with colors orange and blue. The orange curves are solutions with y less than a critical value $y^{(\text{crit})}$. These solutions either flow back to the asymptotic AdS region at $\mu = 0$ with a final value of Y that is less than ℓ, or they to the asymptotic AdS region at $\mu = \mu_*$. The blue curves are solutions with $y < y^{(\text{crit})}$. These solutions all flow back to the asymptotic AdS region $\mu = 0$ with a final value of Y that is greater than ℓ.

2.11.2 BCFT minimal surfaces in $d = 4$

As in the ICFT case, for each $\ell > 0$ there is an infinite family of minimal surfaces satisfying the initial condition $Y(0) = \ell$. We have plotted this family for the case $\ell = 1$ in figure 2.10.

Again, we have identified two subfamilies with colors orange and blue which correspond to solutions with $y < y^{(\text{crit})}$ and $y > y^{(\text{crit})}$ respectively. In addition, we have plotted a purple curve that corresponds to $y = y^{(\text{crit})}$. This curve is the analog of the $d = 2$ circular solution $Y(\mu) = \ell$ in that it is the unique solution reaching the singularity given the initial data $Y(0) = \ell$.

2.11.3 Holographic entanglement entropy for critical solution

In this section we will calculate the holographic entanglement entropy for the critical BCFT curve obtained in the previous section. The entanglement entropy for an RG flow geometry $f(\mu)$ and the critical curve $Y(\mu)$ is given by

$$S = \frac{L^2}{4G_N^{(5)}} \int_{\mu_\varepsilon}^{\mu_*} d\mu \, \frac{f(\mu)^{3/2}}{Y(\mu)^3} \sqrt{Y(\mu)^2 + Y'(\mu)^2}, \tag{2.19}$$

where as in the case $d = 2$, $\mu_\varepsilon = \varepsilon/\ell$ for small ε. Due to the singular behavior of f near $\mu = 0$, the expression for S is divergent. Using the expansion around $\mu = 0$ given in eq (2.12) and (2.14), one can extract the divergent pieces, and one finds that there is a quadratically divergent and logarithmically divergent contribution with respect to the cutoff ε. One can define a regular, finite part of the entanglement entropy by subtracting the appropriate divergent terms and then taking $\varepsilon \to 0$;

$$S_{\text{reg}} = \lim_{\varepsilon \to 0} \left[\frac{L^2}{4G_N^{(5)}} \left(\int_{\mu_\varepsilon}^{\mu_*} d\mu \, \frac{f(\mu)^{3/2}}{Y(\mu)^3} \sqrt{Y(\mu)^2 + Y'(\mu)^2} - \frac{1}{2\varepsilon^2} + \frac{\beta_-^2}{3\ell^2} \log \frac{\ell}{\varepsilon} \right) \right]. \tag{2.20}$$

Note that the logarithmically divergent term depends on the source β_- of the operator deformation. We have evaluated the subtracted finite part of the entanglement entropy as a function of ℓ and β_-. The numerical results for S_{reg} are well approximated by a $1/\ell^2$ dependence for any value of β_-. This was to be expected since the only dimensionful parameter on

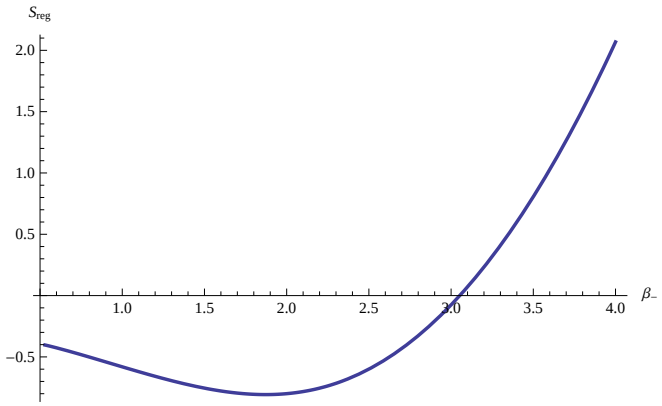

Figure 2.11: The subtracted finite entanglement entropy as a function as a function of β_- for fixed $\ell = 2$.

which S_{reg} can depend is the strip width ℓ, and the dependence must be $1/\ell^2$ as can be seen from (2.20). The dependence on the operator source is more complicated and reasonably well-approximated by a quadratic polynomial in β_-. A representative plot is presented in Figure 2.11. It is an open and interesting question whether either the logarithmically divergent or finite term are universal and can be interpreted analogously to the g-factor in the $d = 2$ system. Note that the integration constant β_- determines the value of μ where the geometry becomes singular and is therefore equivalent to the tension of the cut-off brane in the Takayanagi realization of BCFT. We leave investigations of these questions for future work.

2.12 Discussion

In this paper we have constructed a new holographic description of interface and boundary CFTs utilizing an AdS-slicing ansatz for a holographic RG-flow. In the discussion we compare and contrast this construction with other approaches developed recently in the literature. The construction of Takayanagi et al [181, 101] (see [138] for an earlier, closely related construction) also uses an AdS_d slicing of AdS_{d+1} like that given in (2.8). The bulk space

is cut off by the presence of a brane with AdS_d world volume at a fixed value of μ, which is determined by the tension of the brane via matching conditions. In the RG-flow solutions found in the present paper the brane is replaced by the singularity where $f = 0$. For the RG-flow solution, the minimal surface that is used for the calculation of the entanglement entropy is uniquely determined by the strip width ℓ on the boundary. This is to be contrasted with the calculation of the entanglement entropy in [101], where there is a one-parameter family of extremal surfaces where the minimal area solution is used to calculate the entanglement entropy.

The BCFT RG-flow solutions develop curvature singularities, hence the supergravity approximation, which is only valid for small curvatures, breaks down near the singularity. This behavior is similar to what is found in many Poincaré-sliced RG-flow solutions corresponding to relevant operator deformations such as the GPPZ flow [111]. The interpretation of the Poincaré RG-flow is that the theory becomes massive and is in a gapped phase. Nevertheless, calculations of correlations functions, Wilson loops and entanglement entropy are possible as long as the results are dominated by the region far away from the singularity. We followed the same assumption in the calculation of the entanglement entropy for the AdS-sliced BCFT RG flows presented in this paper.

In some cases the singularities can be resolved by lifting the solution to higher dimensions (see for example the discussion of the Coulomb branch in $\mathcal{N} = 4$ SYM given in [144, 140, 100]). Another example of regular BCFT solutions in six-dimensional supergravity corresponding to a backreacted solution of self-dual strings ending on three branes in six-dimensions was found in [61].

As already remarked in [82], in contrast to the Poincaré-sliced RG flows, it is not possible to explicitly integrate the AdS-sliced RG equations of motion in a first order form based on super potential. Therefore the only solutions we were able to find were numerical. It is an interesting question whether it is possible to find analytic solutions as these would

be very useful for, e.g. the holographic calculation of correlation functions in the BCFT. One approach to construct exact solutions, which has been very fruitful in the past, is to solve BPS conditions for the existence of backgrounds which preserve a subset of super symmetries of the AdS vacuum. This approach has been very successful in constructing half BPS Janus solutions in type IIB [83, 84], M-theory [85, 88] and six dimensional supergravity [60, 63, 62, 61]. It would be very interesting to explore these methods to construct BPS solutions for the the relevant deformations related to the ones in the present paper. If such solutions existed, they would correspond to new interface and boundary CFTs which preserved some superconformal symmetries. Exact solutions would also be important to go beyond the numerical evaluation of the entanglement entropy and hence clarify the physical interpretation of the divergent and finite terms in the entanglement entropy.

In 2-dimensional CFT renormalization group flows, ICFTs and BCFTs have also been discussed from a purely field theoretic point of view. For recent examples concerning flows of minimal model CFTs see e.g. [45, 98, **?**]. Note that in these examples the relevant perturbations do not have the $x_\perp$ dependence as the ones discussed in the present paper. A holographic description of $x_\perp$-independent BCFT flow will entail an ansatz that is different from the Janus ansatz used here. On the other hand it would also be interesting to study the $x_\perp$-dependent relevant perturbations on the field theory side. We leave this for investigation in future work.

Chapter 3

Warped entanglement entropy

Understanding how the holographic principle works beyond the example of anti-de Sitter space is a crucial and beautiful challenge which will elucidate the dynamics of quantum gravity in general backgrounds. A natural example is the geometry describing our universe, which is cosmological in nature, and more closely resembles an FRW/de Sitter type universe. As another example, the geometry describing regions near the horizons of certain astrophysical black holes is not quite anti-de Sitter space but more closely resembles a slight deformation thereof known as the NHEK/warped AdS_3 geometry. There have been several proposals for holographic descriptions of these and other non-AdS spacetimes [**?**, **?**, **?**], and the story is still unfolding.

In this paper we will focus on aspects of the warped AdS_3 geometry and its putative holographic description. As we will describe more concretely below, warped AdS_3 is a deformation of AdS_3 that destroys the boundary asymptotics. The deformation preserves only an $SL(2,\mathbb{R}) \times U(1)$ subgroup of the original $SL(2,\mathbb{R}) \times SL(2,\mathbb{R})$ isometry group of AdS_3. From the point of view of the two-dimensional CFT dual to AdS_3, the warping of AdS_3 corresponds to an irrelevant chiral deformation (which does not die away in the ultraviolet). Geometrically this manifests itself in the destruction of an asymptotically AdS_3 boundary.

Holographic considerations of this geometry began with [?]. Based on the thermodynamic properties of asymptotically warped AdS_3 black holes [161, ?, 160, 42], whose entropy could be written in a suggestive, Cardy-like fashion, it was proposed that it was dual to a two-dimensional conformal(-esque) field theory. Later work embedded and studied warped AdS_3 within string theory [12, 162, 176, 81, 94, 19, 139] and studied properties of two-dimensional field theories, dubbed warped CFTs, whose symmetry structure matches that of warped AdS_3 [129, 80]. Other work studied the wave equation, correlation functions and quasinormal modes of fields in warped AdS_3 [59, 58, 57, 13, 14]. Much of the work on warped AdS_3 has so far focused on thermodynamic properties of the theory and its asymptotic symmetry structure [71, 70]. In this paper we would like to focus instead on entangling properties of asymptotically warped AdS_3 geometries. We do so by exploiting the simple holographic manifestation of the entropy of entanglement of some state in a CFT as an extremal surface in the bulk geometry dual to such a state, as described by [134], generalizing [172, 171]. Though entanglement entropy is a simple property of the quantum state, it has sufficient information to independently verify features derived from the thermodynamics, such as central charges and left- and right-moving temperatures. It can also provide additional insight into the nature of the dual as we will shortly discuss. We now move on to briefly review the warped AdS_3 geometry and the holographic entanglement entropy proposal before summarizing our results and giving an outline of the paper.

3.1 Warped AdS_3

Consider AdS_3 expressed as a real-line or circle fibration over a Lorentzian AdS_2 base space. These geometries can be deformed with a nontrivial warp factor into the warped AdS_3 spacetimes we will consider later. The (spacelike) warped AdS_3 metric in global coordinates

with warp factor $a \in [0, 2)$ is given by[1]

$$ds^2 = \frac{\ell^2}{4}\left(-(1+r^2)\,d\tau^2 + \frac{dr^2}{1+r^2} + a^2(du + r\,d\tau)^2\right). \tag{3.1}$$

The coordinates range over the whole real line, $\{r, \tau, u\} \in \mathbb{R}^3$, although later we will consider compactifying u to recover a near-horizon extremal BTZ geometry. To obtain AdS_3, one sets $a = 1$. The conformal boundary in the case of $a = 1$ is the usual cylinder parsed by null coordinates and looks like a barber-shop pole; see Figure 3.1. The case $a \neq 1$ corresponds to spacelike warped AdS_3, which is the case we shall focus on in this paper. We will also comment on the timelike warped AdS_3 case, whose base space is Euclidean AdS_2, in Section 3.12. For $a \neq 1$ there is no conformal boundary [35], although a generalized notion of "anisotropic conformal infinity" can be defined [131]. We will also consider the geometries in Poincaré-like coordinates with metric

$$ds^2 = \frac{1}{4}\left(-\ell^2\frac{d\psi^2}{x^2} + \ell^2\frac{dx^2}{x^2} + a^2\left(d\phi + \ell\frac{d\psi}{x}\right)^2\right). \tag{3.2}$$

and coordinate ranges $\{\psi, x, \phi\} \in \mathbb{R}^3$.

These spacetimes posses $SL(2,\mathbb{R}) \times U(1)$ isometry for $a \neq 1$ and appear in a Penrose-like near-horizon limit of extremal black holes. In the context of a trivial warp factor $a = 1$, these geometries are locally AdS_3, and we expect the HRT proposal to apply. We will see that our results match field theory expectations, where the field theory is placed at zero left-moving temperature and finite right-moving temperature. This state of the field theory has not yet been considered in the holographic entanglement entropy literature, though it is closely related to the extremal limit of the rotating BTZ black hole, considered in [134].

[1] In the literature, usually in the context of topologically massive gravity, one often sees an alternative convention in which the metric is characterized by parameters $\tilde{\ell}$ and ν related to our parameters by $\tilde{\ell}^2 = \ell^2(\nu^2+3)/4$ and $a^2 = 4\nu^2/(\nu^2+3)$.

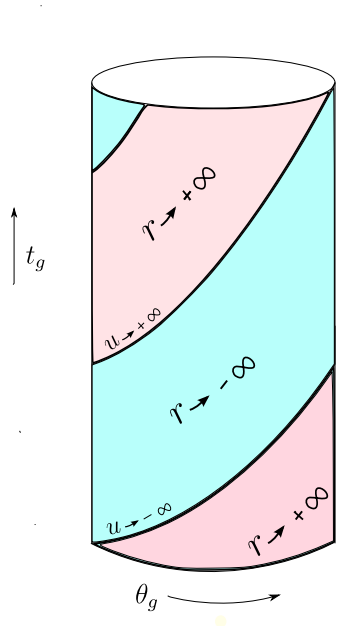

Figure 3.1: This is the global AdS_3 cylinder parameterized by the coordinates (3.1). The coordinates t_g and θ_g represent the usual global coordinates. We will primarily consider sticking to a region of the boundary with $r = \infty$ for simplicity. This figure is taken from [15].

For the case of nontrivial warp factor, the purported holographic duals of the spacetime are referred to as warped CFTs and possess $SL(2,\mathbb{R}) \times U(1)$ symmetry. This symmetry is automatically enhanced to two infinite-dimensional local symmetries [129]: the left-moving $SL(2,\mathbb{R})$ is enhanced to a left-moving Virasoro, while the right-moving $U(1)$ is enhanced to a left-moving $U(1)$ Kac-Moody current algebra (indeed, the term WCFT is used for the case that the $U(1)$ is *not* enhanced to a full Virasoro, which is also possible). Not much is known about these theories (a nontrivial example has only recently been suggested in [72]), but the symmetries can still be used to constrain properties that such a theory could have. This approach has been used successfully in reproducing a Cardy-like formula for the asymptotic growth of states in [80]. The bulk geometries are often considered in the context of topologically massive gravity, but for simplicity we shall restrict ourselves to the case where they are solutions of three-dimensional Einstein gravity with matter fields, as studied

in [93, 12, 81]. In string theory, for example, the warped geometries can be constructed by a hyperbolic, marginal deformation of the $SL(2,\mathbb{R})$ WZW model [136].

3.2 Holographic entanglement

The use of entanglement entropy to study quantum field theories continues to surge due to its relevance to quantum gravity and condensed matter physics and its analytic tractability. Holographically, this has been studied with the Ryu-Takayanagi (RT) proposal [172, 171] for computing the entanglement entropy via geometric methods in the bulk. The proposal now has support for multiple intervals in asymptotically AdS_3 bulk spacetimes [124, 122, 95] and spherical entangling surfaces in any dimension [51]. Strong arguments for the general case are provided in [152] and essentially prove the conjecture. Quantum corrections have been analytically computed in [32], with a general prescription appearing in [96]. Prescriptions for gravitational theories with higher curvature corrections are given in [135, 39, 102, 40, 177] and, for higher spin theories, in [8, 76]. The covariant Hubeny-Rangamani-Takayanagi (HRT) proposal [134] has far less support, though it has passed nontrivial consistency checks [47, 188]. It is natural to wonder how generally the proposal can apply. In this paper, we would like to take a few steps toward understanding the issues of holographic entanglement entropy in warped AdS_3 spacetime and two-dimensional warped conformal field theory ($WCFT_2$). The spacetimes we will study are non-static and will therefore require the covariant proposal. Although these spacetimes are often studied as solutions of topologically massive gravity, here we will consider the case where they are supported by Einstein gravity plus matter, allowing us to use the usual HRT proposal.

The goal of the HRT proposal in [134] is to obtain a holographic prescription for computing the entanglement entropy for time-varying states in QFTs with bulk duals which are non-static, asymptotically AdS spacetimes. To describe the proposal, we consider a $(d+1)$-

dimensional asymptotically AdS spacetime M with d-dimensional boundary ∂M, and we consider a field theory defined on this boundary. We choose a foliation of ∂M by spacelike hypersurfaces (time slices) $\widehat{M_t}$. For each time $t \in \mathbb{R}$, we write the slice $\widehat{M_t}$ as a union of disjoint sets A_t and B_t, and we can compute the entanglement entropy $S_{AB}(t)$ between the degrees of freedom in the two regions for a given state (density matrix) of the full system living on $\widehat{M_t}$.

The HRT proposal is as follows: for each time t, determine the co-dimension 2 extremal surfaces W_t satisfying $\partial W_t = \partial A_t$. If there is more than one extremal surface satisfying these boundary data, then choose the extremal surface $W_{t,\min}$ with smallest area. Then we have

$$S_{AB}(t) = \frac{\text{Area}(W_{t,\min})}{4G_N^{(d+1)}}. \tag{3.3}$$

The question of which homology class to consider is interesting in the context of the covariant proposal [133], but we will not need to consider it here. This is the correct expression for Einstein gravity coupled to matter, which are the theories we will consider here, although subleading corrections in G_N (bulk quantum corrections) will depend on the bulk matter supporting the geometry.

It is worth noting a rather remarkable feature of the above proposal (3.3). In the context of Einstein theories of gravity the entanglement entropy manifests itself in a purely geometric form at leading order in G_N, as the area of an extremal surface. This universal feature is particularly surprising, given that entanglement entropy is a property of the particular quantum state under consideration, which is generally a functional of all the bulk matter fields and not just the metric. It is reminiscent of the universality of the Bekenstein-Hawking entropy of a black hole, which also manifests itself as a geometric area in Einstein theories of gravity, regardless of the matter content that constitutes the black hole.

In our use of this formula, we will keep the slice chosen on the boundary arbitrary but

spacelike. Since we consider exclusively (2+1)-dimensional bulk geometries, this means that our entanglement entropy answers will be phrased in terms of two distinct coordinate separations, which can then be chosen to give a particular spacelike slice. We present the answers in this way because it makes the split into left-moving and right-moving sectors transparent; see (3.28) for one such example. It is important to note that the HRT prescription (and indeed the original Ryu-Takayanagi prescription) is computing the entanglement entropy between regions A_t and B_t defined by the unique geodesic along the *boundary* which connects the two points which define their separation. In other words, once one picks two points on the boundary to connect by a bulk geodesic, there remains an ambiguity in choosing the spacelike curves on the boundary which connect the two points and define the regions A_t and B_t. The holographic entanglement entropy prescription naturally picks the unique geodesic along the boundary which connects the two points as defining the spatial regions A_t and B_t.

To elaborate further, imagine applying the covariant proposal to the Poincaré patch of AdS_3 by picking points on the boundary that are spacelike separated but arbitrary. The length of the regulated bulk geodesic connecting these two points, divided by $4G_N$, is given in terms of CFT quantities as

$$S_{EE} = \frac{c}{3} \log \frac{\sqrt{L_x^2 - L_t^2}}{\epsilon} \,. \tag{3.4}$$

To match with the universal 2D CFT answer, we conclude that the region being picked out on the boundary theory is the geodesic along the boundary which connects the two points, since this curve has length $\sqrt{L_x^2 - L_t^2}$. The fact that in this example the spatial length at fixed time gets replaced with the invariant Minkowskian length is a result of Lorentz invariance. This will not be the case once we introduce a dimensionful scale, e.g. the radius of the cylinder for global AdS_3 or the temperature of a black hole.

3.3 Summary and outline

Although the validity of applying the HRT proposal to spacetimes with different asymptotics is an interesting open question,[2] in this paper we shall pursue a more modest goal. We will set up what is effectively a perturbation theory about the AdS_3 point by considering warping $a = 1+\delta$ and cutting off the $WAdS_3$ spacetime deep in the interior, where it is AdS_3-like. This can be understood as AdS/CFT in the presence of an infinitesimal, irrelevant deformation, a context in which holographic renormalization can be understood perturbatively in the deformation [182, 183].[3] Thus, attacking the problem in this way puts our analysis on firmer footing. We will see that such an approach gives sensible results, and in the regime of large separation in the fiber coordinate, the series can be summed to all orders in δ. The result is precisely that of two-dimensional CFT, with $c_L = c_R = 3\ell a/2G_N$. This exactly matches an independent proposal for the central charge, deduced by demanding consistency with the Cardy formula for two-dimensional CFTs [12]. We will also consider the warped BTZ black hole and again find universal CFT results which allow us to read off the left-moving and right-moving temperatures. Our central charge and temperatures altogether satisfy the Cardy formula and reproduce the entropy of the warped BTZ black hole.

In Section 3.4, we will apply the HRT proposal to locally AdS_3 spacetimes written as a fibration over a Lorentzian AdS_2 base space. In Section 3.7, we will deform these geometries into warped AdS_3 and set up the problem of applying the HRT proposal to these spacetimes. In Section 3.9, we will complete the problem by performing a perturbative application of the HRT proposal to warped AdS_3 geometries, where we will be perturbing around the locally AdS_3 geometries considered in Section 3.4. Finally, we will summarize and look toward future work in Section 3.15.

[2] We stress that calculations like the ones in [**?**], which consider a decoupled IR geometry, are still understood as occurring in an asymptotically AdS spacetime, as discussed in [174].

[3] For a specific implementation in Lifshitz backgrounds with $z = 1 + \epsilon$, see [142].

3.4 AdS_3 in fibered coordinates

We begin our story by considering AdS_3 in fibered Poincaré coordinates and fibered global coordinates. We will see that these coordinate systems are dual to states at zero left-moving and finite right-moving temperature, a feature reflected in the answer for the entanglement entropy. The geometry obtained by compactifying the fiber coordinate appears in a near-horizon limit of the extremal BTZ black hole. If the fiber coordinate remains uncompactified, the geometry is instead the near-horizon limit of a boosted extremal black string.

3.5 Poincaré fibered AdS_3

The metric (3.2) with $a = 1$ reduces to

$$ds^2 = \frac{1}{4}\left(-\ell^2\frac{d\psi^2}{x^2} + \ell^2\frac{dx^2}{x^2} + \left(d\phi + \ell\frac{d\psi}{x}\right)^2\right). \tag{3.5}$$

We choose this parameterization since all coordinates and ℓ can be assigned dimensions of length. Near the conformal boundary, the coordinates ϕ and ψ become null. We would like to determine the affinely parametrized geodesics $x^\mu(\lambda) = (x(\lambda), \phi(\lambda), \psi(\lambda))$. To do so, we notice that this geometry has Killing vectors ∂_ϕ and ∂_ψ, corresponding to translations in ϕ and ψ, and these Killing vectors yield conserved quantities $c_\phi = \dot{x}\cdot\partial_\phi$ and $c_\psi = \dot{x}\cdot\partial_\psi$. We will solve for the geodesics by using these conserved quantities and the affine constraint $c_v = \dot{x}^\mu\dot{x}_\mu$. This gives equations of motion

$$c_\phi = \frac{x\dot{\phi} + \ell\dot{\psi}}{4x}\,, \tag{3.6}$$

$$c_\psi = \frac{\ell\dot{\phi}}{4x}\,, \tag{3.7}$$

$$c_v = \frac{\ell^2\dot{x}^2 + x\dot{\phi}(x\dot{\phi} + 2\ell\dot{\psi})}{4x^2}\,. \tag{3.8}$$

The solutions to these equations are given in Appendix A.1.

We want to compute the length of a geodesic beginning and ending near the conformal boundary at $x_\epsilon \sim \epsilon^2/\ell$, where we have used the UV-IR relation to map our bulk IR cutoff x_ϵ to a dual UV field theory cutoff ϵ [179, 171]. This follows from the quadratic relationship between x and the usual Poincaré coordinate z near the conformal boundary, $x \sim z^2$. Since we chose our geodesics to be affinely parametrized, we can use the solution $x(\lambda)$ to solve for the cutoffs $\pm\lambda_\infty$ in the affine parameter defined by $x(\pm\lambda_\infty) = x_\epsilon$. The regulated length is then given by

$$\text{Length} = \sqrt{c_v}\int_{-\lambda_\infty}^{\lambda_\infty} d\lambda = 2\sqrt{c_v}\,\lambda_\infty, \tag{3.9}$$

which at the end will be c_v-independent, as required by parameterization-invariance of the length. Writing down the leading divergence of λ_∞ in terms of the conserved quantities c_ϕ, c_ψ and c_v gives

$$\lambda_\infty \approx \frac{\ell}{4\sqrt{c_v}}\log\left(\frac{c_v\,\ell\sqrt{4c_\phi^2 - c_v}}{4(c_v c\psi - 4c\phi^2 c\psi)}\,\frac{\ell}{\epsilon}\right), \tag{3.10}$$

we now attempt to trade the conserved quantities c_ϕ and c_ψ for spatial separations on the asymptotic boundary. This entails solving the equations

$$L_\phi \equiv \phi(\lambda_\infty) - \phi(-\lambda_\infty)\ , \qquad L_\psi \equiv \psi(\lambda_\infty) - \psi(-\lambda_\infty)\ , \tag{3.11}$$

to zeroth order in λ_∞ for c_ϕ and c_ψ in terms of L_ϕ and L_ψ. An important point about AdS_3 solutions, which we state here to contrast with the warped AdS_3 solutions of later sections, is that the "non-radial" coordinates (in this case ϕ and ψ) asymptote to constant values as the affine parameter diverges. In other words, one can safely take the limit $\lambda_\infty \to \pm\infty$

in either L_ϕ or L_ψ. The solutions to the geodesic equations of motion have two primary branches, which we call the "cosh-like" and "sinh-like" branches. We will consider the "cosh-like" branch, defined by $x(\lambda_\infty) = -x(-\lambda_\infty)$, although the "sinh-like" branch, defined by $x(\lambda_\infty) = x(-\lambda_\infty)$, can be handled analogously (see Appendix A.1 for details). Using $c = 3\ell/2G_N$, we find

$$S_{\text{EE}} = \frac{c}{3} \log \left(\frac{1}{\epsilon} \sqrt{L_\psi \, \ell \sinh\left(\frac{L_\phi}{2\ell}\right)} \right) . \tag{3.12}$$

We will comment in the next section on what ℓ, the curvature scale, is doing in a field-theory formula. Given that the geometry we are considering is simply a coordinate transformation of the usual Poincaré patch on AdS_3, we could have gotten this answer by performing the appropriate transformations on the usual Poincaré patch answer, $(c/3)\log(L/\epsilon)$. This method is easier since the Poincaré patch is globally static, allowing us to use the time-independent proposal, and the geodesics are semicircles. To see how such an approach works, see Appendix B. We will increasingly rely on using such coordinate transformations as we begin warping the spacetime in the later sections.

3.5.1 Interpretation

We can suggestively rewrite the answer for the entanglement entropy as

$$S_{\text{EE}} = \frac{c}{3} \log \frac{\sqrt{L_\psi \, \ell \sinh\left(\frac{L_\phi}{2\ell}\right)}}{\epsilon} = \frac{c}{6} \log \frac{L_\psi}{\epsilon} + \frac{c}{6} \log \left(\frac{\ell}{\epsilon} \sinh\left(\frac{L_\phi}{2\ell}\right) \right) . \tag{3.13}$$

This answer looks like the ground-state answer in the ψ direction and the finite-temperature answer in the ϕ direction, with the temperature being set by the curvature scale ℓ. Recall that ϕ and ψ are null coordinates on the conformal boundary, so these correspond to the left- and right-movers.

To investigate the dual state corresponding to this bulk geometry, we can write out the bulk metric near the boundary in the Fefferman-Graham expansion [97]:

$$ds^2 = \ell^2 \left(\frac{d\rho^2}{4\rho^2} + h_{ij}(x^i, \rho) dx^i dx^j \right), \qquad h_{ij}(x^i, \rho) = \frac{g^{(0)}_{ij}}{\rho} + g^{(2)}_{ij} + \dots \,. \tag{3.14}$$

In general, the boundary metric $g^{(0)}_{ij}$ determines the trace and covariant divergence of $g^{(2)}_{ij}$ through the equations of motion near the boundary as

$$\text{tr } g^{(2)} \equiv g^{(0)}_{ij} g^{(2)ij} = -\frac{1}{2} R[g^{(0)}_{ij}], \tag{3.15}$$

$$\nabla_i g^{(2)ij} = \nabla^j \text{ tr } g^{(2)}, \tag{3.16}$$

where the covariant derivative is with respect to the metric $g^{(0)}_{ij}$. The expectation value of the stress-energy tensor is then given by the variation of the renormalized on-shell action with respect to $g^{(0)}_{ij}$ [25, **?**], which in two boundary dimensions turns out to be

$$\langle T_{ij} \rangle = \frac{\ell}{8\pi G} \left(g^{(2)}_{ij} - g^{(0)}_{ij} \text{ tr } g^{(2)} \right). \tag{3.17}$$

For the usual Poincaré patch, we identify $g^{(2)}_{ij} = 0$, so we see that $\langle T_{ij} \rangle = 0$. However, for the Poincaré fibered coordinates, since $g^{(2)}_{\phi\phi} = 1/4$ we have

$$\langle T_{\phi\phi} \rangle = \frac{\ell}{32\pi G} = \frac{c}{48\pi} \tag{3.18}$$

with all other components vanishing (the tracelessness of the stress-energy tensor is preserved since $g^{(0)}_{\phi\phi} = 0$). Thus, we are not in the vacuum state of the dual theory and should not have expected to get the universal answer for the vacuum state, which in this case would have

been

$$S_{\rm EE} = \frac{c}{3}\,\log\,\frac{\sqrt{L_\psi L_\phi}}{\epsilon} \tag{3.19}$$

since lengths in the boundary metric are computed with $ds^2 = d\phi\, d\psi$. In fact, we do get the vacuum answer for the ψ-movers, which agrees with $\langle T_{\psi\psi}\rangle = \langle T_{\psi\phi}\rangle = 0$. The ϕ-movers are in an excited state, which agrees with $\langle T_{\phi\phi}\rangle \neq 0$. As it should, the bulk diffeomorphism that takes one from Poincaré coordinates to Poincaré fibered coordinates induces a conformal transformation on the boundary theory, and (3.18) is just what one obtains by conformally transforming the vanishing stress-energy tensor from Poincaré coordinates to Poincaré fibered coordinates.

Now that we have shown that the modes in the ψ direction are in their ground state and the modes in the ϕ direction are excited, the expression for the entanglement entropy is becoming a bit clearer. To make the finite-temperature interpretation more precise, we consider the metric (3.5) with compactified fiber coordinate:

$$ds^2 = \frac{1}{4}\left(-\ell^2\frac{d\psi^2}{x^2} + \ell^2\frac{dx^2}{x^2} + \left(d\phi + \ell\frac{d\psi}{x}\right)^2\right), \qquad \phi \sim \phi + 4\pi r_+\,. \tag{3.20}$$

This is precisely the geometry that appears in a Penrose-like near-horizon limit of the extremal BTZ black hole

$$ds^2 = -\frac{(r^2 - r_+^2)^2}{r^2\ell^2}dt^2 + \frac{\ell^2 r^2}{(r^2 - r_+^2)^2}dr^2 + r^2\left(d\phi - \frac{r_+^2}{\ell r^2}dt\right)^2, \tag{3.21}$$

which has dimensionless $J = M = \frac{2r_+^2}{\ell^2}$ and $S = 4\pi r_+$ in units where $8G = 1$. Defining left-moving and right-moving energies as

$$E_L \equiv M - J = 0, \qquad E_R \equiv M + J, \tag{3.22}$$

and dimensionless left-moving and right-moving temperatures as

$$T_L \equiv \ell \, \frac{\partial E_L}{\partial S} = 0 \,, \qquad T_R \equiv \ell \, \frac{\partial E_R}{\partial S} = \frac{r_+}{\pi \ell} \,, \tag{3.23}$$

we see that the state dual to the background (3.5) is at zero left-moving temperature and finite right-moving temperature. Though it is at zero Hawking temperature, the statistical degeneracy is explained by the Cardy formula and the nonvanishing right-moving temperature:

$$S = \frac{\pi^2}{3}(c_L T_L + c_R T_R) = \frac{\pi^2}{3} \frac{3\ell}{2G_N} \frac{r_+}{\pi \ell} = 4\pi r_+ \,, \tag{3.24}$$

which matches the area of the horizon in coordinates (3.20) or (3.21). We have used $8G_N = 1$ to get to the final expression.

Notice that our answer (3.13) applies for the geometry with compact fiber coordinate (3.5) as long as we consider small L_ϕ. With the thermodynamic language developed above, we can define $\tilde{\phi} = \phi/(2r_+)$, $\tilde{\psi} = r_+\psi/\pi\ell = \psi/\beta_R$ and rewrite the second piece in (3.13) as

$$\frac{c}{6} \log\left(\frac{\ell}{\epsilon} \sinh\left(\frac{L_\phi}{2\ell}\right)\right) \longrightarrow \frac{c}{6} \log\left(\frac{\beta_R}{\epsilon} \sinh\left(\frac{\pi \, L_{\tilde{\phi}}}{\beta_R}\right)\right) , \tag{3.25}$$

where $\tilde{\phi} \sim \tilde{\phi} + 2\pi$ and the first term in (3.13) remains unchanged. The UV-IR relation is fixed to match onto the ground state answer in the limit of small $L_{\tilde{\phi}}$. So we have seen that the entanglement entropy answer for the geometry with a compact fiber coordinate reflects the fact that the right-movers are at finite right-moving temperature.

We pause for a moment to connect to an existing result in the literature, which is the calculation of entanglement entropy in the state dual to the rotating BTZ black hole [134].

Taking the extremal limit of their result, $\beta_R \to \infty$, one finds

$$S_{\text{EE}} = \frac{c}{6} \log \frac{L}{\epsilon} + \frac{c}{6} \log \left(\frac{\beta_R}{\epsilon} \sinh \left(\frac{\pi L}{\beta_R} \right) \right) \tag{3.26}$$

for purely spatial separation on the boundary. This is precisely our answer with $L_{\tilde{\phi}} = L_{\tilde{\psi}} = L$. It seems that the IR limit we have taken to get to the geometry (3.20) has retained the entangling properties of the dual state.

Now we would like to take the limit where the geometry decompactifies, i.e. $r_+/\ell \to \infty$, since this allows us to recover our original geometry (3.5). Notice that in this limit, we are going from having two scales, ℓ and r_+, to just one scale ℓ. Thus, all dimensionful parameters must be measured relative to ℓ.[4] Looking at the left-hand-side of (3.25), we see that this means that the argument of the sinh must remain fixed in this limit, since we want to keep L_ϕ (in units of ℓ) fixed. Expressed in terms of the CFT quantities on the right-hand-side of (3.25), we are taking β_R small with $L_{\tilde{\phi}}/\beta_R$ fixed. We therefore retain the interpretation of the right-movers being at finite temperature in the decompactification limit. With compact fiber coordinate, the expression (3.13) can be understood in relation to the DLCQ limit which freezes the ψ-movers to their ground state [24].

To aid with understanding taking arbitrary spacelike slices, we note here that the expression for the length of an extremal geodesic in the rotating BTZ background for arbitrary spacelike separation on the boundary can be written:

$$S_{EE} = \frac{c}{6} \log \left[\frac{\beta_L \beta_R}{\pi^2 \epsilon^2} \sinh \left(\frac{\pi \Delta x_L}{\beta_L} \right) \sinh \left(\frac{\pi \Delta x_R}{\beta_R} \right) \right] \tag{3.27}$$

$$= \frac{c}{6} \log \left[\frac{\beta_L}{\pi \epsilon} \sinh \left(\frac{\pi \Delta x_L}{\beta_L} \right) \right] + \frac{c}{6} \log \left[\frac{\beta_R}{\pi \epsilon} \sinh \left(\frac{\pi \Delta x_R}{\beta_R} \right) \right] \tag{3.28}$$

for $x_L = \phi + t$ and $x_R = \phi - t$. Again, the contribution to the entanglement entropy splits up

[4] The role of the lattice spacing ϵ will not be important for this argument.

into distinct contributions from the left- and right-moving sectors. This is analogous to how the contribution to the thermodynamic entropy splits into left- and right-moving sectors in the Cardy formula.

3.6 Global fibered AdS_3

The global fibered AdS_3 metric is obtained by setting $a = 1$ in (3.1) to obtain

$$ds^2 = \frac{\ell^2}{4}\left(-(1+r^2)\,d\tau^2 + \frac{dr^2}{1+r^2} + (du + r\,d\tau)^2\right). \tag{3.29}$$

All coordinates are dimensionless while ℓ has dimensions of length. The coordinates u and τ become null near the part of the boundary reached by $r \to \pm\infty$, which is the region to which we shall restrict our attention; see Figure 3.1 for the precise parameterization of the boundary cylinder in these coordinates. One can write conservation equations for affinely parameterized geodesics just like in the Poincaré fibered case. In this case, we label the conserved quantities corresponding to translations in τ and u by c_τ and c_u respectively, while $c_v = \dot{x}^\mu \dot{x}_\mu$. After some manipulation, the conservation equations can be written as follows:

$$\dot{r}^2 = \left(\frac{c_v}{(\ell/2)^2}\right) r^2 - \left(\frac{2c_u c_\tau}{(\ell/2)^4}\right) r - \frac{c_u^2 - c_\tau^2 - (\ell/2)^2 c_v}{(\ell/2)^4}\,, \tag{3.30}$$

$$\dot{\tau} = \frac{c_u}{(\ell/2)^2}\frac{r}{r^2+1} - \frac{c_\tau}{(\ell/2)^2}\frac{1}{r^2+1}\,, \tag{3.31}$$

$$\dot{u} = \frac{c_\tau}{(\ell/2)^2}\frac{r}{r^2+1} + \frac{c_u}{(\ell/2)^2}\frac{1}{r^2+1}\,. \tag{3.32}$$

Imposing the condition $c_v > 0$ ensures that the geodesics determined by these equations are spacelike. For equation (3.30), there are "cosh-like" and "sinh-like" solution branches according to whether $c_u^2 - c_v(\ell/2)^2 > 0$ and $c_u^2 - c_v(\ell/2)^2 < 0$, respectively. The solutions

are presented in Appendix A.2.

We now wish to calculate the leading divergent piece of the length of these geodesics. The approach is identical to the previous section, so we will not repeat the details here. Using the UV-IR relation $r_\infty \sim \epsilon^{-2}$ for dimensionless cutoff ϵ, we find

$$\lambda_\infty \approx \frac{(\ell/2)}{\sqrt{c_v}} \log\left(\frac{c_v(\ell/2)^2}{\sqrt{(c_u^2 - c_v(\ell/2)^2)(c_\tau^2 + c_v(\ell/2)^2)}}\frac{1}{\epsilon^2}\right). \tag{3.33}$$

We can now trade in the conserved quantities c_u and c_τ for coordinate separations L_u and L_τ on the boundary and recover

$$S_{\text{EE}} = \frac{c}{3}\log\left(\frac{1}{\epsilon}\sqrt{\sin\left(\frac{L_\tau}{2}\right)\sinh\left(\frac{L_u}{2}\right)}\right). \tag{3.34}$$

We will stick to $L_\tau < 2\pi$ on the boundary to maintain spacelike separation between the two endpoints (τ is a null coordinate that winds up the cylinder). Just as in the Poincaré fibered case (3.12) we see that the u-moving sector seems to be at finite temperature, with the temperature scale set by ℓ (recall that our coordinate u is dimensionless), while the τ-moving sector is in its ground state. The appearance of the sine function is simply from the compact $U(1)$ of the global AdS_3 cylinder. One can perform a Fefferman-Graham analysis by repeating the steps of Section 3.5.1, but the details are the same and we omit them here.

The result for the "sinh-like" branch is similar:

$$S_{\text{EE}} = \frac{c}{3}\log\left(\frac{1}{\epsilon}\sqrt{\cos\left(\frac{L_\tau}{2}\right)\cosh\left(\frac{L_u}{2}\right)}\right). \tag{3.35}$$

Notice that the length remains well-defined when $L_u \to 0$ and $L_\tau \to 0$, as it should since the geodesic is going through the bulk from $r = -\infty$ to $r = \infty$ in this limit. We mention this branch due to its relevance to the metric (3.1) with compact fiber coordinate. This is the self-dual orbifold considered first in [73] and studied extensively in [24, 27]. The

geometry is locally AdS_3 and has an AdS_2 factor, but a compact fiber coordinate causes the two boundaries at $r = +\infty$ and $r = -\infty$ to become disconnected, though they are *causally connected* through the bulk. The entanglement between the asymptotic boundaries was computed via a reduction to AdS_2/CFT_1 in [20]. Our answer can be used to compute quantities like the holographic thermo-mutual information (HTMI) in these horizon-less backgrounds, as defined in [159], directly in AdS_3.

3.7 Spacelike $WAdS_3$

We have seen in the previous sections how to apply the covariant HRT proposal to locally AdS_3 spacetimes written as a real-line fibration over AdS_2. The results agree with the universal CFT_2 answers for a state at zero left-moving temperature and finite right-moving temperature. We now move on to the case of nontrivial warping. We will set up the problem with general warping parameter $a \neq 1$ and only specify our peturbative expansion about AdS_3 with $a = 1 + \delta$ at a later point in our analysis.

3.8 Global coordinates analysis

We consider the metric (3.1), and we determine the affinely parameterized geodesics $x^\mu(\lambda) = (\tau(\lambda), u(\lambda), r(\lambda))$ in this geometry. The metric has Killing vectors ∂_τ and ∂_u corresponding to translations in τ and u, and they yield conserved quantities $c_\tau = \dot{x} \cdot \partial_\tau$ and $c_u = \dot{x} \cdot \partial_u$, respectively. Since we consider affinely parameterized geodesics, the square speed $c_v = \dot{x}^\mu \dot{x}_\mu$

along the geodesic is also conserved. The corresponding conservation equations are

$$c_\tau = (\ell/2)^2 \left(a^2 r \left(r\dot{\tau} + \dot{u}\right) - \left(r^2+1\right)\dot{\tau}\right), \tag{3.36}$$

$$c_u = (\ell/2)^2 a^2 \left(r\dot{\tau} + \dot{u}\right), \tag{3.37}$$

$$c_v = \frac{(\ell/2)^2 \left[-\left(r^2+1\right)^2 \dot{\tau}^2 + a^2\left(r^2+1\right)\left(r\dot{\tau}+\dot{u}\right)^2 + \dot{r}^2\right]}{r^2+1}. \tag{3.38}$$

To solve these equations, it helps to manipulate them into the following form:

$$\dot{r}^2 = -\left(\frac{c_u^2(1-a^2) - (\ell/2)^2 a^2 c_v}{(\ell/2)^4 a^2}\right) r^2 - \left(\frac{2c_u c_\tau}{(\ell/2)^4}\right) r - \frac{c_u^2 - a^2 c_\tau^2 - (\ell/2)^2 a^2 c_v}{(\ell/2)^4 a^2}, \tag{3.39}$$

$$\dot{\tau} = \frac{c_u}{(\ell/2)^2}\frac{r}{r^2+1} - \frac{c_\tau}{(\ell/2)^2}\frac{1}{r^2+1}, \tag{3.40}$$

$$\dot{u} = \frac{c_\tau}{(\ell/2)^2}\frac{r}{r^2+1} + \frac{c_u}{(\ell/2)^2 a^2}\frac{1}{r^2+1} + \frac{c_u}{(\ell/2)^2}\left(\frac{1-a^2}{a^2}\right)\frac{r^2}{r^2+1}. \tag{3.41}$$

Equation (3.39) is now a decoupled, separable differential equation that can be integrated to determine $r(\lambda)$. The solution to (3.39) can then be plugged into equations (3.40) and (3.41), which can be integrated to obtain $\tau(\lambda)$ and $u(\lambda)$, respectively. Notice also that setting $a = 1$ in these equations gives the system of equations (3.30), (3.31), and (3.32). The equations become a-independent in the limit $c_u = 0$, though such a limit does not seem particularly useful for understanding warped AdS_3; see Appendix A.3.1. The general solutions to these equations can be found in Appendix A.3. We simply note here that the solution for $u(\lambda)$ has a piece that grows linearly with λ, unlike in the AdS_3 case. This means that the relation between c_u and L_u will necessarily involve λ_∞. This complicates the analysis, as we shall see shortly.

Let us focus on the "cosh-like" branch with $0 < a < 2$ and fix $c_v = 1$. This includes the squashed and stretched cases. In our approach, we first write the length of the geodesic in

terms of the conserved quantities and the cutoff in the holographic coordinate r:

$$\lambda_\infty = \frac{1}{\sqrt{c_1}} \cosh^{-1}\left[\frac{-c_2 + 2c_1 r_\infty}{\sqrt{c_2^2 + 4c_1 c_3}}\right], \tag{3.42}$$

where we have used the definitions in (A.17) and require $c_1 > 0$. This expression holds for general warping a as well as for the AdS_3 case of $a = 1$ (the a-dependence is buried in c_1 and c_3). Taking $c_1 r_\infty \gg c_2$ and restoring the original constants of motion c_u and c_τ gives[5]

$$\lambda_\infty \approx \frac{\log\left[\frac{c_1 r_\infty}{\sqrt{c_2^2+4c_1c_3}}\right]}{\sqrt{c_1}} = \frac{\log\left[r_\infty \frac{a^2(1+c_u^2)-c_u^2}{\sqrt{(-a^2+c_u^2)(a^2(1+c_\tau^2+c_u^2)-c_u^2)}}\right]}{\sqrt{1+(1-1/a^2)c_u^2}}, \tag{3.43}$$

where we have set $c_v = \ell/2 = 1$. Although the geodesic equations for $r(\lambda)$, $\tau(\lambda)$, and $u(\lambda)$ are soluble, to write the answer for the length in terms of coordinate separations on an asymptotic boundary (instead of in terms of conserved quantities as done above) there remains the task of inverting limits of those solutions to obtain the conserved quantities c_u and c_τ in terms of separations on the boundary L_u and L_τ. The equation for the τ coordinate is simply generalized from the AdS case:

$$c_\tau = \sqrt{c_1}\cot\left(\frac{L_\tau}{2}\right) = \sqrt{\frac{c_u^2(a^2-1)+a^2}{a^2}}\cot\left(\frac{L_\tau}{2}\right), \tag{3.44}$$

which holds as long as $L_\tau < \pi$. The new feature in these spacetimes, which is different from asymptotically AdS spacetimes, is that the relation between c_u and L_u involves λ_∞:

$$2\left(-1+\frac{1}{a^2}\right)c_u\lambda_\infty + \log\left(\frac{c_u + \sqrt{1+c_u^2-\frac{c_u^2}{a^2}}}{c_u - \sqrt{1+c_u^2-\frac{c_u^2}{a^2}}}\right) = L_u\,. \tag{3.45}$$

In other words, one cannot keep both c_u and L_u fixed as the cutoff is scaled large. This

[5] One cannot in general be so cavalier in taking $c_1 r_\infty \gg c_2$ without any restrictions on L_u, since c_2 depends on c_u, which depends on λ_∞. In our case, however, this can be consistently realized by taking $r_\infty \gg 1$.

follows directly from the linear divergence of $u(\lambda)$ with λ, as would occur in an $AdS_2 \times \mathbb{R}$ background. One could at this point try to proceed by solving for c_u in terms of L_u and λ_∞ and plug c_u and c_τ into (3.43). This would then be an equation for λ_∞ that can be solved to determine the length. Unfortunately, such an approach has two obstacles, one conceptual and one technical. The conceptual obstacle is that this would correspond to fully applying the HRT proposal in an asymptotically warped AdS_3 spacetime, and it is unclear whether such a prescription makes sense. The technical obstacle (at least in this approach) is that (3.45) is a transcendental equation for c_u. In the case of $AdS_2 \times \mathbb{R}$, which can be realized as the $a \to 0$ limit of warped AdS_3, the left-hand-side of the analog of (3.45) has only the piece linear in λ_∞ and such a method can be carried out.

In the next section, we will show that setting up a perturbative expansion about the AdS_3 point by considering warping parameter $a = 1 + \delta$ will allow us to solve this equation order-by-order in δ.

3.9 Perturbative entanglement entropy

Given that a nonperturbative application of the HRT prescription to asymptotically warped AdS_3 spacetimes is suspect, here we will try to infinitesimally perturb around the AdS_3 point and use the AdS/CFT dictionary, which presumably contains as one of its entries the HRT prescription. Deep in the IR, the geometry (3.1) is close to AdS_3, and it is only in the UV that the nontrivial warping parameter begins to destroy the asymptotics. If we cut off our spacetime before this happens, then we are at low enough energies where our analysis will be on firmer ground. Viewed in this way, we have a conformal field theory which we perturb by an infinitesimal, irrelevant operator. Holographic renormalization can then be understood perturbatively in this infinitesimal source [182, 183]. We will find that in a certain limit we can sum the perturbative expansion to *all* orders. The resulting answer takes the precise

form of a two-dimensional CFT and reproduces the warping-dependent central charge and left- and right-moving temperatures postulated previously in the literature.

3.10 Perturbative expansion

We imagine that the warping parameter is close to 1, i.e. $a = 1 + \delta$ for $|\delta| \ll 1$. It is in this sense which we expand about the AdS_3 point $a = 1$. Such a perturbative expansion will help us solve (3.45) for c_u order-by-order in δ. The solutions below follow a simple pattern at each order, and though we list the general formulae for arbitrary order, we have technically only checked that they are true to tenth order. Expanding

$$c_u = c_{u,0} + \delta\, c_{u,1} + \delta^2 c_{u,2} + \cdots\,, \tag{3.46}$$

we solve (3.45) to get

$$c_{u,0} = (\ell/2)\coth\frac{L_u}{2}\,, \tag{3.47}$$

$$c_{u,1} = \frac{1}{2}((\ell/2) - 4\lambda_\infty + (\ell/2)\cosh L_u)\coth\frac{L_u}{2}\,\mathrm{csch}^2\frac{L_u}{2}\,, \tag{3.48}$$

$$c_{u,n} = \left(\sum_{j=0}^{n-1}\sum_{i=0}^{n}\lambda_\infty^i(\ell/2)^{n-i}k_{ij}^{(n)}\cosh(jL_u)\right)\coth\frac{L_u}{2}\,\mathrm{csch}^{2n}\frac{L_u}{2}\,; \qquad n>1\,, \tag{3.49}$$

where the $k_{ij}^{(n)}$ are calculable n- and λ_∞-dependent constants. We require $|\delta^n\, c_{u,n}| \ll |\delta^{n-1} c_{u,n-1}|$ to assure convergence of our perturbative expansion. This can be satisfied by taking

$$L_u \gtrsim 1\,, \qquad |\lambda_\infty\,\delta| \ll 1\,. \tag{3.50}$$

L_u is being measured in units of ℓ. The latter condition ensures that we stay in an AdS_3-like part of the geometry and not get into the $WAdS_3$ asymptotic. Notice that from the point of view of perturbing about AdS_3, this is an eminently sensible condition; regardless of how small one takes δ, the geometry looks wildly different from AdS_3 for sufficiently large λ_∞, so we need to constrain their product. Incidentally, the curvature invariants of $WAdS_3$ are all finite and continuously connected to the AdS_3 case $a = 1$, so they are not a good way to classify where to cut off the spacetime for a well-defined perturbation theory. When computing the length, we keep only the leading divergent piece (in r_∞) at each order. This gives the following result for the entanglement entropy:

$$S_{\text{EE}} = \frac{\ell}{4G_N}\left[\left(1+\delta\coth^2\frac{L_u}{2}\right)\log\left(r_\infty \sin\frac{L_\tau}{2}\sinh\frac{L_u}{2}\right)\right] + \\ \frac{\ell}{4G_N}\sum_{i=2}^{\infty}\delta^i\,(-1)^{i+1}\coth^2\frac{L_u}{2}\operatorname{csch}^{2(i-1)}\frac{L_u}{2}\left[\log\left(r_\infty \sin\frac{L_\tau}{2}\sinh\frac{L_u}{2}\right)\right]^i\left(\sum_{j=0}^{i-2}c_{ij}\cosh(jL_u)\right). \tag{3.51}$$

The constants c_{ij} are all positive. Notice that the zeroth order piece is precisely the answer for AdS_3 given in (3.34), as it should be. Unfortunately, the series does not seem simply summable unless we take the scaling limit $L_u \gg 1$, in which case we use our knowledge of the c_{ij} and sum the series to get

$$S_{\text{EE}} = \frac{\ell}{4G_N}\left[(1+\delta)\log\left(r_\infty \sin\frac{L_\tau}{2}\sinh\frac{L_u}{2}\right)\right] - \\ \frac{\ell}{4G_N}\,e^{-L_u}\left[-1+4\delta\log\left(r_\infty \sin\frac{L_\tau}{2}\sinh\frac{L_u}{2}\right)+e^{-4\delta\log\left(r_\infty \sin\frac{L_\tau}{2}\sinh\frac{L_u}{2}\right)}\right] \tag{3.52}$$

to leading order in L_u. Notice that the first two terms in the second line are suppressed by a factor of e^{-L_u} relative to the first line and can safely be dropped. Up to an overall constant,

the last term in the second line can be written as

$$\left(\sin\frac{L_\tau}{2}\right)^{-4\delta}\left(r_\infty^{-4\delta}e^{-L_u(1+2\delta)}\right). \tag{3.53}$$

For $\delta > 0$, this is suppressed relative to the first line without further qualification and can be dropped. For $\delta < -1/2$, this term grows with L_u and cannot be neglected. However, for $-1/2 < \delta < 0$, there is a competition between the factor containing $r_\infty \sim e^{\lambda_\infty} \gg 1$ and the factor containing $L_u \gg 1$. In this regime, for a given δ and r_∞, one simply needs to choose L_u sufficiently large ($L_u(1+2\delta) \gg -4\delta\lambda_\infty$) such that the resulting expression is dominated by the expression in the first line.

By combining these observations, we find that if $\delta > -1/2$, then the leading behavior of the entanglement entropy in the large-L_u regime is

$$S_{\text{EE}} = \frac{\ell}{2G_N}(1+\delta)\log\left(\frac{1}{\epsilon}\sqrt{\sin\frac{L_\tau}{2}\exp\left(\frac{L_u}{2}\right)}\right), \tag{3.54}$$

where we have used the UV-IR relation $r_\infty \sim 1/\epsilon^2$. Since we are sourcing an infinitesimal irrelevant operator and computing perturbatively, the UV-IR relation used should remain that of AdS/CFT. We have also replaced the hyperbolic sine function with an exponential function, since corrections are subleading in our expansion in e^{-L_u}. As usual, numerical factors are absorbed into a redefinition of the cutoff ϵ.

We see that for $a = 1+\delta$, the perturbative expansion in the large-L_u gives simply the two-dimensional CFT answer of (3.34) upon identifying the coefficient of the logarithm with $c/3$:

$$c_L = c_R = \frac{3\ell}{2G_N}(1+\delta)\,. \tag{3.55}$$

The equality of c_L and c_R is due to a lack of diffeomorphism anomaly, since we are working

in Einstein gravity. These are precisely the central charges of [12], conjectured by demanding consistency with the Cardy formula (we will reproduce this check in Section 3.14).[6] One of these central charges has been produced through an asymptotic symmetry group analysis [69]. Identifying the functional form of S_{EE} with the AdS_3 result (3.34) allows us to conclude that the dual state lives on a cylinder charted by null coordinates τ and u.

It is important to keep in mind that the entanglement entropy computed in (3.54) is understood as an expansion to zeroth order in e^{-L_u} but to *all* orders in δ. This approach can in principle be extended to lower orders in L_u, and the appearance of the logarithmic term in our general formulae suggests that the answer will remain roughly in the form of the CFT_2 answer, except the logarithm will have an L_u-dependent prefactor. This is consistent with the existence of a single Virasoro algebra, since it seems the answer only picks up additional u-dependence while keeping the τ-dependence the same. Our result at leading order in e^{-L_u} seems to suggest that warped CFTs behave like ordinary CFTs in the IR, for large L_u. The IR restriction is due to cutting off our spacetime deep in the bulk and is independent of the large L_u restriction. The similarity to CFT_2 jibes well with the fact that the deep interior of the $WAdS_3$ geometry is AdS_3-like. We will discuss the physical meaning of large L_u in Section 3.13. We will also go beyond the small warping limit in Section 3.14 by arguing that warped CFTs are CFT-like generally, as long as one takes an infrared limit and studies large L_u.

Performing the same perturbative expansion in the case of Poincaré coordinates would give a result that can be obtained simply by coordinate transforming our current answer as

[6] To facilitate comparison with the notation of [12], one should take $a^2 \to \beta^2$ and $\ell^2 \to (4-\beta^2)\ell^2/3$. Notice that as $\beta^2 \to 4$, which is the limit in which the central charge of [12] vanishes, there is an infinite rescaling that allows our central charge to remain finite.

in Appendix B.2, and it is given by

$$S_{\text{EE}} = \frac{\ell}{2G_N}(1+\delta)\log\left(\frac{1}{\epsilon}\sqrt{L_\psi \ell \exp\left(\frac{L_\phi}{2\ell}\right)}\right). \tag{3.56}$$

This is again the appropriate answer at large L_ϕ for a two-dimensional CFT, now on the Minkowski plane charted by null coordinates ϕ and ψ, as presented in (3.12). Taking the fiber coordinate L_u large in the global coordinate system corresponds to taking the fiber coordinate L_ϕ large in Poincaré coordinates. In the case of Poincaré coordinates, however, we can simultaneously take L_ψ large if we want to consider a particular time slice $L_\phi = L_\psi$.

Due to the convergence of the perturbative expansion for any warping parameter $a > 1/2$ in the large fiber-coordinate regime, we conjecture that the nonperturbative answer for the entanglement entropy for a state at zero left-moving temperature and finite right-moving temperature, in the large fiber-coordinate regime, is given by (3.56) for a state on the plane or (3.54) for a state on the cylinder. We will expound on this conjecture in Section 3.14 after providing some more evidence for our approach. However, we will henceforth use the nonperturbative parameter a in our formulae.

3.11 Finite temperature

In the limit of large separation in the fiber coordinate, we can match our results with those of two-dimensional CFT even at finite temperature. Since black holes in warped AdS_3 are given by discrete quotients of the vacuum spacetime, they are locally warped AdS_3 [16]. This is analogous to BTZ black holes in AdS_3. Due to the local equivalence, we can exhibit local coordinate transformations that take us from the geometry with a black hole to the geometry without a black hole. We will stick to the stretched case $a > 1$ to avoid closed

timelike curves. The metric for the warped BTZ black hole is given by

$$\frac{ds^2}{\ell^2} = \frac{3dt^2}{4-a^2} + \frac{dr^2}{4(r-r_+)(r-r_-)} + \frac{6\sqrt{3}}{(4-a^2)^{3/2}}\left(ar - \sqrt{r_+ r_-}\right) dt d\theta + \frac{9r}{(4-a^2)^2}\left((a^2-1)r + r_+ + r_- - 2a\sqrt{r_+ r_-}\right) d\theta^2 \,. \tag{3.57}$$

We will restrict to the stretched case $a > 1$ to avoid the presence of closed timelike curves at large radial coordinate. The answer for the entanglement entropy in a warped BTZ background can be reproduced by coordinate transforming our previous answer. The coordinate transformations can be found in Section 5 of [16]. Performing such a transformation to (3.54), we find

$$S_{\text{EE}} = \frac{\ell a}{G_N} \log\left(\frac{r_+ - r_-}{\epsilon^2} \exp\left(\sqrt{\frac{3}{a^2(4-a^2)}}\,\Delta t + \frac{\pi\Delta\theta}{\beta_L}\right) \sinh\frac{\pi\Delta\theta}{\beta_R}\right), \tag{3.58}$$

with dimensionless temperatures

$$\beta_L^{-1} = T_L = \frac{3}{2\pi(4-a^2)}\left(r_+ + r_- - \frac{2}{a}\sqrt{r_+ r_-}\right), \tag{3.59}$$

$$\beta_R^{-1} = T_R = \frac{3(r_+ - r_-)}{2\pi(4-a^2)} \,. \tag{3.60}$$

Due to the compactification of θ, there can exist many spacelike geodesics in this geometry, distinguished by their winding number and directionality. The expression $\Delta\theta$ refers to the separation in a noncompact θ, i.e. without modding by 2π. We can ignore the global topology by considering $\Delta\theta \ll 2\pi$. This is consistent with the large-L_u limit taken in the previous section, since that limit can be accomodated by taking Δt large. Adding winding will only increase the length of the geodesic,[7] so we see that our answer is valid in the regime considered.

[7]Note that this would be more subtle if we considered the squashed case $a < 1$, since for large enough r winding in θ corresponds to a timelike direction and can *decrease* the length of the geodesic.

In the case of AdS_3 with $a = 1$, the coordinates are such that one picks a constant-time slice by requiring $\Delta t = 0$. It is important to note that this case corresponds to the BTZ black hole in a rotating coordinate system, and our answer for $a = 1$ is the universal CFT_2 answer for such a dual state. Since we are using a rotating coordinate system, it is not necessary that the functional form of our answer precisely match the form of (3.28). The parameters β_L and β_R give the inverse left-moving and right-moving temperatures of the BTZ black hole in this frame, and we see that this match extends to the warped BTZ case as well; the dimensionful temperatures (3.59) and (3.60) match precisely with those of [16]. In Section 3.14 we will show that these temperatures, combined with the central charge (3.55), satisfy the Cardy formula. Finally, implementing an appropriate homology constraint suffices to reproduce the thermodynamic black hole entropy in the limit where we consider the entire boundary density matrix without tracing out any degrees of freedom.

3.12 A vacuum state proposal

We have produced the universal CFT results for states dual to spacelike warped AdS_3 and the warped BTZ black hole. However, as our formulae in the previous sections illustrate, none of these states can be considered the vacuum state. The proposal in [80] is that the timelike warped AdS_3 geometry is a suitable candidate for the vacuum state in both topologically massive gravity and a specific string theory example that reduces to Einstein gravity plus matter. The proposed vacuum geometry (which is in fact Gödel space) can be written as

$$\frac{ds^2}{\ell^2} = -\frac{3dt^2}{4-a^2} + \frac{3dr^2}{4r(4-a^2+3r)} - \frac{6ar\sqrt{3}}{(4-a^2)^{3/2}}dtd\theta + \frac{3r(4-a^2-3r(a^2-1))}{(4-a^2)^2}d\theta^2\,, \quad (3.61)$$

where θ is a compact coordinate with $\theta \sim \theta + 2\pi$. For $a^2 > 1$ this geometry has closed timelike curves for $r > (4-a^2)/3(a^2-1)$ (see [151, 29] for a discussion). In our perturbative

approach, we can take $r_\infty \delta \ll 1$, which is sufficient to excise the region with closed timelike curves. Notice that we can get to this geometry by taking the warped BTZ black hole (3.57) and performing the identifications

$$r_+ = 0, \qquad r_- = \frac{a^2 - 4}{3}, \qquad t \to it, \qquad \theta \to i\theta \ . \tag{3.62}$$

If we replace the exponential function in (3.58) with a hyperbolic sine (i.e. start with a precise match to 2D CFT instead of a match only at large fiber coordinate), then we can perform these identifications on the entanglement entropy result to get, for $\Delta t = 0$,

$$S_{\text{EE}} = \frac{\ell a}{2G_N} \log\left(\frac{\sin(L_\theta/2)}{\epsilon}\right). \tag{3.63}$$

We see that this is the ground state answer for a two-dimensional CFT on a cylinder with a compact spatial coordinate θ. Unfortunately, this is merely illustrative because it runs afoul of the requirement of large fiber-coordinate separation. The correct way to get the answer in our framework is to keep the entire expression (3.51) and perform the identifications necessary to get to timelike warped AdS. From here, there does not appear to be a sensible regime in which the series can be summed and reduces to a two-dimensional CFT answer.

3.13 The geometric meaning of large fiber-coordinate separation

We now discuss the meaning of the limit of large fiber-coordinate separation L_ϕ on a field theory calculation of entanglement entropy. Note that the limit is not necessarily a restriction on the spatial size, $(L_\phi L_\psi)^{1/2}$, for which our result holds.[8] The different spatial sizes lie on

[8]Here we are referring to spacelike warped AdS_3 in Poincaré coordinates (3.2), where the fiber coordinate is denoted by ϕ, and there is no restriction on the separation in the other coordinate ψ. The dual state is

spacelike slices boosted with respect to one another. For example, large spatial sizes are accommodated by taking $L_\psi \sim L_\phi$, which results in a "mostly spacelike" slice, whereas small spatial sizes are accommodated by taking L_ψ small, which makes the slice more null. Nevertheless, imposing large L_ϕ without constraining the system size *does* impose a physical restriction on the reduced density matrix. Unlike the case of the vacuum state on the Minkowski plane, there is no Lorentz symmetry relating the different observers on their different spacelike slices. In the case of spacelike warped AdS_3, our result for S_{EE} exhibits that there is a finite right-moving temperature turned on, which breaks Lorentz invariance. In the case of warped BTZ black holes, there is also a finite left-moving temperature. Thus, Lorentz transformations connecting different observers act nontrivially and lead to a different reduced density matrix. On the other hand, for the vacuum state on the plane the answer can be boosted and replaced with the invariant Minkowskian interval, as shown in (3.4). The entanglement entropy in this case is only sensitive to the length of the spatial interval and not the orientation of the spatial slice, whereas when Lorentz invariance is broken it is sensitive to both.

3.14 Nonperturbative conjecture

We have seen that the perturbative series we constructed converges for $a > 1/2$ in the large fiber-coordinate regime. Recall that the physically relevant range is $a \in [0, 2)$, so we fail to capture part of the parameter space. The region $a \in [0, 1/2)$ includes the interesting case of $\mathrm{AdS}_2 \times \mathbb{R}$, which can be reached by taking $a \to 0$ and rescaling the fiber coordinate $u \to u/a$ in (3.1).

The convergence of our series seems to suggest that our results for the entanglement entropy hold nonperturbatively in the warping. We conjecture this to be true. This claim

on the Minkowski plane and has finite right-moving temperature.

requires a UV-IR relation of the form $r_\infty \sim 1/\epsilon^2$ to hold nonperturbatively. In our perturbative approach we could make use of this UV-IR relation since we were working in the context of AdS/CFT, where it is known to be true. Extending the requirement into the nonperturbative regime is a natural choice. With it, we claim that our perturbative expansion is sufficient to capture the nonperturbative dynamics entering into the entanglement entropy.

A nontrivial check on this nonperturbative proposal is the Cardy formula. Our answers for S_{EE} allow us to read off left-moving and right-moving temperatures and the central charge. We now claim that all these results hold nonperturbatively. The central charge is given universally as

$$c_L = c_R = \frac{3\ell a}{2G_N}\,. \tag{3.64}$$

For the warped BTZ black hole, our proposal allows us to identify the left-moving and right-moving temperatures as (3.59) and (3.60) nonperturbatively in a. These temperatures and the central charge reproduce the entropy of the warped BTZ black hole through the Cardy formula:

$$S = \frac{A}{4G_N} = \left(\frac{3\pi\ell}{2G_N(4-a^2)}\left(ar_+ - \sqrt{r_+ r_-}\right)\right) = \frac{\pi^2}{3}(c_L T_L + c_R T_R). \tag{3.65}$$

3.15 Summary and outlook

We have taken the first steps toward understanding holographic entanglement entropy in the context of asymptotically warped AdS_3 spacetimes in Einstein gravity. We began by considering AdS_3 as a real-line fibration over AdS_2, a coordinate system relevant to the study of extremal black holes. The calculation of the entanglement entropy indicated a state at zero left-moving and finite right-moving temperature, as expected.

Deforming the fibration by a nontrivial warp factor leads to the warped AdS_3 geometries,

appearing in the near-horizon limit of extremal Kerr black holes at constant polar angle. To connect with the HRT proposal in AdS/CFT, we constructed a perturbation theory about the AdS_3 point with trivial warping. For $a = 1 + \delta$, one can compute the length of the necessary geodesic perturbatively in δ to all orders. The general answer is not particularly illuminating, except in the limit of large separation in the fiber coordinate. Recall that the $U(1)$ isometry originating from translation invariance in the fiber coordinate is what is expected to enhance to an infinite-dimensional $U(1)$ Kac-Moody algebra in the boundary theory. In this limit, the answer takes the universal form predicted by two-dimensional CFT. Interpreting our answer as a CFT answer allows us to read off the purported central charge of the dual theory, which is given by $c = 3\ell a/2G_N$. Since we are working in Einstein gravity, there is no diffeomorphism anomaly and $c_L = c_R = c$. Furthermore, heating up the dual state with a warped BTZ black hole in the bulk again leads to universal two-dimensional CFT answers, with the left- and right-moving temperatures appearing appropriately in the entanglement entropy. Altogether, the central charge and left- and right-moving temperatures identified in this way satisfy the Cardy formula and thus reproduce the black hole entropy in the bulk. The central charge we have identified from the entanglement entropy calculation has been previously produced in the literature [12] by *demanding* consistency with the Cardy formula. Our approach implements the covariant holographic entanglement entropy proposal and consistency with the Cardy formula is instead a promising output. Taking our results at face value, they seem to suggest that warped CFTs behave like ordinary CFTs in the IR; this matches the intuition garnered from asymptotically warped AdS_3 spacetimes in holography, since their deep interiors are AdS_3-like for small warping. Our perturbative expansion also shows that there exists nontrivial fiber-coordinate dependence at subleading order in the separation of the fiber coordinate, suggesting that the full theory is not a standard conformal field theory. How to implement a proposal for holographically computing entanglement entropy in asymptotically warped AdS_3 spacetimes, without taking an IR limit, remains an open

question.

The most immediate way one can make progress on the questions discussed in this paper is by studying the constraints of warped CFT on field-theoretic calculations of entanglement entropy. It has been shown in [80] that warped conformal invariance is strongly constraining and allows one to reproduce a Cardy-like formula for the asymptotic growth in the density of states by using the modular covariance of the partition function. As shown in [130], the calculation of entanglement entropy in the vacuum and finite-temperature states of two-dimensional CFT can be conformally mapped to the calculation of a partition function. The constrained form of the partition function then allows one to write down the universal formulas for two-dimensional CFT. Such a procedure may prove fruitful in the case of warped CFTs as well, although one of the primarily difficulties is due to warped CFTs not having natural Euclidean descriptions. Obtaining a universal entanglement entropy formula for simple states of warped CFTs will allow one to determine if our holographic results are indicating the existence of a second hidden Virasoro algebra or if the infinite-dimensional $U(1)$ is sufficient to constrain the answers in the way we have presented.

It is also interesting to see how far the analogy with two-dimensional CFT can be taken. For example, it is possible that for large separation in the $U(1)$ coordinate, with an appropriate IR limit, the field-theoretic calculation of entanglement entropy in a warped CFT reproduces the CFT result. A simpler question is the constraint on correlation functions: it can be shown [129] that left-translation invariance, left-scale invariance, and right-translation invariance constrain the vacuum two-point function of local operators ϕ_i to be of the form

$$\langle \phi_i(x^-, x^+)\phi_j(y^-, y^+)\rangle = \frac{f_{ij}(x^- - y^-)}{(x^+ - y^+)^{\lambda_i+\lambda_j}} \ , \tag{3.66}$$

where λ_i is the weight of the operator ϕ_i. Furthermore, the symmetries are automatically enhanced to an infinite-dimensional left-moving $U(1)$ Kac-Moody algebra and a left-moving

Virasoro algebra. If the analogy to two-dimensional CFT is to be taken seriously, these symmetries should provide a constraint on f_{ij} such that in the limit of large separation $x^- - y^-$ and in an appropriate infrared regime the answer reduces to that of two-dimensional CFT. Even if this simplification occurs, however, it does not imply that the theory can be described by an ordinary two-dimensional CFT in this regime. The entanglement entropy in the states we have considered and the vacuum two-point function give limited information about the theory and do not elucidate its full dynamics.

Another home for the study of warped AdS_3 and warped BTZ black holes is topologically massive gravity, a higher curvature theory of gravity. There has been some work on extending the holographic entanglement entropy proposal to this theory [177], although as far as we are aware no manifestly successful proposal has been put forth. Indeed, accomodating the diffeomorphism anomaly seems nontrivial. Nevertheless, since the bulk theory is three-dimensional we expect the analysis to be analytically tractable. Given our study of finite-temperature solutions, it is clear that a proposal for topologically massive gravity which reproduces the CFT_2 answer for empty, warped AdS_3 will also reproduce the correct answer for the warped BTZ black hole, as shown in Section 3.11.

We have seen that the method of holographically computing entanglement entropy, devised in AdS/CFT, can be adapted to the case of warped AdS_3 holography. It provides further evidence that a sharp holographic correspondence can be developed in this context. The perturbative approach we implemented may be a promising way to study entanglement entropy in more general spacetimes continuously connected to AdS_{d+2}. It can also be adapted to the NHEK geometry, where one would like to independently deduce $c_L = 12J$.

Chapter 4

A higher spin Lifshitz black hole

In the past few years there has been a renewed interest in higher spin gravity in various dimensions following the work of Vasiliev and collaborators (see [187] for a review). In the present paper we focus on higher spin theories in three spacetime dimensions. Gaberdiel and Gopakumar proposed a duality of the two dimensional W_N minimal model CFTs to three dimensional Vasiliev theory [103]. The original proposal has passed many checks and some refinements in recent years, see e.g. [106, 105, 104, 52, 54, 11, 166, 128]. An interesting feature of the three dimensional Vasiliev theory [169] is that while it is a complicated nonlinear theory coupling an infinite tower of higher spin fields to scalar matter, if the scalars are linearized, the theory can be reformulated in terms of a Chern-Simons theory with an infinite dimensional gauge algebra $hs(\lambda) \times hs(\lambda)$ [41, 37, 168]. The deformation parameter λ is associated with the 't Hooft coupling of the dual CFT [103]. The Chern-Simons theory simplifies if $\lambda = \pm N$, where N is an integer and the theory reduces to Chern-Simons theory with gauge group $SL(N,\mathbb{R}) \times SL(N,\mathbb{R})$ and is purely topological, corresponding to a theory of massless fields of spin $2, 3, \cdots, N$. Note that Einstein gravity with negative cosmological constant is included by taking $N = 2$ [189, 1].

The simplest solutions of the Chern-Simons theory correspond to AdS_3 vacua. The

asymptotic symmetry of the AdS vacuum in $SL(N,\mathbb{R}) \times SL(N,\mathbb{R})$ higher spin gravity depends on the embedding of a $SL(2,\mathbb{R})$ sub-algebra in $SL(N,\mathbb{R})$. For the principal embedding one obtains W_N symmetry [49, 126], whereas for non-principal embeddings other higher spin algebras such as $W_N^{(2)}$ can occur [9, 48].

The construction of black holes in AdS/CFT is important since (large) black holes describe the dual CFT in thermal equilibrium at finite temperature. The BTZ solution [31] of three dimensional gravity has been a very important part of exploring the AdS/CFT correspondence (see [143] for a review). In higher spin theories the definition of what constitutes a black hole is nontrivial since the metric field transforms under higher spin gauge transformations [49] and hence the standard geometric characterization of a black hole, i.e. the existence of a horizon is not gauge invariant. In [120] a new criterion was proposed which uses the holonomy of the Chern-Simons gauge field around the contractable euclidean time circle to characterize a regular black hole. The holonomy condition has been applied to various black holes in 3 dimensional higher spin theories [53, 75, 55, 56] and it has been checked by comparing bulk and CFT calculations of thermal correlation functions [146, 107, 108], see [10] for a review and a more extended list of references. Note that there are some puzzles remaining, for example there are two different proposals for the entropy, namely the "holomorphic" [120] and the "canonical" [165, 165] one. See [164, 147, 76, 8] for recent work on the two proposals and their possible relation.

In the Chern-Simons formulation of of higher spin gravity, the W_N extension of the Virasoro symmetry of the boundary theory is obtained via the Drinfeld-Sokolov reduction by specifying asymptotic boundary fall off conditions for the gauge fields and considering nontrivial gauge transformations which respect these boundary conditions. If the boundary conditions are consistent then the boundary charges are integrable, finite and conserved and generate the (extended) symmetry algebra.

It is a very interesting question whether the higher spin gravity/CFT duality in three

dimensions can be generalized to non-AdS backgrounds. In [109, 3] a general recipe and examples including Lobachevsky ($\mathbb{R} \times AdS_2$), Lifshitz, Schrödinger and warped AdS backgrounds were given. More recently the same philosophy was applied to flat space holography in [4, 114].

In the present paper we are interested in a construction and detailed analysis of higher spin realizations of asymptotically Lifshitz spacetimes. Such spacetimes provide candidates for a holographic description of field theories with Lifshitz scaling invariance. These theories exhibit an anisotropic scaling symmetry with respect to space and time $\vec{x} \to \lambda \vec{x}$ and $t \to \lambda^z t$, with $z \neq 1$ and are important in various condensed matter systems (see [137] for references). In [137] a holographic Lifshitz spacetime solution of a gravity theory coupled to anti-symmetric tensor fields in four dimension was given. Subsequently Lifshitz space times have been ground in many (super)gravity theories, see e.g. [90, 23, 91, 116]. In holographic theories black hole or black brane solutions provide the dual description of field theories at finite temperature (and chemical potential if the black holes are charged). For Lifshitz spacetimes the construction of black holes was initiated in [74, 38, 158, 22], but most solutions in the literature are only known numerically.

In the present paper we focus mainly on the simplest three dimensional higher spin theory which is based on $SL(3,\mathbb{R}) \times SL(3,\mathbb{R})$ Chern-Simons theory and corresponds to gravity coupled to a massless spin three field. For simplicity, most explicit calculations are performed in this theory, but we shall also comment on generalizations to $N > 3$ and $hs(\lambda)$.

The structure of the paper is as follows: In section 4.1 we give a brief review of the Chern-Simons formulation of higher spin gravity. In section 4.2 we review some salient features of field theories which enjoy Lifshitz scaling symmetry, and we discuss the holographic realization of such theories. We then review how the Lifshitz spacetime can be obtained as a solution to $SL(3,\mathbb{R}) \times SL(3,\mathbb{R})$ Chern-Simons theory, and we demonstrate that the algebra generating Lifshitz isometries can be realized in a higher spin context.

In section 4.3 we construct black hole solutions with Lifshitz scaling, focusing on the simplest case of non-rotating black holes. We discuss the gauge freedom and the holonomy conditions as well as the thermodynamics. When the holonomy conditions are solved to express the temperature and chemical potential in terms of the extensive parameters there are six different branches. Only two of the six have positive temperature and entropy and are hence physically sensible. We consider two additional conditions on the branches, first the local thermodynamic stability and second the existence of a radial gauge where the metric exhibits a regular horizon and find that only one branch satisfies all of these conditions.

In section 4.4 we discuss generalizations of our work including the possibility of constructing rotating black hole solutions as well as Lifshitz black holes in $hs(\lambda)$ higher spin theory.

We close with a brief discussion of our results in section 4.5. For completeness we summarize our conventions for $SL(3,\mathbb{R})$ and $hs(\lambda)$ in an appendix.

4.1 Chern-Simons formulation of higher spin gravity

The Chern-Simons formulation of three dimensional (higher spin) gravity is based on two copies of the Chern-Simons action at level k and $-k$ and gauge group $SL(N,\mathbb{R})\times SL(N,\mathbb{R})$.

$$S = S_{CS}[A] - S_{CS}[\bar{A}] \tag{4.1}$$

where

$$S_{CS}[A] = \frac{k}{4\pi}\int \mathrm{tr}\Big(A\wedge dA + \frac{2}{3}A\wedge A\wedge A\Big). \tag{4.2}$$

The equations of motion are simply flatness conditions,

$$F = dA + A \wedge A = 0, \qquad \bar{F} = d\bar{A} + \bar{A} \wedge \bar{A} = 0. \tag{4.3}$$

Ordinary gravity is given by the case $N = 2$; in the following we will mainly focus on the case $N = 3$. This theory was studied in detail in [49] and it was shown that the CS theory is equivalent to AdS gravity coupled to a massless spin three field. The vielbein and spin connection take values in the $SL(3, \mathbb{R})$ Lie algebra and are related to the CS gauge fields as follows:

$$e_\mu = \frac{l}{2}(A_\mu - \bar{A}_\mu), \qquad \omega_\mu = \frac{1}{2}(A_\mu + \bar{A}_\mu). \tag{4.4}$$

In the following we set the length scale l to one for notational ease. Using the expression of the vielbein (4.4) in terms of the connection, the metric and spin 3 field can be expressed as

$$g_{\mu\nu} = \frac{1}{2}\,\mathrm{tr}(e_\mu e_\nu), \qquad \phi_{\mu\nu\rho} = \frac{1}{6}\,\mathrm{tr}(e_{(\mu} e_\nu e_{\rho)}). \tag{4.5}$$

The gauge transformations act on the Chern-Simons connections as follows

$$\delta A = d\Lambda + [A, \Lambda], \qquad \delta\bar{A} = d\bar{\Lambda} + [A, \bar{\Lambda}]. \tag{4.6}$$

In the construction of asymptotically AdS as well as asymptotically Lifshitz spacetimes, we employ a special choice of coordinates and choice of gauge. We define a radial coordinate ρ, where the holographic boundary will be located at $\rho \to \infty$. In addition we define a timelike coordinate t and a space like coordinate x, which can be either compact or non-compact and hence the boundary has either the topology of $\mathbb{R} \times S^1$ or $\mathbb{R} \times \mathbb{R}$. The "radial gauge" that

we will use is constructed by defining $b = \exp(\rho L_0)$ and setting

$$A_\mu = b^{-1} a_\mu \, b + b^{-1} \partial_\mu b, \qquad \bar{A}_\mu = b \, \bar{a}_\mu b^{-1} + b \, \partial_\mu (b^{-1}). \tag{4.7}$$

where $a_\mu = a_\mu(t, x)$ and $\bar{a}_\mu = \bar{a}_\mu(t, x)$ do not depend on ρ.

4.2 Lifshitz spacetimes

Quantum field theories which exhibit a scaling symmetry which is anisotropic with respect to space and time

$$t \to \lambda^z t, \qquad x \to \lambda x \tag{4.1}$$

appear in many condensed matter systems. The dynamical scaling coefficient $z \neq 1$ breaks relativistic symmetry. If one augments the symmetry of the theory to include space and time translations, then one obtains a theory that is said to possess Lifshitz symemtry. Lifshitz symmetry can therefore be encoded as a Lie algebra generated by time translations H, spatial translations P and Lifshitz scalings D satisfying the following structure relations:

$$[P, H] = 0 \qquad [D, H] = zH \qquad [D, P] = P. \tag{4.2}$$

In two dimensions, conformal symmetry (with $z = 1$) implies a conserved, traceless and symmetric stress tensor. For theories with Lifshitz scaling the stress tensor does not have to be symmetric, since they do not possess boost invariance. The stress-energy complex for field theories in 1+1 dimensions with Lifshitz scaling exponent z contains the following objects: the energy density $\mathcal{E}$, the energy flux $\mathcal{E}^x$, the momentum density $\mathcal{P}_x$ and the stress energy

tensor Π^x_x. These quantities satisfy the following conservation equations (see e.g. [170]):

$$\partial_t \mathcal{E} + \partial_x \mathcal{E}^x = 0, \qquad \partial_t \mathcal{P}_x + \partial_x \Pi^x_x = 0. \tag{4.3}$$

In addition, the Lifshitz scaling with exponent z implies a modified tracelessness condition

$$z\mathcal{E} + \Pi^x_x = 0. \tag{4.4}$$

The Lifshitz symmetries of a (1+1)-dimensional metric can be realized holographically with the following metric:

$$ds^2 = L^2\Big(d\rho^2 - e^{2z\rho}dt^2 + e^{2\rho}dx^2\Big) \tag{4.5}$$

where the Lifshitz scaling transformation corresponds to a translation $\rho \to \rho + \ln\lambda$. This metric is not a solution of Einstein gravity with negative cosmological constant; one has to add matter or higher derivative terms to the action to obtain it as a solution.

One can realize the $z = 2$ Lifshitz metric in the $SL(3,\mathbb{R}) \times SL(3,\mathbb{R})$ higher spin theory [3] by choosing the radial gauge as in (4.7) and by choosing the following connections $a = a_\mu\, dx^\mu$ and $\bar{a} = \bar{a}_\mu\, dx^\mu$:

$$a = W_2\, dt + L_1\, dx, \qquad \bar{a} = W_{-2}\, dt + L_{-1}\, dx. \tag{4.6}$$

It follows from (4.5) that this connection reproduces the Lifshitz metric (4.5) with scaling exponent $z = 2$. Lifshitz spacetimes with critical exponents $z > 2$ can be obtained using $SL(N,\mathbb{R}) \times SL(N,\mathbb{R})$ Chern-Simons theory with $N > 3$.

4.2.1 Asymptotically Lifshitz connections

Focusing on $N = 3$ and $z = 2$, we explore Chern-Simons connections that behave asymptotically like Lifshitz. In this section, we use primes to denote derivatives with respect to x and overdots to denote derivatives with respect to t. With the gauge connections defined in (4.7), we look for the most general, flat connections with the property that

$$A - A_{\text{Lif}} \sim \mathcal{O}(1), \qquad \text{as } \rho \to \infty \tag{4.7}$$

$$\bar{A} - \bar{A}_{\text{Lif}} \sim \mathcal{O}(1), \qquad \text{as } \rho \to \infty \tag{4.8}$$

where A_{Lif} and $\bar{A}_{\text{Lif}}$ are the Lifshitz connections specified in (4.6). The most general connections that obey these asymptotics are obtained by adding terms to the Lifshitz connections a in (4.6) proprotional to W_0, W_{-1}, W_{-2} and L_0, L_{-1} (and similarly for $\bar{a}$). In particular, we consider the following ansatz:

$$a_t = W_2 + \ell_{t,0}L_0 + \ell_{t,-1}L_{-1} + w_{t,0}W_0 + w_{t,-1}W_{-1} + w_{t,-2}W_{-2}, \tag{4.9}$$

$$a_x = L_1 + \ell_{x,0}L_0 + \ell_{x,-1}L_{-1} + w_{x,0}W_0 + w_{x,-1}W_{-1} + w_{x,-2}W_{-2}. \tag{4.10}$$

Before applying flatness conditions, we allow all coefficients $\ell_{t,i}, \ell_{x,i}, w_{t,m}, w_{x,m}$ to be arbitrary functions of t and x. By suitable gauge transformations, we can set

$$w_{x,0} = 0, \qquad w_{x,-1} = 0, \qquad \ell_{x,0} = 0. \tag{4.11}$$

Employing the same notation as used in the higher spin black holes, we denote

$$\ell_{x,-1} = -\mathcal{L}, \qquad w_{x,-2} = \mathcal{W}, \tag{4.12}$$

and, after applying the flatness conditions[1], we obtain

$$a_t = W_2 - 2\mathcal{L}W_0 + \frac{2}{3}\mathcal{L}'W_{-1} - 2\mathcal{W}L_{-1} + \Big(\mathcal{L}^2 - \frac{1}{6}\mathcal{L}''\Big)W_{-2}, \tag{4.13}$$

$$a_x = L_1 - \mathcal{L}L_{-1} + \mathcal{W}W_{-2}, \tag{4.14}$$

where henceforth, an over-dot denotes a t-derivative and a prime denotes an x-derivative. Flatness also results in the following evolution equations for $\mathcal{L}$ and $\mathcal{W}$:

$$\dot{\mathcal{L}} = 2\mathcal{W}' \tag{4.15}$$

$$\dot{\mathcal{W}} = \frac{4}{3}(\mathcal{L}^2)' - \frac{1}{6}\mathcal{L}'''. \tag{4.16}$$

If we follow the same procedure for the barred sector, imposing the condition (4.8), then we find the following asymptotically Lifshitz connections:

$$\bar{a}_t = W_{-2} - 2\bar{\mathcal{L}}W_0 - \frac{2}{3}\bar{\mathcal{L}}'W_1 + 2\bar{\mathcal{W}}L_1 + \Big(\bar{\mathcal{L}}^2 - \frac{1}{6}\bar{\mathcal{L}}''\Big)W_2, \tag{4.17}$$

$$\bar{a}_x = L_{-1} - \bar{\mathcal{L}}L_1 - \bar{\mathcal{W}}W_2. \tag{4.18}$$

where again the flatness conditions produce evolution equations for the barred quantities

$$\dot{\bar{\mathcal{L}}} = -2\bar{\mathcal{W}}', \tag{4.19}$$

$$\dot{\bar{\mathcal{W}}} = -\frac{4}{3}(\bar{\mathcal{L}}^2)' + \frac{1}{6}\bar{\mathcal{L}}''', \tag{4.20}$$

which can be obtained, from (4.15) and (4.16) by replacing $\mathcal{L}$ and $\mathcal{W}$ by $\bar{\mathcal{L}}$ and $-\bar{\mathcal{W}}$. The signs were chosen so that we can now express the quantities appearing in the energy-momentum

[1] See [125] for discussion of closely related connections and their symmetries.

complex (4.3) in terms of the parameters appearing in the connection as follows:

$$\begin{aligned}
\mathcal{E} &= \mathcal{W} + \bar{\mathcal{W}}, \\
\mathcal{P}_x &= \mathcal{L} - \bar{\mathcal{L}}, \\
\Pi^x_x &= -2\mathcal{W} - 2\bar{\mathcal{W}}, \\
\mathcal{E}^x &= -\Big(\frac{4}{3}\mathcal{L}^2 - \frac{1}{6}\partial_x^2\mathcal{L}\Big) + \Big(\frac{4}{3}\bar{\mathcal{L}}^2 - \frac{1}{6}\partial_x^2\bar{\mathcal{L}}\Big).
\end{aligned} \tag{4.21}$$

It is straightforward to verify that that evolution equations (4.15) and (4.16) imply the equations for the Lifshitz stress-tensor complex (following the terminology of [170]) with $z = 2$, given by (4.3) and (4.4).

4.2.2 Realization of Lifshitz symmetries

We now show that among the gauge transformations that leave the connections (4.13) and (4.14) form-invariant, there exist those that realize the Lifshitz algebra as a Poisson algebra of boundary charges. To begin, recall that for each gauge parameter Λ, the standard definition of the variations of asymptotic symmetry boundary charges in Chern-Simons theory is as follows [49]:

$$\delta Q(\Lambda) = -\frac{k}{2\pi}\int_{-\infty}^{\infty} dx\, \mathrm{tr}(\Lambda \delta A_x). \tag{4.22}$$

We now show that there exist gauge parameters $\Lambda_H, \Lambda_P, \Lambda_D$ that leave the asymptotically Lifshitz connections form-invariant. Moreover, we show that the variations $\delta Q(\Lambda_H), \delta Q(\Lambda_P)$ and $\delta Q(\Lambda_D)$ as defined in (4.22) are integrable and yield charges $Q(\Lambda_H), Q(\Lambda_P)$ and $Q(\Lambda_D)$ that realize the Lifshitz algebra as a Poisson algebra.

As our first step, we determine the most general gauge parameter that results in a gauge transformation that leaves the asymptotically Lifshitz connections form-invariant. The radial

gauge (4.7) is preserved under gauge transformations if and only if the gauge parameter is of the form

$$\Lambda(\rho, t, x) = b^{-1}(\rho)\lambda(t, x)b(\rho). \tag{4.23}$$

Given this form, gauge transformations are characterized by the function λ and act on the connections as follows:

$$\delta_\lambda a_\mu = \partial_\mu \lambda + [a_\mu, \lambda]. \tag{4.24}$$

Now consider a general gauge parameter λ;

$$\lambda = \sum_{i=-1}^{1} \epsilon_i L_i + \sum_{m=-2}^{2} \chi_m W_m, \tag{4.25}$$

where $\epsilon_i = \epsilon_i(t, x)$ and $\chi_m = \chi_m(t, x)$. Gauge transformations are now explicitly given by

$$\delta_\lambda a_t = -2\delta\mathcal{L}W_0 + \frac{2}{3}(\delta\mathcal{L})'W_{-1} - 2\delta\mathcal{W}L_{-1} + \left(2\mathcal{L}\delta\mathcal{L} - \frac{1}{6}(\delta\mathcal{L})''\right) W_{-2}, \tag{4.26}$$

$$\delta_\lambda a_x = -\delta\mathcal{L}L_{-1} + \delta\mathcal{W}W_{-2}, \tag{4.27}$$

and enforcing form-invariance of the connections allows one to solve for all parameters ϵ_i and

χ_i in terms of the two parameters $\epsilon = \epsilon_1$ and $\chi = \chi_2$.

$$\begin{aligned}
\epsilon_0 &= -\epsilon', \\
\epsilon_{-1} &= -\mathcal{L}\epsilon + \frac{1}{2}\epsilon'' - 2\mathcal{W}\chi, \\
\chi_1 &= -\chi', \\
\chi_0 &= -2\mathcal{L}\chi + \frac{1}{2}\chi'', \\
\chi_{-1} &= \frac{2}{3}\mathcal{L}'\chi + \frac{5}{3}\mathcal{L}\chi' - \frac{1}{6}\chi''', \\
\chi_{-2} &= \mathcal{W}\epsilon + \mathcal{L}^2\chi - \frac{1}{6}\mathcal{L}''\chi - \frac{7}{12}\mathcal{L}'\chi' - \frac{2}{3}\mathcal{L}\chi'' + \frac{1}{24}\chi''''.
\end{aligned} \tag{4.28}$$

Form-invariance also gives evolution equations for ϵ and χ

$$\dot{\epsilon} = \frac{8}{3}\mathcal{L}\chi' - \frac{1}{6}\chi''', \tag{4.29}$$

$$\dot{\chi} = 2\epsilon', \tag{4.30}$$

and it constrains the forms of the variations $\delta\mathcal{L}$ and $\delta\mathcal{W}$

$$\delta\mathcal{L} = \epsilon\mathcal{L}' + 2\epsilon'\mathcal{L} + 2\chi\mathcal{W}' + 3\chi'\mathcal{W} - \frac{1}{2}\epsilon''', \tag{4.31}$$

$$\delta\mathcal{W} = \mathcal{W}'\epsilon + 3\mathcal{W}\epsilon' + \Big(\frac{4}{3}(\mathcal{L}^2)' - \frac{1}{6}\mathcal{L}'''\Big)\chi + \Big(\frac{8}{3}\mathcal{L}^2 - \frac{3}{4}\mathcal{L}''\Big)\chi' - \frac{5}{4}\mathcal{L}'\chi'' - \frac{5}{6}\mathcal{L}\chi''' + \frac{1}{24}\chi''''. \tag{4.32}$$

Now that we know the precise form of the most general gauge parameters leaving the connections form-invariant, we attempt to identify which of these parameters Λ_H, Λ_P and Λ_D lead to charges that satisfy a Lifshitz algebra. To find these parameters, we first notice that given the Lifshitz metric (4.5), the Lifshitz algebra is geometrically realized by the following

killing vectors:

$$\xi_H = \partial_t, \tag{4.33}$$

$$\xi_P = \partial_x, \tag{4.34}$$

$$\xi_D = \partial_\rho - x\partial_x - zt\partial_t. \tag{4.35}$$

Explicitly, one easily verifies that

$$[\xi_P, \xi_H] = 0, \qquad [\xi_D, \xi_H] = 2\xi_H, \qquad [\xi_D, \xi_P] = \xi_P. \tag{4.36}$$

This is precisely the Lifshitz algebra (4.2) with $z = 2$. These killing vectors generate spacetime diffeomorphisms, and there is a standard realization diffeomorphisms as gauge transformations in Chern-Simons theory via field-dependent gauge parameters [28]

$$\Lambda = -\xi^\mu A_\mu. \tag{4.37}$$

For the asymptotically Lifshitz connections of section 4.2.1, we expect that there exists a realization of the Lifshitz algebra, but it is not immediately obvious which gauge parameters one should pick that yield charges satisfying this algebra. However, motivated by the method of generating diffeomorphisms via gauge transformations, we try the following:

$$\Lambda_H = -(\xi_H)^\mu A_\mu = b^{-1}(-a_t)b, \tag{4.38}$$

$$\Lambda_P = -(\xi_P)^\mu A_\mu = b^{-1}(-a_x)b, \tag{4.39}$$

$$\Lambda_D = -(\xi_D)^\mu A_\mu = b^{-1}(-L_0 + xa_x + 2ta_t)b. \tag{4.40}$$

These gauge parameters leave the asymptotically Lifshitz connections form-invariant because one can show that there exists choices of the parameters ϵ and χ that lead to these gauge pa-

rameters. To see this explicitly, notice that given $\epsilon(t,x)$ and $\chi(t,x)$, if we let $\widehat{\lambda}(\epsilon(t,x),\chi(t,x))$ denote the gauge parameter $\lambda(t,x)$ of (4.25) obtained after all ϵ_i and χ_m have been substituted for their expressions in terms of ϵ and χ in (4.28), then we have

$$\Lambda_H = b^{-1}\widehat{\lambda}(0,-1)b, \tag{4.41}$$

$$\Lambda_P = b^{-1}\widehat{\lambda}(-1,0)b, \tag{4.42}$$

$$\Lambda_D = b^{-1}\widehat{\lambda}(x,2t)b. \tag{4.43}$$

We now have candidates for gauge parameters from which to construct charges that satisfy the Lifshitz algebra. Using the definition (4.22), we find that the expressions for the variations of the charges corresponding to these gauge parameters are integrable and give

$$Q(\Lambda_H) = \frac{2k}{\pi}\int_{-\infty}^{\infty} dx\mathcal{W}, \tag{4.44}$$

$$Q(\Lambda_P) = \frac{2k}{\pi}\int_{-\infty}^{\infty} dx\mathcal{L}, \tag{4.45}$$

$$Q(\Lambda_D) = -\frac{2k}{\pi}\int_{-\infty}^{\infty} dx(2t\mathcal{W} + x\mathcal{L}). \tag{4.46}$$

To determine the Poisson algebra of these charges, we recall that for any two gauge parameters Λ and Γ, one has [49, 28]

$$\{Q(\Lambda), Q(\Gamma)\} = \delta_\Lambda Q(\Gamma). \tag{4.47}$$

We assume that the fields $\mathcal{L}$ and $\mathcal{W}$ vanish sufficiently rapidly as $x \to \pm\infty$ to ensure that any boundary terms encountered in computing the gauge-variations of the charges vanish.

After some tedious but straightforward calculation, we find that

$$\{Q(\Lambda_H), Q(\Lambda_P)\} = 0, \tag{4.48}$$

$$\{Q(\Lambda_D), Q(\Lambda_H)\} = 2Q(\Lambda_H), \tag{4.49}$$

$$\{Q(\Lambda_D), Q(\Lambda_P)\} = Q(\Lambda_P). \tag{4.50}$$

This is precisely the Lifshitz algebra (4.2). In two dimensions we expect that the Lifshitz algebra will be extended to an infinite-dimensional algebra, in analogy with the extension of global conformal symmetry to a Virasoro algebra. A proposal for an infinite-dimensional extension of the Lifshitz symmetry was made in [68] and can be investigated using the Chern-Simons formulation.

4.3 Non-rotating Lifshitz black hole

The most general solutions of the Chern-Simons theory have connections A and $\bar{A}$ which are independent. We relate the barred and unbarred charges by setting

$$\bar{a}_x = -a_x^T, \qquad \bar{a}_t = a_t^T, \tag{4.1}$$

leaving the solutions to be characterized by only by the unbarred connection a_μ. Consequently, the expression for the metric (4.5) is diagonal, i.e. the g_{tx} component of the metric vanishes.

4.3.1 Most general non-rotating black hole solutions

Restricting ourselves to $SL(3,\mathbb{R}) \times SL(3,\mathbb{R})$ Chern-Simons, we start with a generalization of the ansatz (4.9), (4.10) in which we allow for source terms as coefficients of the generators W_2 and L_1 in the temporal components of the connections. This changes the asymptotics,

but as we will see presently, this extra freedom will allow us to interpret the resulting solutions as finite energy excitations above the asymptotic Lifshitz vacuum. We also restrict our attention to coordinate-independent connection coefficients. Our general ansatz for the unbarred sector is

$$a_t = \ell_{t,1}L_1 + w_{t,2}W_2 + \ell_{t,0}L_0 + \ell_{t,-1}L_{-1} + w_{t,1}W_1 + w_{t,0}W_0 + w_{t,-1}W_{-1} + w_{t,-2}W_{-2}, \quad (4.2)$$

$$a_x = L_1 + \ell_{x,0}L_0 + \ell_{x,-1}L_{-1} + w_{x,0}W_0 + w_{x,-1}W_{-1} + w_{x,-2}W_{-2}. \quad (4.3)$$

Notice that the ansatz (4.9), (4.10) of the last section is a special case of this ansatz obtained by setting $\ell_{t,1} = 0$ and $w_{t,2} = 1$. In order for this ansatz to be a solution of our theory we need to impose the flatness conditions which constrain the connections;

$$\begin{aligned}
w_{t,1} &= 0, \\
\ell_{x,0} &= 0, \\
w_{t,-1} &= \ell_{t,1}w_{x,-1}, \\
\ell_{t,0} &= -w_{t,2}w_{x,-1}, \\
\ell_{t,-1} &= \ell_{t,1}\ell_{x,-1} - 2w_{t,2}w_{x,-2}, \\
w_{t,0} &= \ell_{t,1}w_{x,0} + 2\ell_{x,-1}w_{t,2}, \\
w_{t,-2} &= \ell_{x,-1}^2 w_{t,2} + \ell_{t,1}w_{x,-2} + w_{x,0}w_{t,2}w_{x,-2} - \frac{1}{4}w_{2,t}w_{x,-1}^2.
\end{aligned} \quad (4.4)$$

These conditions seems to indicate that a flat solution is specified by parameters $\ell_{t,1}, \ell_{x,-1}$ and $w_{t,2}, w_{x,0}, w_{x,-1}, w_{x,-2}$. However we have not fixed all the gauge freedom, and some of these parameters are gauge artifacts. In order to see which of these parameters are the charges and sources of the theory and which of them can be gauged away, it suffices to look at the only gauge invariant quantities of the theory: the holonomies. A quick inspection of the holonomies around the thermal and angular cycles shows that the following quantities

distinguish different solutions

$$\begin{aligned}
\mu_2 &= w_{t,2}, \\
\mu_1 &= \ell_{t,1} + \frac{1}{3} w_{x,0} w_{t,2}, \\
\mathcal{L} &= -\ell_{x,-1} + \frac{1}{12} w_{x,0}^2, \\
\mathcal{W} &= w_{x,-2} + \frac{1}{54} \left(18 \ell_{x,-1} w_{x,0} - w_{x,0}^3 \right).
\end{aligned} \tag{4.5}$$

Under these identifications we will interpret μ_1, μ_2 and $4\mathcal{L}, -4\mathcal{W}$ as sources and their conjugate charges. We will expand on this interpretation in section 4.3.3. Finally, to obtain a generic solution for the barred sector, we take $\bar{A} = -A^T$ replacing μ_i by $\bar{\mu}_i$ and $\mathcal{L}$, $\mathcal{W}$ by $\bar{\mathcal{L}}$ and $\bar{\mathcal{W}}$. Limiting out attention to non non-rotating solutions implies setting $\bar{\mu}_i = -\mu_i$, $\bar{\mathcal{L}} = \mathcal{L}$ and $\bar{\mathcal{W}}$.

Note that for a non-vanishing source μ_1, the connection (4.2) has a nonzero L_1 component and does not satisfy the criterion for an asymptotically Lifshitz connection (4.7). This indicates that the source μ_1 deforms the Lifshitz vacuum just as in the case of the higher spin CFTs. We note that it was shown in [**?**] that in the case of the asymptotically AdS theory with a deformation by a source still enjoys the full W_3 symmetry. It is quite likely that this is the case for our solution too, but we have not shown it.

4.3.2 Holonomy conditions

In the context of Chern-Simons higher spin theories, black hole solutions need to satisfy certain holonomy conditions and should have a thermodynamical interpretation [120, 53]. In particular, the requirement of a smooth Euclidean geometry implies that the thermal holonomy of the Chern-Simons connection is trivial;

$$\mathcal{P} \exp\left(\oint_t dt A_t \right) = \mathbf{1}, \tag{4.6}$$

where $\mathbf{1}$ is the $SL(3,\mathbb{R})$ identity, and the thermal cycle is from $t = 0$ to $t = 2\pi i$. This condition can be recast in more than one equivalent way. Diagonalizing a_t, and noting that a_t is constant, we find that the condition of a trivial thermal holonomy is equivalent to the following condition on the eigenvalues λ_1, λ_2, and λ_3 of a_t;

$$e^{2\pi i\lambda_1} = e^{2\pi i\lambda_2} = e^{2\pi i\lambda_3} = 1. \tag{4.7}$$

This means that each eigenvalue of a_t must be an integer. Since A_t is an element of $\mathfrak{sl}(3,\mathbb{R})$, it must be traceless, and this gives a second requirement on the eigenvalues; they must sum to zero.

$$\lambda_1 + \lambda_2 + \lambda_3 = 0. \tag{4.8}$$

The simplest nontrivial solution is then $(\lambda_1, \lambda_2, \lambda_3) = (0, 1, -1)$. This solution contains the famous BTZ black hole and its higher spin generalizations studied in [120].

In order to find black hole solutions one demands that the connections (4.2) and (4.3) obey (4.7) and (4.8). These conditions can be cast in a computationally convenient light. Employing the Cayley-Hamilton theorem, we note that every 3-by-3 complex matrix X satisfies its own characteristic polynomial. This means that there exist complex numbers $\Theta_0, \Theta_1, \Theta_2$ for which

$$X^3 = \Theta_0 I + \Theta_1 X + \Theta_2 X^2. \tag{4.9}$$

In particular, this allows one to compute any integer power of X knowing only the coefficients of the characteristic polynomial, and therefore allows for evaluation of the matrix exponential of X in terms of these coefficients. In the special case that X is traceless, which is the case for the argument of the exponential in the thermal holonomy, there are simple expressions

for the coefficients of the characteristic polynomial, which therefore serve to determine the thermal holonomy completely;

$$\Theta_0 = \det(X), \qquad \Theta_1 = \frac{1}{2}\,\mathrm{tr}(X^2), \qquad \Theta_2 = 0. \tag{4.10}$$

Applying this to the triviality condition (4.6), we find that the eigenvalues of a_t are related to the characteristic polynomial coefficients;

$$\Theta_0 = (2\pi i)^3 \lambda_1\lambda_2\lambda_3, \qquad \Theta_1 = -2\pi^2(\lambda_1^2+\lambda_2^2+\lambda_3^2). \tag{4.11}$$

In the case of, for example, the BTZ black hole, with $(\lambda_1, \lambda_2, \lambda_3) = (0, 1, -1)$ one obtains

$$\Theta_0 = 0, \qquad \Theta_1 = -4\pi^2, \qquad \Theta_2 = 0. \tag{4.12}$$

In the context of finding a higher spin Lifshitz black hole solutions, we see no compelling reason to choose the BTZ holonomy conditions over others, but we do so anyway because they are simple and non-trivial. In principle, however, any conditions on the eigenvalues λ_j satisfying (4.7) and (4.8) should give rise to independent solutions. Applying the conditions (4.12) to our solution, we obtain the following holonomy conditions:

$$0 = 3\mathcal{L}\mu_1^2 + 9\mathcal{W}\mu_1\mu_2 + 4\mathcal{L}^2\mu_2^2 - \frac{3}{4}, \tag{4.13}$$

$$0 = 108\mathcal{W}^2\mu_2^3 + 8\mathcal{L}^2\mu_2\left(9\mu_1^2 - 4\mathcal{L}\mu_2^2\right) + 27\mathcal{W}\left(\mu_1^3 + 4\mathcal{L}\mu_1\mu_2^2\right). \tag{4.14}$$

These two equations can be used to solve for any two of $\mathcal{L}, \mathcal{W}, \mu_1, \mu_2$ in terms of the remaining two. In the next section we shall argue that thermodynamically $\mathcal{L}$ and $\mathcal{W}$ are charges and μ_1, μ_2 are the conjugate potentials.

4.3.3 Action and entropy

Since the black holes we are studying are gravitational solutions, we need to check that the Chern-Simons theory provides a correct variational principle. Let I_0 denote the euclidean Chern-Simons action. The on-shell, euclidean action $I_0^{\rm os}$, namely the action in which the equations of motion have been used, is given by a boundary term

$$I_0^{\rm os} = -\frac{k}{4\pi}\int d\phi\, dt\ {\rm tr}(a_t a_x) + \frac{k}{4\pi}\int d\phi\, dt\ {\rm tr}(\bar{a}_t \bar{a}_x), \tag{4.15}$$

and evaluating the action on our non-rotating connections gives [30];

$$I_0^{\rm os} = -4k\big(2\mathcal{L}\mu_1 + 3\mathcal{W}\mu_2\big). \tag{4.16}$$

However $I_0^{\rm os}$ does not obey a thermodynamically sensible variational principle because the on-shell variation of I_0 is

$$(\delta I_0)^{\rm os} = 8k\big(\mathcal{L}\delta\mu_1 + \mathcal{W}\delta\mu_2\big) + \delta(4k\mu_2\mathcal{W}). \tag{4.17}$$

The third term spoils the identification of μ_1, μ_2 with sources having conjugate charges $\mathcal{L}$ and $\mathcal{W}$. As discussed in [77, 30], in the context of the higher spin black holes, it is possible to obtain a canonical action I_1 that is thermodynamically sensible by adding a boundary term to I_0. When we evaluate I_1 on our non-rotating solutions, we obtain

$$I_1^{\rm os} = -8k(\mu_1\mathcal{L} + 2\mu_2\mathcal{W}), \tag{4.18}$$

and it has the corresponding on-shell variaton

$$(\delta I_1)^{\rm os} = 8k(\mathcal{L}\delta\mu_1 + \mathcal{W}\delta\mu_2). \tag{4.19}$$

This relation follows directly from the holonomy conditions (4.13) and (4.14). Taking derivatives of the conditions with respect to the sources, one can show that

$$\frac{\partial \mathcal{L}}{\partial \mu_1} = -\frac{6\mu_1\mathcal{L} - 18\mu_2\mathcal{W}}{3\mu_1^2 - 16\mu_2^2\mathcal{L}}, \qquad \frac{\partial \mathcal{W}}{\partial \mu_2} = -\frac{8\mathcal{L}(\mu_1\mathcal{L} - 3\mu_2\mathcal{W})}{3\mu_1^2 - 16\mu_2^2\mathcal{L}}, \tag{4.20}$$

$$\frac{\partial \mathcal{L}}{\partial \mu_2} = \frac{16\mu_2\mathcal{L}^2 - 9\mu_1\mathcal{W}}{3\mu_1^2 - 16\mu_2^2\mathcal{L}}, \qquad \frac{\partial \mathcal{W}}{\partial \mu_1} = \frac{16\mu_2\mathcal{L}^2 - 9\mu_1\mathcal{W}}{3\mu_1^2 - 16\mu_2^2\mathcal{L}}. \tag{4.21}$$

Using these expression one can easily show that that μ_1, μ_2 are conjugate to $\mathcal{L}$ and $\mathcal{W}$ respectively;

$$\frac{\partial I_1^{\text{os}}}{\partial \mu_1} = 8k\mathcal{L}, \qquad \frac{\partial I_1^{\text{os}}}{\partial \mu_2} = 8k\mathcal{W}. \tag{4.22}$$

The following integrability relation follows immediately from the equality of mixed partial derivatives:

$$\frac{\partial \mathcal{W}}{\partial \mu_1} = \frac{\partial \mathcal{L}}{\partial \mu_2}. \tag{4.23}$$

The entropy S is naturally a function of the charges $\mathcal{L}, \mathcal{W}$. It can can be obtained by performing a Legendre transform of $I_1^{\text{os}}(\mu_1, \mu_2)$ with respect to the conjugate variables $\mathcal{L}$ and $\mathcal{W}$.

$$\begin{aligned} S(\mathcal{L}, \mathcal{W}) &= \frac{\partial I_1^{\text{os}}}{\partial \mu_1}\mu_1 + \frac{\partial I_1^{\text{os}}}{\partial \mu_2}\mu_2 - I_1^{\text{os}} \\ &= 8k\big(2\mu_1\mathcal{L} + 3\mu_2\mathcal{W}\big). \end{aligned} \tag{4.24}$$

Moreover, using the holonomy conditions one can easily verify that the following inverse thermodynamic relations are:

$$\frac{\partial S}{\partial(8k\mathcal{L})} = \mu_1, \qquad \frac{\partial S}{\partial(8k\mathcal{W})} = \mu_2. \tag{4.25}$$

4.3.4 Temperature and grand potential

Recall that for any thermodynamic system, the grand potential is defined as follows in terms of the thermal partition function:

$$\Phi = -\frac{1}{\beta} \ln Z. \tag{4.26}$$

Using the saddle point approximation, we identify the on-shell, Euclidean Chern-Simons action with the log of the partition function, so we obtain

$$\Phi = \frac{1}{\beta} I_1^{\text{os}}. \tag{4.27}$$

The thermodynamic potential Φ is associated with the grand canonical ensemble and has as natural variables the temperature T and the chemical potential α. These can be related to μ_1, μ_2 as follows.

In euclidean signature we have chosen the periodicity of the euclidean time circle to be 1. A different euclidean periodicity β is equivalent to keeping the periodicity equal to 1 and rescaling A_t by a factor of β. This leads us to re-express the potentials μ_1, μ_2 in terms of β (or the temperature T) and a higher spin potential α.

$$\mu_1 = \beta\alpha = \frac{1}{T}\alpha, \qquad \mu_2 = \beta = \frac{1}{T}. \tag{4.28}$$

This prescription also ensures that after the rescaling, the connections have Lifshitz asymptotics.

In thermodynamics it is a well known fact that the grand canonical potential has the

following differential

$$d\Phi = -SdT - Qd\alpha. \tag{4.29}$$

It follows that the entropy S and charge Q can be computed as appropriate partial derivatives of the grand potential;

$$\left.\frac{\partial\Phi}{\partial T}\right|_{\alpha} = -S, \qquad \left.\frac{\partial\Phi}{\partial\alpha}\right|_{T} = -Q. \tag{4.30}$$

For the Lifhsitz black hole, the grand potential Φ is related to the on shell action I_1^{os} via (4.27) which is turn is given by (4.18), giving

$$\Phi = -8k\Big(\alpha\mathcal{L} + 2\mathcal{W}\Big). \tag{4.31}$$

Using the holonomy conditions (4.13) and (4.14) to eliminate derivatives with respect to α, T one can calculate the entropy

$$S = -\left.\frac{\partial\Phi}{\partial T}\right|_{\alpha} = \frac{1}{T}8k\Big(2\alpha\mathcal{L} + 3\mathcal{W}\Big). \tag{4.32}$$

Note that the entropy agrees with (4.24). The charge conjugate to the potential α is given by

$$Q = -\left.\frac{\partial\Phi}{\partial\alpha}\right|_{T} = -8k\mathcal{L}. \tag{4.33}$$

We can use the thermodynamic relation between grand potential and the internal energy (which we can identify with the mass of the black hole) to obtain a formula for the energy[2]

[2]Notice that it follows from (4.34) that the Gibbs-Duhem relation $E = TS + \alpha Q$ doesn't hold for our black hole solution, since it would imply $\Phi = 0$. This is a common feature of black hole thermodynamics which has been noticed at various points in the literature (see e.g. [**?**][110]).

E;

$$E = \Phi + TS + \alpha Q = 8k\mathcal{W}. \tag{4.34}$$

Note that this result agrees with the identification of $\mathcal{W}$ with the energy in the holographic Lifshitz em-complex given in (4.21). We can perform one last consistency check by solving the holonomy conditions with S and Q as independent variables, it is straightforward to verify that the First Law of thermodynamics is indeed satisfied;

$$dE = TdS + \alpha dQ. \tag{4.35}$$

4.3.5 Branches

After clarifying the thermodynamical interpretation of the parameters in the connection, we are ready to look for black hole solutions to the holonomy conditions (4.13) and (4.14). In this section we will express the intensive parameters T and α in terms of the extensive parameters $\mathcal{L}$ and $\mathcal{W}$. Note that due to the nonlinear nature of the holonomy conditions, there will be multiple branches which can be interpreted as different phases of the theory.

In order to simplify the calculation it proves useful to replace $\mathcal{W}$ by a parameter θ which is given by

$$\mathcal{W} = \sqrt{\frac{16\mathcal{L}^3}{27}}\sin\theta. \tag{4.36}$$

Using (4.25), we eliminate μ_1, μ_2 in the first holonomy condition (4.13) in favor of derivatives of the entropy with respect to $\mathcal{L}$ and θ.

$$64k^2\mathcal{L} = 9\left(\frac{\partial S}{\partial \theta}\right)^2 + 4\mathcal{L}^2\left(\frac{\partial S}{\partial \mathcal{L}}\right)^2. \tag{4.37}$$

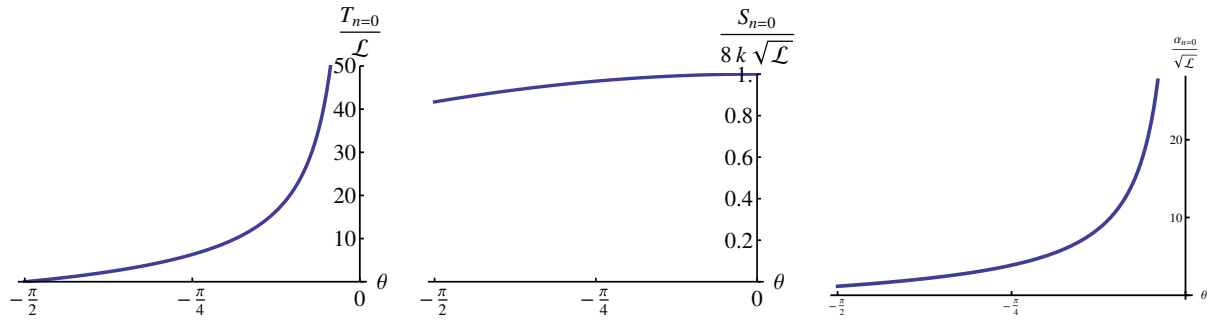

Figure 4.1: Temperature, entropy and chemical potential of the $n = 0$ branch

This partial differential equation for S is solved by the following family of solutions parametrized by a constant C.

$$S(\mathcal{L}, \theta) = 8k\sqrt{\mathcal{L}} \cos\left(\frac{\theta}{3} + C\right). \tag{4.38}$$

Inserting this in the second holonomy condition (4.14) gives us a restriction for C given by

$$\sin(3C) = 0, \tag{4.39}$$

which indicates that $C = n\pi/3$ for $n = 0, .., 5$. Hence there are six different solutions labelled by n. All of these solutions can be regarded as thermodynamical branches of a Lifshitz black hole. The branches $n = 1, 2, 3, 4$ all show pathologies that make them unphysical. The $n = 1$ case has negative temperature for all values of $\theta, \mathcal{L}$, while $n = 2$ has both negative temperature and entropy. Finally, the $n = 3, 4$ branches have strictly negative entropy.

Consequently, only the branches with $n = 0$ and $n = 5$ seem to be physically sensible. The entropy and temperature of the first brach ($n = 0$) read

$$S_{n=0} = 8k\sqrt{\mathcal{L}} \cos\left(\frac{\theta}{3}\right), \qquad T_{n=0} = -\frac{4\mathcal{L}}{\sqrt{3}} \frac{\cos\theta}{\sin\frac{\theta}{3}}, \qquad \alpha_{n=0} = -2\sqrt{\frac{\mathcal{L}}{3}} \frac{\cos\frac{2\theta}{3}}{\cos\frac{\theta}{3}}. \tag{4.40}$$

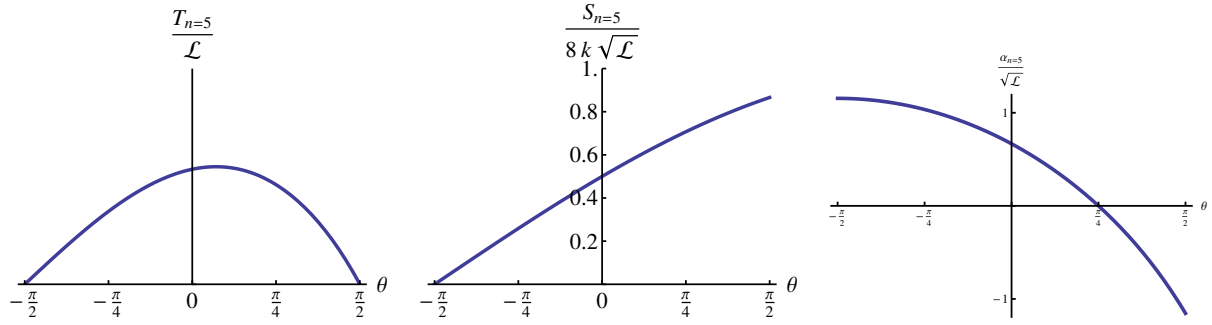

Figure 4.2: Temperature, entropy and chemical potential of the $n = 5$ branch

This implies that for the temperature to be positive, one needs $-\pi/2 < \theta < 0$, which imposes the constraint $-\sqrt{16\mathcal{L}^3/27} < \mathcal{W} < 0$. In this range, the entropy has its minimum at zero temperature, in accordance with the third law of thermodynamics. Note that under this constraint, the energy (4.34) is negative, but bounded from below. In section 4.3.8 we will discuss a simple radial gauge for which this solution looks explicitly like a black hole. Interestingly, this gauge only exists for this branch and $n = 4$, which has exactly the same entropy but with the opposite sign. This does not mean that other branches do not have black hole gauges, as we have not explored non-radial gauges. For now, the plots of the temperature and entropy as a function of θ for a fixed value of $\mathcal{L}$, are shown in figure 4.1.

The sixth branch ($n = 5$) shows the following behavior with respect to $\mathcal{L}$ and θ

$$S_{n=5} = 8k\sqrt{\mathcal{L}}\cos\left(\frac{\theta+5\pi}{3}\right), \qquad T_{n=5} = \frac{4\mathcal{L}}{\sqrt{3}}\frac{\cos\theta}{\cos\frac{2\theta+\pi}{6}}, \qquad \alpha_{n=5} = 2\sqrt{\frac{\mathcal{L}}{3}}\frac{\cos\frac{2\theta+\pi}{3}}{\cos\frac{2\theta+\pi}{6}}. \quad (4.41)$$

This branch has positive values of temperature and entropy for all values of $\theta \in [-\pi/2, \pi/2]$, as shown in figure 4.2.

4.3.6 Entropy as a function of intensive parameters

Study of the stability and thermodynamical dominance of the different branches requires an expression for the entropy as a function of intensive parameters. This, in turn, requires us to

solve the holonomy conditions for $\mathcal{L}, \mathcal{W}$ in terms of α, T, and then write the entropy using (4.32) as a function of α and T only. The first holonomy condition (4.13) is linear in $\mathcal{W}$ and can be easily solved;

$$\mathcal{W} = -\frac{12\alpha^2\mathcal{L} + 12\mathcal{L}^2 - 3T^2}{36\alpha}. \tag{4.42}$$

Plugging this into the second holonomy condition (4.14), twe obtain the following quartic equation for $\mathcal{L}$.

$$256\mathcal{L}^4 - 576\alpha^2\mathcal{L}^3 + (432\alpha^4 - 96\,T^2\mathcal{L}^2 + (36\alpha^2T^2 - 108\,\alpha^6)\mathcal{L} + 27\alpha^4T^2 + 9T^4 = 0. \tag{4.43}$$

This implies the existence of four branches. Even though the number of branches is different from the ones found in last section, one can see that appropriately gluing together these branches, one obtains the solutions we studied in section 4.3.5. For positive temperature, the only branches with positive entropy can be found in figure 4.3. Note that branch IV has been plotted for a negative value of α because its entropy is negative otherwise.

One can check that I and II branches map back to the $n = 0$ branch from the previous section, while III and IV are related to the $n = 5$ branch. Figure 4.3b shows the grand potential (4.31) as a function of the temperature for fixed chemical potential. In the case of negative α, the only sensible branch is IV, and it dominates the thermodynamics. However, for a positive value of α, branch I ($n = 0$) takes over.

We should note that the phase diagrams displayed in section 4.3.5 and 4.3.6 look very similar to the ones obtained for the asymptotically AdS higher spin black holes discussed in [53, 75, 55, 56]. This is no surprise since the holonomy equations are identical. The Lifshitz black hole differs from the AdS higher spin black hole however in the identification of temperature and chemical potential as well as the charges. Hence the physical interpretation

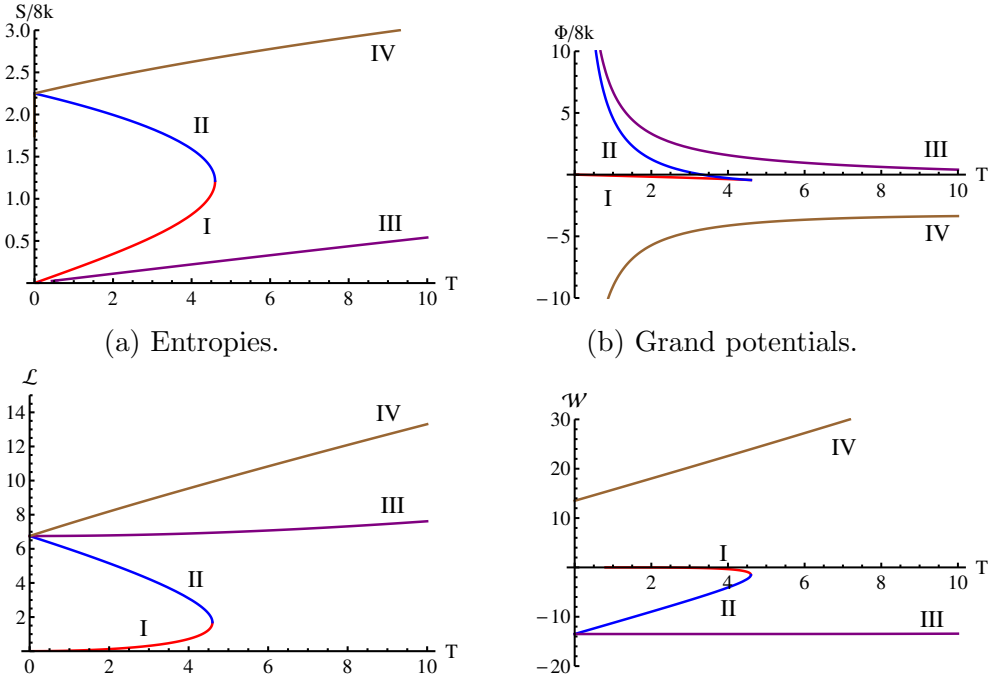

(a) Entropies.

(b) Grand potentials.

(c) $\mathcal{L}$ charge.

(d) $\mathcal{W}$ charge.

Figure 4.3: Entropies, Grand potentials and extensive variables for the four branches as a function of the temperature, at fixed α. I,II and III branches have been plotted for $\alpha = 3$, while branch IV has $\alpha = -3$

of the quantities and physical constraints (such as positive temperature) are different.

It is interesting to study the high temperature limit of these solutions. Branch I cannot reach high temperatures at fixed α. However, in the high α limit, the temperature can be arbitrarily high at the point of maximum entropy. This point is defined by a concrete value of θ, so the high α limit can only be reached by taking $\mathcal{L}$ to infinity, as can be seen by looking at equations (4.40). In that case the temperature grows like $\mathcal{L}$ while the entropy grows like $\sqrt{\mathcal{L}}$. This implies

$$S_{n=0} \sim \sqrt{T}. \tag{4.44}$$

The same can be checked for branch IV. In the limit of high temperature, one finds that

$$\mathcal{L} = \frac{\sqrt{3}T}{4} + 3^{3/4}\sqrt{\frac{T}{32}}|\alpha| + \mathcal{O}(1), \tag{4.45}$$

$$S = -\frac{3^{1/4}\mathrm{sgn}(\alpha)}{\sqrt{8}}\sqrt{T} + \mathcal{O}(1). \tag{4.46}$$

Hence for negative α we obtain again

$$S_{n=5} \sim \sqrt{T}. \tag{4.47}$$

This temperature scaling (4.44) and (4.47) is expected for a theory dual to a quantum field theory with $z = 2$ anisotropic Lifshitz scaling symmetry in two dimensions [115].

4.3.7 Local stability in the grand canonical ensemble

Local thermodynamical stability is associated with the subadditivity of the entropy, as discussed in [118, ?] this condition is equivalent to demanding that the Hessian matrices of $-S$

and $-\beta\Phi$ are positive definite.

$$H_{mn} = \frac{\partial^2(-S)}{\partial x_m \partial x_n}, \qquad W_{mn} = \frac{\partial^2(-\beta\Phi)}{\partial y_m \partial y_n} \tag{4.48}$$

Which Matrix one has to consider depends on whether one describes the thermodynamic state of the system in terms of extensive parameters x_i or intensive parameters y_i respectively.

In the case of our Lifshitz black hole solution, the extensive parameters can be regarded as the charges $\mathcal{L}$ and $\mathcal{W}$, while the intensive parameters can be regarded as β and $\beta\alpha$. Evaluation of the eigenvalues of the Hessian H_{nm} for the $n = 5$ branch shows that this condition can't be satisfied for any value of $\mathcal{L}$ and $\mathcal{W}$, so the $n = 5$ branch is locally unstable. Demanding positive definiteness of the Hessian for the $n = 0$ branch requires that $\theta \in (-3\cos^{-1}\left(\frac{3^{1/4}}{\sqrt{2}}\right), 0)$. This is exactly the regime of θ covered by the curve representing branch I in figure 4.3.

One can further check that this result is consistent with the description in terms of potentials. Computation of the eigenvalues of W_{nm} for the four branches studied in section 4.3.6, indeed shows that branch I is locally stable, while II is not.

4.3.8 Metric and black hole gauge

We now investigate the question whether a gauge exists in which the metric of the Lifshitz black hole solutions displays a regular horizon. In fact, we demonstrate that for some branches one can maintain radial gauge and choose some of the residual gauge such that g_{tt} contains a double zero and g_{xx} is regular.

We begin again with the ansatz (4.9), (4.10) and the flatness conditions (4.4), where again the barred sector is determined by the non-rotating condition $\bar{a}_x = -a_x^T$ and $\bar{a}_t = a_t^T$. We also regard equations (4.5) as a reparametrization of $w_{t,2}, l_{t,1}, l_{x,-1}$, and $w_{x,-2}$ as functions of the charges and potentials $\mathcal{L}, \mathcal{W}, \mu_1, \mu_2$, and the residual gauge parameter $w_{x,0}$. Next, we

solve for the value of $w_{x,0}$ for which the corresponding metric derived from (4.5) has a double zero in g_{tt} at some value of $\rho = \rho_h$, the location of the corresponding horizon. To do this, first we note that the metric component g_{tt} can be written as

$$g_{tt} = -(e^{2\rho}p_1 - e^{-2\rho}p_2)^2 - (e^{\rho}p_3 - e^{-\rho}p_4)^2 \tag{4.49}$$

where p_i are ρ-independent coefficients given by

$$p_1 = \mu_2 \tag{4.50}$$

$$p_3 = \mu_1 - \mu_2\frac{w_{x,0}}{3} \tag{4.51}$$

$$p_2 = -\left(\frac{w_{x,0}}{3}\right)^3\frac{\mu_1}{4} + \mathcal{W}\mu_1 + \mathcal{L}^2\mu_2 + \left(\frac{w_{x,0}}{3}\right)^4\frac{\mu_2}{16} + \frac{w_{x,0}}{3}2\mathcal{W}\mu_2 + \frac{1}{2}\mathcal{L}\frac{w_{x,0}}{3}\left(2\mu_1 + \frac{w_{x,0}}{3}\mu_2\right) \tag{4.52}$$

$$p_4 = \mathcal{L}\mu_1 - \left(\frac{w_{x,0}}{3}\right)^2\frac{3}{4}\mu_1 + \frac{w_{x,0}}{3}\mathcal{L}\mu_2 + \left(\frac{w_{x,0}}{3}\right)^3\frac{\mu_2}{4} + 2\mathcal{W}\mu_2 \tag{4.53}$$

It is clear that g_{tt} is zero if and only if each term in parentheses on the right hand side of (4.49) is zero for the same value of ρ_h which implies that $p_2/p_1 = (p_4/p_3)^2$. Using the expressions above for $p_1, \ldots, p_4$, this constraint is equivalent to the following cubic equation for $w_{x,0}$:

$$w_{x,0}^3 - 36\mathcal{L}w_{x,0} - 108\mathcal{W} = 0. \tag{4.54}$$

The three solutions are given by

$$w_{x,0} = 4\sqrt{3\mathcal{L}}\cos\left(\frac{\cos^{-1}(\sin\theta)}{3} + m\frac{2\pi}{3}\right), \tag{4.55}$$

with $m = 0, 1, 2$. However the only solution with a positive and real horizon $\rho_h = \sqrt[4]{p_2/p_1} =$

$\sqrt{p_4/p_3}$ is the one with $m = 2$, which can be simplified to

$$w_{x,0} = -4\sqrt{3\mathcal{L}}\sin\left(\frac{\theta}{3}\right). \tag{4.56}$$

The horizon is then located at

$$\rho_h = \sqrt{\mathcal{L}\left(2\cos\frac{2\theta}{3} - 1\right)}. \tag{4.57}$$

It seems that we did not need to impose the holonomy conditions in order to find this black hole gauge. However, we still need to check that the metric and the spin three field in this gauge are smooth around the cycle $t \sim t + 2\pi i$. this implies the following conditions

$$1 = \sqrt{\frac{g_{tt}}{-2g_{\rho\rho}}}\bigg|_{\rho_h}, \qquad 1 = \sqrt{\frac{\psi_{xtt}}{-2\psi_{x\rho\rho}}}\bigg|_{\rho_h}. \tag{4.58}$$

Direct substitution of the charges and sources for the six branches found in previous sections shows that only the $n = 0, 4$ cases satisfy these identities. This can mean that this gauge is appropriate for those two solutions, while the other branches require giving up the radial gauge chosen in equation (4.7). As we have argued in section 4.3.5, the $n = 3$ branch does not seem to be physically sensible. For this reason we will focus our attention in branch $n = 0$. The values of the spin fields at the horizon in this branch obey the following relations

$$g_{tt}|_{\rho_h} = 0, \qquad g'_{tt}|_{\rho_h} = 0, \qquad g_{xx}|_{\rho_h} = 4\mathcal{L}, \qquad \psi_{xxx}|_{\rho_h} = 2\mathcal{W}. \tag{4.59}$$

So we can recast our expresion for the entropy as

$$S = \frac{4k}{\pi}A\cos\left[\frac{1}{3}\sin^{-1}\left(\frac{3^{\frac{3}{2}}\psi_3}{A^3}\right)\right] \tag{4.60}$$

where

$$A = 2\pi\sqrt{g_{xx}|_{\rho_h}}, \qquad \psi_3 = \psi_{xxx}|_{\rho_h}, \tag{4.61}$$

which is very similar to the entropy formula found for asymptotically AdS higher spin black holes [**?**]. It would be interesting to investigate whether the local thermodynamic instability of the $n = 5$ branch discussed in section 4.3.7 and the absence of a regular horizon are related. However, it is an open and interesting question, if for the $n = 5$ branch there is a more general radial gauge choice (along the lines of [9]) which has a regular horizon.

4.4 Generalizations

In this section we will present some observations on possible generalizations of our $SL(3,\mathbb{R})$ results obtained in the previous sections.

4.4.1 Rotating solutions

In the present paper we have limited ourselves to non-rotating solutions, for which the connections A and $\bar{A}$ are related by equation (4.1). Since the two Chern-Simons connections $A, \bar{A}$ are independent, it is clear that constructing a solution with angular momentum entails lifting the condition (4.1). This also means that there will be two holonomy conditions for the A and the $\bar{A}$ connection. Recall that in the $SL(3,\mathbb{R}) \times SL(3,\mathbb{R})$ black hole first discussed in [120] a rotating higher spin black hole is obtained by choosing modular parameter to be complex $\tau = \Omega + i\beta$, where Ω is the potential dual to the angular momentum. For the Lifshitz black holes this cannot work quite the same way and we present some observations here. Note that in the holographic dictionary or the stress energy complex of a Lifshitz theory (4.4.1) the angular momentum (i.e. the momentum along the x direction if we take

x to be compact) is identified with $\mathcal{L} - \bar{\mathcal{L}}$, whose conjugate potential is $\mu_1 - \bar{\mu}_1$ and the energy is identified with $\mathcal{W} + \bar{\mathcal{W}}$, whose conjugate potential is $\mu_2 + \bar{\mu}_2$. Hence it is likely that a rotating solution can be constructed by choosing a connections with $\mu_1 \neq \bar{\mu}_1$ and keeping the indentification of the temperature β the same as in the non-rotating case. The expressions for the metric and higher spin fields are much more complicated. This implies also that the analysis of the black hole gauge done section 4.3.8 becomes more involved, and we leave these questions for future work. We also note that, to our knowledge, no rotating Lifshitz black hole solutions have been constructed using the standard supergravity actions. Hence constructing such solutions in higher spin gravity might be interesting.

4.4.2 Lifshitz vacuum for $hs(\lambda)$

In this section we discuss some steps in generalizing the construction of Lifshitz black holes from $SL(3,\mathbb{R})$ to $hs(\lambda)$, note that this generalization will also include the case of $SL(N,\mathbb{R})$ by choosing $\lambda = N$, where the infinite-dimensional Lie algebra reduces to $SL(N,\mathbb{R})$. Our conventions for $hs(\lambda)$ are summarized in appendix C.2.

A Lifshitz vacuum in the $hs(\lambda)$ theory can be easily constructed as follows

$$
\begin{aligned}
a_t &= \frac{1}{\sqrt{\mathrm{tr}(V^s_{s-1}V^s_{-(s-1)})}}V^s_{s-1}, & a_x &= \frac{1}{\sqrt{\mathrm{tr}(V_1^2V_{-1}^2)}}V_1^2 \\
\bar{a}_t &= \frac{1}{\sqrt{\mathrm{tr}(V^s_{s-1}V^s_{-(s-1)})}}V^s_{-(s-1)}, & \bar{a}_x &= -\frac{1}{\sqrt{\mathrm{tr}(V_1^2V_{-1}^2)}}V_{-1}^2.
\end{aligned}
\tag{4.1}
$$

Note that since

$$
[V_1^2, V^s_{s-1}]_\star = 0, \qquad [V_{-1}^2, V^s_{-(s-1)}]_\star = 0, \tag{4.2}
$$

this satisfies the flatness condition for a connection in the radial gauge. The gauge connections A_μ and the metric are obtained from (4.1) by adapting the formulae (4.5) and using

$b = \exp(\rho V_0^2)$ It follows that the metric is of the form.

$$ds^2 = -e^{2(s-1)\rho} dt^2 + e^{2\rho} dx^2 + d\rho^2. \tag{4.3}$$

Hence we can realize an asymptotically Lifshitz metric in the $hs(\lambda)$ theory for any $z = 2, 3, 4, \cdots$, by setting $s = z + 1$. Note that some higher spin fields will be non-vanishing for this $hs(\lambda)$ Lifshitz vacuum. By setting $\lambda = N$, the infinite-dimensional $hs(\lambda)$ gauge algebra truncates to a finite-dimensional $SL(N, \mathbb{R})$, and the connections give Lifshitz vacua with $z = N - 1, N - 2, \cdots, 2$. Note that the generators V_0^2, V_1^2 and V_2^3 form a Lifshitz sub algebra. The generalization of the evolution equations (4.15) and (4.16) to the case of $hs(\lambda)$ is an interesting open problem.

4.4.3 An $hs(\lambda)$ Lifshitz black hole

Here we limit ourself to the BH for $z = 2$, which is related to the $hs(\lambda)$ black hole with a chemical potential for the spin three charge, which is most extensively studied in the literature. The connection is given by

$$a_x = V_1^2 + \tilde{\mathcal{L}} V_{-1}^2 + \tilde{\mathcal{W}} V_{-2}^3 + \tilde{\mathcal{U}} V_{-3}^4 + \cdots \tag{4.4}$$

$$a_t = \tilde{\mu}_1 a_x + \tilde{\mu}_2 (a_x \star a_x) \mid_{\text{traceless}} . \tag{4.5}$$

Here, $\tilde{\mathcal{L}}, \tilde{\mathcal{W}}, \tilde{\mathcal{U}}$, etc are associated with charges of spin $2, 3, 4, \cdots$. We have tilded all quantities to distinguish them from the quantities appearing in the higher spin black hole reviewed in the appendix C.2.

By construction the connection (4.4) satisfied the flatness condition. To define a regular black hole in a higher spin Chern-Simons theory one has to impose a holonomy condition on the gauge connection around the euclidean time circle. The holonomy condition which

we choose is again that the holonomy is equal to the BTZ holonomy for the $hs(\lambda)$ black hole defined in appendix C.2. One might object that in the case of the Lifshitz BH this condition seems less well motivated since there is no analog of a BTZ black hole for an asymptotically Lifshitz spacetime, however a better way to think about this is that the BTZ holonomy simply states that the holonomy of the BH is in the center of $hs(\lambda)$ (see [108] for a discussion on how the center of $hs(\lambda)$ is defined).

If we compare the holonomy associated with a_t defined in (4.4) and the higher spin black hole holonomy (C.9) one recognizes that they are the same upon the following identifications

$$\tilde{\mu}_1 = 2\pi\tau, \qquad \tilde{\mu}_2 = -2\pi\alpha. \tag{4.6}$$

Furthermore the charges can also be identified

$$\tilde{\mathcal{L}} = -\frac{2\pi}{k}\mathcal{L}, \qquad \tilde{\mathcal{W}} = -\frac{\pi}{2k}\mathcal{W}, \quad \cdots \tag{4.7}$$

Since there is a one-to-one map of parameters one might ask how this can be different than the $hs(\lambda)$ [145]. The answer lies in the fact that while (this was true for the $SL(3,\mathbb{R})$ case too) the holonomy conditions have the same functional form, the interpretations of $\tilde{\mu}_1$ and $\tilde{\mu}_2$ are different. The inverse temperature β and the chemical potential $\tilde{\alpha}$ can be related to $\tilde{\mu}_1$ and $\tilde{\mu}_2$ following the the $SL(3,\mathbb{R})$ Lifshitz black hole example

$$\tilde{\mu}_1 = \beta\tilde{\alpha}, \qquad \tilde{\mu}_2 = \beta. \tag{4.8}$$

This means that the most natural regime for the Lifshitz black hole , i.e. $\tilde{\beta}$ finite and $\tilde{\alpha}$ small, is not the same regime as the one which allows the perturbative solution of the holonomy conditions first obtained in [145]. Indeed if we take the limit $\tilde{\alpha} \to 0$, this is equivalent for the higher spin black hole to taking the limit $\tau \to 0$ and keeping α finite, i.e. taking an infinite

temperature limit and finite chemical potential.

4.5 Discussion

In this paper we have discussed the construction of holographic spacetimes dual to field theory with Lifshitz $z = 2$ scaling symmetry . In addition we have constructed black hole solutions in these theories. One interesting feature of these theories is that the connections, holonomy conditions and thermodynamic relations are all very similar to the higher spin black holes first constructed in [120]. This can be traced back to the fact that the Lifshitz black hole connections and the higher spin black hole connections are related by replacing t, x by $\bar{z}, z$ respectively. Note however that the interpretation of the parameters is quite different. First, the holographic identification of the stress energy complex of the QFT with Lifshitz symmetry and the role of the fields $\mathcal{L}$ and $\mathcal{W}$ are quite different for the Lifshitz theory compared to the W_3 CFT. Second, for the Lifshitz black hole solutions the identification of the temperature and higher spin chemical potential is in some sense reversed compared to the higher spin black hole, this leads to a different interpretation of the thermodynamics. The solution of the holonomy conditions has different branches, which we can interpret as different thermodynamic phases. We have shown that only one branch (branch I of section 4.3.6) has 1. positive entropy and 2. positive temperature, 3. is locally thermodynamically stable and 4. enjoys a radial gauge with a regular horizon. All other branches do not satisfy one or more of these conditions and are therefore physically not satisfying.

We have briefly discussed generalizations of the black hole solutions found in this paper. It would be interesting to study Lifshitz black hole solutions in $hs(\lambda)$ further, since there exists a concrete proposal for a dual CFT and the Lifshitz theories could be interpreted as deformations of the CFT. Furthermore since it is possible to couple scalar matter consistently there are independent probes of the geometry of the black hole. To make progress one has to

solve the holonomy conditions either exactly or maybe less ambitiously determine wether it is possible to solve the holonomy conditions perturbatively for small $\tilde{\alpha}$ and finite temperature. We plan to return to these interesting questions in the future.

Appendix A

Warped AdS Geodesics

A.1 AdS_3 in Poincaré fibered coordinates

There are four solution branches for the geodesics in the background (3.5). To obtain these solutions, one solves equations (3.6) and (3.7) for $\dot{\psi}$ and $\dot{\phi}$ in terms of x, plugs the result back into (3.8), and then integrates the resulting equation to obtain

$$x_{c,\pm}(\lambda) = \frac{\ell c_v}{4c_\psi c_\phi \pm 2\sqrt{c_\psi^2\left(-\left(c_v - 4c_\phi^2\right)\right)}\cosh\left(\frac{2\sqrt{c_v}(\lambda-\lambda 0)}{\ell}\right)}\,, \tag{A.1}$$

$$x_{s,\pm}(\lambda) = \frac{\ell c_v}{4c_\psi c_\phi \pm 2\sqrt{c_\psi^2\left(c_v - 4c_\phi^2\right)}\sinh\left(\frac{2\sqrt{c_v}(\lambda-\lambda 0)}{\ell}\right)}\,. \tag{A.2}$$

We typically refer to the solutions (A.1) as the "cosh-like" branch and to those in (A.2) as the "sinh-like" branch. The differences between these branches will be clarified in the next section when we consider global coordinates. Note that in the process of obtaining these four solutions, one made the assumption that $c_v - 4c_\phi^2 < 0$ to get the "cosh-like" branch, while one assumed that $c_v - 4c_\phi^2 > 0$ to obtain the "sinh-like" branch. Each of these solutions for x can then be combined with the other conservation equations to find the following corresponding

solutions for ϕ:

$$\phi_{c,\pm}(\lambda) = \widehat{\phi}_{c,\pm} + 2\ell \coth^{-1}\left(\frac{\sqrt{c_v}c_\psi \coth\left(\frac{\sqrt{c_v}(\lambda-\lambda 0)}{\ell}\right)}{2c_\psi c_\phi \mp \sqrt{c_\psi^2\left(-\left(c_v-4c_\phi^2\right)\right)}}\right), \tag{A.3}$$

$$\phi_{s,\pm}(\lambda) = \widehat{\phi}_{s,\pm} \mp 2\ell \coth^{-1}\left(\frac{\sqrt{c_v}c_\psi}{\mp 2c_\psi c_\phi \tanh\left(\frac{\sqrt{c_v}(\lambda-\lambda 0)}{\ell}\right) + \sqrt{c_\psi^2\left(c_v-4c_\phi^2\right)}}\right), \tag{A.4}$$

and the following for ψ:

$$\psi_{c,\pm}(\lambda) = \widehat{\psi}_{c,\pm} + \frac{\ell\sqrt{c_v}\left(4c_\phi\sqrt{4c_\phi^2-c_v}\sinh\left(\frac{2\sqrt{c_v}(\lambda-\lambda 0)}{\ell}\right) + \left(c_v-4c_\phi^2\right)\sinh\left(\frac{4\sqrt{c_v}(\lambda-\lambda 0)}{\ell}\right)\right)}{2c_\psi\left(\left(c_v-4c_\phi^2\right)\cosh\left(\frac{4\sqrt{c_v}(\lambda-\lambda 0)}{\ell}\right) + c_v + 4c_\phi^2\right)}, \tag{A.5}$$

$$\psi_{s,\pm}(\lambda) = \widehat{\psi}_{s,\pm} \pm \frac{\ell\sqrt{c_v}\left(c_v-4c_\phi^2\right)\cosh\left(\frac{2\sqrt{c_v}(\lambda-\lambda 0)}{\ell}\right)}{\pm 2c_\psi\left(c_v-4c_\phi^2\right)\sinh\left(\frac{2\sqrt{c_v}(\lambda-\lambda 0)}{\ell}\right) + 4c_\phi\sqrt{c_\psi^2\left(c_v-4c_\phi^2\right)}}. \tag{A.6}$$

At first glance one might be concerned about the continuity of the "cosh-like" branch solutions because of the presence of the function $\coth^{-1}$. However, we see that the argument of the $\coth^{-1}$ is of the form $\alpha\coth(\beta\lambda+\gamma)$ where α, β, and γ are real, and this ensures that the overall solution is continuous. Similar remarks hold for the sinh branch.

A.2 AdS_3 in global fibered coordinates

The geodesics of (3.29) are obtained by first solving (3.39) to obtain the following four solution branches:

$$r_{\pm,c}(\lambda) = \frac{c_u c_\tau}{c_v(\ell/2)^2} \pm \frac{\sqrt{(c_u^2-c_v(\ell/2)^2)(c_\tau^2+c_v(\ell/2)^2)}}{c_v(\ell/2)^2}\cosh\left(\frac{\sqrt{c_v}}{(\ell/2)}(\lambda-\lambda_0)\right), \tag{A.7}$$

$$r_{\pm,s}(\lambda) = \frac{c_u c_\tau}{c_v(\ell/2)^2} \mp \frac{\sqrt{-(c_u^2-c_v(\ell/2)^2)(c_\tau^2+c_v(\ell/2)^2)}}{c_v(\ell/2)^2}\sinh\left(\frac{\sqrt{c_v}}{(\ell/2)}(\lambda-\lambda_0)\right). \tag{A.8}$$

The different branches can be clarified by considering the parametrization of the boundary in these coordinates found in Appendix A of [15]. The two solutions in the "cosh-like" branch give geodesics that go from $r = +\infty$ or $r = -\infty$ back to $r = +\infty$ or $r = -\infty$, respectively, depending on the sign of the solution chosen. The two branches in the "sinh-like" solution correspond to geodesics that go from $r = +\infty$ to $r = -\infty$ or vice versa. In this paper we primarily restrict attention to "cosh-like" branch solutions. If we define

$$f_c(\lambda) = e^{\frac{\sqrt{c_v}(\lambda-\lambda 0)}{(\ell/2)}} h_c \,, \qquad h_c = \sqrt{(c_u^2 - c_v(\ell/2)^2)\,(c_\tau^2 + c_v(\ell/2)^2)}\,, \tag{A.9}$$

$$f_s(\lambda) = e^{\frac{\sqrt{c_v}(\lambda-\lambda 0)}{(\ell/2)}} hs \,, \qquad h_s = \sqrt{-(c_u^2 - c_v(\ell/2)^2)\,(c_\tau^2 + c_v(\ell/2)^2)}\,, \tag{A.10}$$

then the corresponding solutions for τ can be written as

$$\tau_{\pm,c}(\lambda) = \widehat{\tau}_{\pm,c} - \cot^{-1}\left(\frac{f_c(\lambda)^2 \pm 2c_\tau c_u f_c(\lambda) + (c_\tau^2 - c_v(\ell/2)^2)\,(c_u^2 - c_v(\ell/2)^2)}{2\sqrt{c_v}(\ell/2)\,(c_u^2 c_\tau - c_v c_\tau(\ell/2)^2 \pm c_u f_c(\lambda))}\right)\,, \tag{A.11}$$

$$\tau_{\pm,s}(\lambda) = \widehat{\tau}_{\pm,s} - \cot^{-1}\left(\frac{f_s(\lambda)^2 \mp 2c_\tau c_u f_s(\lambda) + (c_\tau^2 - c_v(\ell/2)^2)\,(c_u^2 - c_v(\ell/2)^2)}{2\sqrt{c_v}(\ell/2)\,(c_u^2 c_\tau - c_v c_\tau(\ell/2)^2 \mp c_u f_s(\lambda))}\right)\,. \tag{A.12}$$

The seeming discontinuity of the function $\mathrm{arccot}(y)$ at $y = 0$ is not important since it can be glued onto $\mathrm{arccot}(y) + \pi$ there and continue smoothly to negative values of the argument. This can potentially introduce a shift of π into L_τ, which is important and needs to be tracked.[1] Now if we define

$$g_{c,\pm}(\lambda) = c_u \cosh\left(\frac{\sqrt{c_v}}{(\ell/2)}\,(\lambda - \lambda_0)\right) \pm (\ell/2)\sqrt{c_v}\sinh\left(\frac{\sqrt{c_v}}{(\ell/2)}\,(\lambda - \lambda_0)\right)\,, \tag{A.13}$$

$$g_{s,\pm}(\lambda) = (\ell/2)\sqrt{c_v}\cosh\left(\frac{\sqrt{c_v}}{(\ell/2)}\,(\lambda - \lambda_0)\right) \pm c_u \sinh\left(\frac{\sqrt{c_v}}{(\ell/2)}\,(\lambda - \lambda_0)\right)\,, \tag{A.14}$$

[1] An easy way to not have to deal tracking constant shifts like this one is to do the naive calculation first and obtain a function of the form $\sin((L_\tau + c)/2)$ in the entanglement entropy answer for the "cosh-like" branch, with c an overall constant that has not been carefully tracked. Requiring the length to vanish when $L_\tau \to 0$ now fixes $c = 0$.

the solutions for u become

$$u_{\pm,c}(\lambda) = \widehat{u}_{\pm,c} + \frac{1}{2}\log\left(\frac{\left(c_u - (\ell/2)\sqrt{c_v}\right)\left(((\ell/2)^2 c_v + c_\tau^2)\, g_{c,+}(\lambda) \pm c_\tau h_c\right)}{\left((\ell/2)\sqrt{c_v} + c_u\right)\left(((\ell/2)^2 c_v + c_\tau^2)\, g_{c,-}(\lambda) \pm c_\tau h_c\right)}\right), \tag{A.15}$$

$$u_{\pm,s}(\lambda) = \widehat{u}_{\pm,s} + \frac{1}{2}\log\left(\frac{\left(c_u - (\ell/2)\sqrt{c_v}\right)\left(((\ell/2)^2 c_v + c_\tau^2)\, g_{s,+}(\lambda) \pm c_\tau h_s\right)}{\left((\ell/2)\sqrt{c_v} + c_u\right)\left(((\ell/2)^2 c_v + c_\tau^2)\, g_{s,-}(\lambda) \mp c_\tau h_s\right)}\right). \tag{A.16}$$

A.3 Warped AdS_3 in global fibered coordinates

To simplify our expressions for geodesics in the background (3.1) with $a \neq 1$, we define

$$c_1 = -\frac{c_u^2 - a^2 c_u^2 - (\ell/2)^2 a^2 c_v}{(\ell/2)^4 a^2}, \qquad c_2 = \frac{2}{(\ell/2)^4} c_u c_\tau, \qquad c_3 = \frac{c_u^2 - a^2 c_\tau^2 - (\ell/2)^2 a^2 c_v}{(\ell/2)^4 a^2}, \tag{A.17}$$

This illuminates the general form of (3.39):

$$\dot{r}^2 = c_1 r^2 - c_2 r - c_3\,. \tag{A.18}$$

The general solution with $c_v > 0$ has four branches depending on the sign of the combination $c_2^2 + 4c_1c_3$. We ignore the case $c_2^2 + 4c_1c_3 = 0$ which yields an exponentially decaying solution. For $c_2^2 + 4c_1c_3 > 0$, there are two "cosh-like" branches $r_{\pm,c}$ and for $c_2^2 + 4c_1c_3 < 0$, there are two "sinh-like" branches $r_{\pm,s}$:

$$r_{\pm,c}(\lambda) = \frac{c_2}{2c_1} \pm \sqrt{\left(\frac{c_2}{2c_1}\right)^2 + \frac{c_3}{c_1}}\cosh\left(\sqrt{c_1}(\lambda - \lambda_0)\right), \tag{A.19}$$

$$r_{\pm,s}(\lambda) = \frac{c_2}{2c_1} \mp \sqrt{-\left(\frac{c_2}{2c_1}\right)^2 - \frac{c_3}{c_1}}\sinh\left(\sqrt{c_1}(\lambda - \lambda_0)\right). \tag{A.20}$$

Comparing these solutions to (A.7) and (A.8), we find the same qualitative behavior in $r(\lambda)$ for both the warped and non-warped cases. Moreover, setting $a = 1$ in these warped solutions

yields precisely (A.7) and (A.8), as one would expect since the form of the r equation is left unaltered by non-trivial warping. The form of the τ equation is unaltered by warping, so we expect the corresponding solution to be of the same form. However, notice that the last term in (3.40) only appears in the case $a \neq 1$ where there is non-trivial warping, and this changes the qualitative behavior of the solutions. In particular, manipulating the second and third terms allows one to write the u equation as

$$\dot{u} = \frac{c_u}{(\ell/2)^2 a^2} - \frac{c_u}{(\ell/2)^2}\frac{r^2}{r^2+1} + \frac{c_\tau}{(\ell/2)^2}\frac{r}{r^2+1}, \tag{A.21}$$

from which it becomes clear that integration of the first term with respect to λ leads to a term in the solution for u that diverges linearly with λ. This is just like the $\mathrm{AdS}_2 \times \mathbb{R}$ case.

A.3.1 $c_u = 0$

A simple limit in which we can compute the length of the geodesic in terms of separations in τ and u at large r is for $c_u = 0$. In this case, the equations of motion become a-independent and we are forced onto the "sinh-like" branch. The answer is then just given by the answer for AdS_3 in global fibered coordinates with $c_u = 0$:

$$\text{Length} \sim \log\left(\sqrt{\cos\left(\frac{L_\tau}{2}\right)}\frac{\ell}{\epsilon}\right). \tag{A.22}$$

It is not a problem that the argument of the log does not begin to vanish in the $L_\tau = \tau(\lambda_\infty) - \tau(-\lambda_\infty) \to 0$ limit, since we are on the "sinh-like" branch and so $r(\lambda_\infty) \neq r(-\lambda_\infty)$. Thus, the endpoints remain well-separated in the limit $L_\tau \to 0$.

Appendix B

AdS_3 entanglement entropy via coordinate transformations

For completeness, in this section we show how one can translate from entanglement entropy answers in Poincaré coordinates to global coordinates, or vice versa, by performing the appropriate coordinate transformations. The only point one needs to be careful about is the mapping of the UV cutoff. As an illustrastive example, we will begin with showing how to get the answer in global coordinates from the answer in the Poincaré patch, within which it is easiest to compute. We then show how to go from Poincaré fibered coordinates to global fibered coordinates. Such methods will come in handy when we go from warped AdS_3 to the warped BTZ black hole in Section 3.11.

B.1 Global coordinates from Poincaré patch

Recall that AdS_3 can be defined as an embedded submanifold of $\mathbb{R}^{2,2}$ defined by the constraint

$$X_0^2 - X_1^2 - X_2^2 + X_3^2 = 1 \tag{B.1}$$

where X_0, X_1, X_2, X_3 are the standard coordinates on $\mathbb{R}^{2,2}$. The embedding coordinates for global AdS_3 are

$$X_0 = \ell \cosh\rho \cos t_g \,, \qquad X_1 = \ell \sinh\rho \sin\theta_g \,, \tag{B.2}$$

$$X_2 = \ell \sinh\rho \cos\theta_g \,, \qquad X_3 = \ell \cosh\rho \sin t_g \,, \tag{B.3}$$

while for Poincaré AdS_3 they are

$$X_0 = \frac{1}{2z}(z^2 + \ell^2 + x^2 - t^2) \,, \qquad X_1 = \frac{\ell x}{z} \,, \tag{B.4}$$

$$X_2 = \frac{1}{2z}(z^2 - \ell^2 + x^2 - t^2) \,, \qquad X_3 = \frac{\ell t}{z} \,. \tag{B.5}$$

To get from global coordinates to Poincaré coordinates we use the transformations

$$\begin{aligned}
\frac{X_0^2 + X_3^2}{\ell^2} = \cosh^2\rho = \frac{1}{4\ell^2 z^2}(z^2 + \ell^2 + x^2 - t^2)^2 + \frac{t^2}{z^2} \,, \\
\frac{X_3}{X_0} = \tan t_g = \frac{2\ell t}{(z^2 + \ell^2 + x^2 - t^2)} \,, \\
\frac{X_1}{X_2} = \tan\theta_g = \frac{2\ell x}{(z^2 - \ell^2 + x^2 - t^2)} \,.
\end{aligned}$$

The inverse transformations are given by

$$\begin{aligned}
\frac{\ell^2}{X_0 - X_2} = z = \frac{\ell}{\cosh\rho\cos t_g - \sinh\rho\cos\theta_g} \,, \\
\frac{\ell X_1}{X_0 - X_2} = x = \frac{\ell \sinh\rho \sin\theta}{\cosh\rho\cos t_g - \sinh\rho\cos\theta_g} \,, \\
\frac{\ell X_3}{X_0 - X_2} = t = \frac{\ell \cosh\rho \sin t_g}{\cosh\rho\cos t_g - \sinh\rho\cos\theta_g} \,.
\end{aligned}$$

Using either set of relationships, we can see that for $t = t_g = 0$ and $z = 0$, $\rho = \infty$, we get $x = \ell \sin\theta_g/(1 - \cos\theta_g)$. We want to show that $L_x/\epsilon_P = (x_2 - x_1)/\epsilon_P$, when written in terms of L_θ, is $L_x/\epsilon_P \propto \sin(L_\theta/2)/\epsilon_g$. Our answer for the length of the curve in Poincaré

coordinates is

$$\frac{c}{6}\log\left(\frac{L_x}{z_1}\right)+\frac{c}{6}\log\left(\frac{L_x}{z_2}\right)=\frac{c}{3}\log\left(\frac{L_x}{\sqrt{z_1 z_2}}\right) \tag{B.6}$$

where we have picked two different endpoints z_1 and z_2 for the curve. Using $z=\frac{2\ell e^{-\rho}}{1-\cos\theta_g}$ as the asymptotic coordinate transformation between the coordinates gives

$$\frac{L_x}{\sqrt{z_1 z_2}}=\left(\frac{\sin\theta_{g,2}}{1-\cos\theta_{g,2}}-\frac{\sin\theta_{g,1}}{1-\cos\theta_{g,1}}\right)\frac{\sqrt{(1-\cos\theta_{g,1})(1-\cos\theta_{g,2})}}{2e^{-\rho}} \tag{B.7}$$

$$=\frac{\sin\left(\frac{L_\theta}{2}\right)}{e^{-\rho}}\,, \tag{B.8}$$

where we have picked $\rho_1=\rho_2=\rho$ to fix to a constant cutoff surface. We then use $e^{-\rho}\sim\frac{a}{L}\sim\epsilon$ and recover

$$S_{global}=\frac{c}{3}\log\frac{\sin\frac{L_\theta}{2}}{\epsilon}=\frac{c}{3}\log\frac{\sin(l\pi/L)}{\epsilon} \tag{B.9}$$

upon identifying $L_\theta=\theta_{g,2}-\theta_{g,1}=2\pi l/L$ for total circumference L.

B.2 Global fibered from Poincaré fibered

We now map the Poincaré fibered answer onto the global fibered answer. The coordinate transformations between these two metrics are

$$\phi=\ell\log\left(\frac{e^\sigma\cot(\tau/2)-1}{e^\sigma\cot(\tau/2)+1}e^u\right),\quad \psi=\frac{\cosh\sigma\sin\tau}{\sinh\sigma+\cosh\sigma\cos\tau}\,,\quad x=\frac{1}{\sinh\sigma+\cosh\sigma\cos\tau}\,,$$

which asymptotically ($\sigma\to\infty$) become

$$\phi=\ell u\,,\qquad \psi=\tan(\tau/2)\,,\qquad x=\frac{2e^{-\sigma}}{1+\cos\tau}\,.$$

From these relations we see that

$$L_\phi = \ell L_u\,, \qquad L_\psi = \tan(\tau_2/2) - \tan(\tau_1/2)\,,$$

and

$$\frac{1}{\sqrt{x_1 x_2}} = \frac{\sqrt{(1+\cos\tau_1)(1+\cos\tau_2)}}{2e^{-\sigma}}\,,$$

since we will be assuming we are at different points x_1, x_2 at the two ends of the curve in Poincaré fibered coordinates, whereas for global fibered coordinates we will assume we are at the same σ coordinate at both endpoints of the curve. Our Poincaré fibered answer was found to be

$$S = \frac{c}{3}\,\log\left(\frac{\sqrt{L_\psi \ell \sinh\frac{L_\phi}{2\ell}}}{\epsilon}\right), \tag{B.10}$$

where to get here the cutoff relation $x \sim \epsilon^2/\ell$ was employed. Translating back, we find

$$\epsilon \to \sqrt{\epsilon_1\epsilon_2} = \sqrt{\ell\sqrt{x_1 x_2}}$$

gives us

$$\begin{aligned} S &= \frac{c}{3}\,\log\sqrt{\frac{(\tan(\tau_2/2)-\tan(\tau_1/2))\sqrt{(1+\cos\tau_1)(1+\cos\tau_2)}}{2e^{-2\sigma}}\sinh\frac{L_u}{2}} \\ &= \frac{c}{3}\,\log\sqrt{\frac{\sin(L_\tau/2)\sinh(L_u/2)}{e^{-2\sigma}}} = \frac{c}{3}\,\log\left(\frac{1}{\epsilon}\sqrt{\sin\left(\frac{L_\tau}{2}\right)\sinh\left(\frac{L_u}{2}\right)}\right) \end{aligned}$$

where we have used the relation $\epsilon \sim e^{-\sigma}$ for what is now a dimensionless UV cutoff. This is precisely the answer for global fibered coordinates (3.34).

Appendix C

Higher-Spin

C.1 Explicit $SL(3,\mathbb{R})$ representation

The $SL(2,\mathbb{R})$ generators of the principal embedding are given by the following matrices

$$L_{-1} = \begin{pmatrix} 0 & \sqrt{2} & 0 \\ 0 & 0 & \sqrt{2} \\ 0 & 0 & 0 \end{pmatrix}, \qquad L_1 = \begin{pmatrix} 0 & 0 & 0 \\ -\sqrt{2} & 0 & 0 \\ 0 & -\sqrt{2} & 0 \end{pmatrix}, \qquad L_0 = \begin{pmatrix} 1 & 0 & 0 \\ 0 & 0 & 0 \\ 0 & 0 & -1 \end{pmatrix}. \tag{C.1}$$

and the spin 3 generators, on which we omit the superscript $^{(3)}$ for notational simplicity, are as follows:

$$W_{-2} = \begin{pmatrix} 0 & 0 & 2 \\ 0 & 0 & 0 \\ 0 & 0 & 0 \end{pmatrix}, \qquad W_{-1} = \begin{pmatrix} 0 & \frac{1}{\sqrt{2}} & 0 \\ 0 & 0 & -\frac{1}{\sqrt{2}} \\ 0 & 0 & 0 \end{pmatrix}, \qquad W_0 = \begin{pmatrix} \frac{1}{3} & 0 & 0 \\ 0 & -\frac{2}{3} & 0 \\ 0 & 0 & \frac{1}{3} \end{pmatrix} \tag{C.2}$$

$$W_1 = \begin{pmatrix} 0 & 0 & 0 \\ -\frac{1}{\sqrt{2}} & 0 & 0 \\ 0 & \frac{1}{\sqrt{2}} & 0 \end{pmatrix}, \qquad W_2 = \begin{pmatrix} 0 & 0 & 0 \\ 0 & 0 & 0 \\ 2 & 0 & 0 \end{pmatrix}. \tag{C.3}$$

If we define $(T_1, T_2, \ldots, T_8) = (L_1, L_0, L_{-1}, W_2, \ldots W_{-2})$, then traces of all pairs of generators are given by

$$\mathrm{tr}(T_i T_j) = \left(\begin{array}{ccc|ccc} & & -4 & 0 & \cdots & 0 \\ & 2 & & \vdots & \ddots & \vdots \\ -4 & & & 0 & \cdots & 0 \\ \hline 0 & \cdots & 0 & & & 4 \\ & & & & & \\ \vdots & \ddots & \vdots & & & \\ & & & & & \\ 0 & \cdots & 0 & 4 & & \end{array}\right) \qquad \begin{array}{ccc} & & \\ & & \\ & & \\ & & \\ & -1 & \\ & & \frac{2}{3} \\ & & \\ & & \end{array} \tag{C.4}$$

C.2 $hs(\lambda)$ conventions and black hole

Here we follow the conventions of [146] and [108]. The main formulas we use are, the lone star products

$$V_m^s \star V_n^t = \frac{1}{2} \sum_{u=1,2,\cdots}^{s+t-|s-t|-1} g_u^{st}(m,n;\lambda) V_{m+n}^{s+t-u}. \tag{C.5}$$

The star product is used to define the commutator between Lie algebra generator and is denotes by $[\cdot,\cdot]_\star$. For the elements of the Lie-algebra V_m^s one has $|m| < s$ (the generators are zero otherwise). The elements $V_{-1,0,1}^2$ form a SL(2,R) sub algebra and V_m^s form spin s representation

$$[V_m^2, V_n^t]_* = \Big(m(t-1) - n\Big) V_{m+n}^t. \tag{C.6}$$

The algebra has a unit element denoted by X_0^1, the trace is defines by

$$Tr(X) = X|_{V_0^1}. \tag{C.7}$$

A $hs(\lambda)$ black hole with a chemical potential for the spin 3 charge (this can be generalized to arbitrary spin s) has the following connections

$$\begin{aligned} a_z &= V_1^2 - \frac{2\pi}{k}\mathcal{L}V_{-1}^2 - \frac{\pi}{2k}\mathcal{W}V_{-2}^3 + \mathcal{U}V_{-3}^4 + \cdots, \\ a_{\bar{z}} &= -\frac{\alpha}{\bar{\tau}}(a_z \star a_z)\,|_{\text{traceless}}\,. \end{aligned} \tag{C.8}$$

The holonomy around the time circle is given by $H = e^{\omega}$ with

$$\omega = 2\pi\big(\tau a_z + \bar{\tau} a_{\bar{z}}\big). \tag{C.9}$$

The holonomy condition for the black hole is that the holonomy is the same as the holonomy of the BTZ black hole

$$H = H_{BTZ}. \tag{C.10}$$

where ω_{BTZ} is given by

$$\omega_{BTZ} = 2\pi\tau V_1^2 + \frac{\pi}{\tau}V_{-1}^2. \tag{C.11}$$

This condition is equivalent to the following conditions on the powers of ω (see eq. 2.17 of [108]).

$$Tr(\omega^n) = \frac{1}{\lambda}\lim_{t\to 0}\left(\partial_t^n \frac{\sin\pi\lambda t}{\sin\pi t}\right). \tag{C.12}$$

These conditions have been solved perturbatively in the chemical potential α and one gets the charges $\mathcal{L}, \mathcal{W}, \mathcal{U}, \cdots$ as a power series in α (and depending on τ), such that as $\alpha \to 0$ one gets back the BTZ black hole.

Bibliography

[1] A. Achucarro and P.K. Townsend. A Chern-Simons Action for Three-Dimensional anti-De Sitter Supergravity Theories. *Phys.Lett.*, B180:89, 1986.

[2] Ian Affleck and Andreas W.W. Ludwig. Universal noninteger 'ground state degeneracy' in critical quantum systems. *Phys.Rev.Lett.*, 67:161–164, 1991.

[3] H. Afshar, M. Gary, D. Grumiller, R. Rashkov, and M. Riegler. Non-AdS holography in 3-dimensional higher spin gravity - General recipe and example. *JHEP*, 1211:099, 2012.

[4] Hamid Afshar, Arjun Bagchi, Reza Fareghbal, Daniel Grumiller, and Jan Rosseel. Higher spin theory in 3-dimensional flat space. *Phys.Rev.Lett.*, 111:121603, 2013.

[5] Ofer Aharony, Leon Berdichevsky, Micha Berkooz, and Itamar Shamir. Near-horizon solutions for D3-branes ending on 5-branes. *Phys.Rev.*, D84:126003, 2011.

[6] Ofer Aharony, Steven S. Gubser, Juan Martin Maldacena, Hirosi Ooguri, and Yaron Oz. Large N field theories, string theory and gravity. *Phys.Rept.*, 323:183–386, 2000.

[7] Tameem Albash and Clifford V. Johnson. Holographic Entanglement Entropy and Renormalization Group Flow. *JHEP*, 1202:095, 2012.

[8] Martin Ammon, Alejandra Castro, and Nabil Iqbal. Wilson Lines and Entanglement Entropy in Higher Spin Gravity. *JHEP*, 1310:110, 2013.

[9] Martin Ammon, Michael Gutperle, Per Kraus, and Eric Perlmutter. Spacetime Geometry in Higher Spin Gravity. *JHEP*, 1110:053, 2011.

[10] Martin Ammon, Michael Gutperle, Per Kraus, and Eric Perlmutter. Black holes in three dimensional higher spin gravity: A review. *J.Phys.*, A46:214001, 2013.

[11] Martin Ammon, Per Kraus, and Eric Perlmutter. Scalar fields and three-point functions in D=3 higher spin gravity. *JHEP*, 1207:113, 2012.

[12] Dionysios Anninos. Hopfing and Puffing Warped Anti-de Sitter Space. *JHEP*, 0909:075, 2009.

[13] Dionysios Anninos. Sailing from Warped AdS(3) to Warped dS(3) in Topologically Massive Gravity. *JHEP*, 1002:046, 2010.

[14] Dionysios Anninos and Tarek Anous. A de Sitter Hoedown. *JHEP*, 1008:131, 2010.

[15] Dionysios Anninos, Mboyo Esole, and Monica Guica. Stability of warped AdS(3) vacua of topologically massive gravity. *JHEP*, 0910:083, 2009.

[16] Dionysios Anninos, Wei Li, Megha Padi, Wei Song, and Andrew Strominger. Warped AdS(3) Black Holes. *JHEP*, 0903:130, 2009.

[17] Dionysios Anninos, Joshua Samani, and Edgar Shaghoulian. Warped Entanglement Entropy. 2013.

[18] Benjamin Assel, Costas Bachas, John Estes, and Jaume Gomis. Holographic Duals of D=3 N=4 Superconformal Field Theories. *JHEP*, 1108:087, 2011.

[19] Tatsuo Azeyanagi, Diego M. Hofman, Wei Song, and Andrew Strominger. The Spectrum of Strings on Warped $AdS_3 \times S^3$. *JHEP*, 1304:078, 2013.

[20] Tatsuo Azeyanagi, Tatsuma Nishioka, and Tadashi Takayanagi. Near Extremal Black Hole Entropy as Entanglement Entropy via AdS(2)/CFT(1). *Phys.Rev.*, D77:064005, 2008.

[21] Dongsu Bak, Michael Gutperle, and Shinji Hirano. A Dilatonic deformation of AdS(5) and its field theory dual. *JHEP*, 0305:072, 2003.

[22] Koushik Balasubramanian and John McGreevy. An Analytic Lifshitz black hole. *Phys.Rev.*, D80:104039, 2009.

[23] Koushik Balasubramanian and K. Narayan. Lifshitz spacetimes from AdS null and cosmological solutions. *JHEP*, 1008:014, 2010.

[24] Vijay Balasubramanian, Jan de Boer, M.M. Sheikh-Jabbari, and Joan Simon. What is a chiral 2d CFT? And what does it have to do with extremal black holes? *JHEP*, 1002:017, 2010.

[25] Vijay Balasubramanian and Per Kraus. A Stress tensor for Anti-de Sitter gravity. *Commun.Math.Phys.*, 208:413–428, 1999.

[26] Vijay Balasubramanian and Per Kraus. Space-time and the holographic renormalization group. *Phys.Rev.Lett.*, 83:3605–3608, 1999.

[27] Vijay Balasubramanian, Asad Naqvi, and Joan Simon. A Multiboundary AdS orbifold and DLCQ holography: A Universal holographic description of extremal black hole horizons. *JHEP*, 0408:023, 2004.

[28] Maximo Banados. Global charges in Chern-Simons field theory and the (2+1) black hole. *Phys.Rev.*, D52:5816, 1996.

[29] Maximo Banados, Glenn Barnich, Geoffrey Compere, and Andres Gomberoff. Three dimensional origin of Godel spacetimes and black holes. *Phys.Rev.*, D73:044006, 2006.

[30] Maximo Banados, Rodrigo Canto, and Stefan Theisen. The Action for higher spin black holes in three dimensions. *JHEP*, 1207:147, 2012.

[31] Maximo Banados, Claudio Teitelboim, and Jorge Zanelli. The Black hole in three-dimensional space-time. *Phys.Rev.Lett.*, 69:1849–1851, 1992.

[32] Taylor Barrella, Xi Dong, Sean A. Hartnoll, and Victoria L. Martin. Holographic entanglement beyond classical gravity. *JHEP*, 1309:109, 2013.

[33] Jacob D Bekenstein. Black holes and the second law. *Lettere Al Nuovo Cimento (1971–1985)*, 4(15):737–740, 1972.

[34] Jacob D Bekenstein. Black holes and entropy. *Physical Review D*, 7(8):2333, 1973.

[35] Ingemar Bengtsson and Patrik Sandin. Anti de Sitter space, squashed and stretched. *Class.Quant.Grav.*, 23:971–986, 2006.

[36] Raphael Benichou and John Estes. Geometry of Open Strings Ending on Backreacting D3-Branes. *JHEP*, 1203:025, 2012.

[37] E. Bergshoeff, M.P. Blencowe, and K.S. Stelle. Area Preserving Diffeomorphisms and Higher Spin Algebra. *Commun.Math.Phys.*, 128:213, 1990.

[38] Gaetano Bertoldi, Benjamin A. Burrington, and Amanda Peet. Black Holes in asymptotically Lifshitz spacetimes with arbitrary critical exponent. *Phys.Rev.*, D80:126003, 2009.

[39] Arpan Bhattacharyya, Apratim Kaviraj, and Aninda Sinha. Entanglement entropy in higher derivative holography. *JHEP*, 1308:012, 2013.

[40] Arpan Bhattacharyya, Menika Sharma, and Aninda Sinha. On generalized gravitational entropy, squashed cones and holography. 2013.

[41] M.P. Blencowe. A Consistent Interacting Massless Higher Spin Field Theory in $D = (2+1)$. *Class.Quant.Grav.*, 6:443, 1989.

[42] Adel Bouchareb and Gerard Clement. Black hole mass and angular momentum in topologically massive gravity. *Class.Quant.Grav.*, 24:5581–5594, 2007.

[43] Raphael Bousso. A Covariant entropy conjecture. *JHEP*, 9907:004, 1999.

[44] J. David Brown and M. Henneaux. Central Charges in the Canonical Realization of Asymptotic Symmetries: An Example from Three-Dimensional Gravity. *Commun.Math.Phys.*, 104:207–226, 1986.

[45] Ilka Brunner and Daniel Roggenkamp. Defects and bulk perturbations of boundary Landau-Ginzburg orbifolds. *JHEP*, 0804:001, 2008.

[46] Pasquale Calabrese and John L. Cardy. Entanglement entropy and quantum field theory. *J.Stat.Mech.*, 0406:P06002, 2004.

[47] Robert Callan, Jian-Yang He, and Matthew Headrick. Strong subadditivity and the covariant holographic entanglement entropy formula. *JHEP*, 1206:081, 2012.

[48] Andrea Campoleoni, Stefan Fredenhagen, and Stefan Pfenninger. Asymptotic W-symmetries in three-dimensional higher-spin gauge theories. *JHEP*, 1109:113, 2011.

[49] Andrea Campoleoni, Stefan Fredenhagen, Stefan Pfenninger, and Stefan Theisen. Asymptotic symmetries of three-dimensional gravity coupled to higher-spin fields. *JHEP*, 1011:007, 2010.

[50] John L. Cardy. Boundary Conditions, Fusion Rules and the Verlinde Formula. *Nucl.Phys.*, B324:581, 1989.

[51] Horacio Casini, Marina Huerta, and Robert C. Myers. Towards a derivation of holographic entanglement entropy. *JHEP*, 1105:036, 2011.

[52] Alejandra Castro, Rajesh Gopakumar, Michael Gutperle, and Joris Raeymaekers. Conical Defects in Higher Spin Theories. *JHEP*, 1202:096, 2012.

[53] Alejandra Castro, Eliot Hijano, Arnaud Lepage-Jutier, and Alexander Maloney. Black Holes and Singularity Resolution in Higher Spin Gravity. *JHEP*, 1201:031, 2012.

[54] Chi-Ming Chang and Xi Yin. Higher Spin Gravity with Matter in AdS_3 and Its CFT Dual. *JHEP*, 1210:024, 2012.

[55] Bin Chen, Jiang Long, and Yi-nan Wang. Black holes in Truncated Higher Spin AdS_3 Gravity. *JHEP*, 1212:052, 2012.

[56] Bin Chen, Jiang Long, and Yi-Nan Wang. Phase Structure of Higher Spin Black Hole. *JHEP*, 1303:017, 2013.

[57] Bin Chen, Bo Ning, and Zhi-bo Xu. Real-time correlators in warped AdS/CFT correspondence. *JHEP*, 1002:031, 2010.

[58] Bin Chen and Zhi-bo Xu. Quasi-normal modes of warped black holes and warped AdS/CFT correspondence. *JHEP*, 0911:091, 2009.

[59] Bin Chen and Zhi-bo Xu. Quasinormal modes of warped AdS(3) black holes and AdS/CFT correspondence. *Phys.Lett.*, B675:246–251, 2009.

[60] Marco Chiodaroli, Eric D'Hoker, Yu Guo, and Michael Gutperle. Exact half-BPS string-junction solutions in six-dimensional supergravity. *JHEP*, 1112:086, 2011.

[61] Marco Chiodaroli, Eric D'Hoker, and Michael Gutperle. Holographic duals of Boundary CFTs. *JHEP*, 1207:177, 2012.

[62] Marco Chiodaroli, Eric D'Hoker, and Michael Gutperle. Simple Holographic Duals to Boundary CFTs. *JHEP*, 1202:005, 2012.

[63] Marco Chiodaroli, Michael Gutperle, and Darya Krym. Half-BPS Solutions locally asymptotic to AdS(3) x S**3 and interface conformal field theories. *JHEP*, 1002:066, 2010.

[64] Demetrios Christodoulou. Reversible and irreversible transformations in black-hole physics. *Physical Review Letters*, 25:1596–1597, 1970.

[65] Demetrios Christodoulou and Remo Ruffini. Reversible transformations of a charged black hole. *Physical Review D*, 4(12):3552–3555, 1971.

[66] A. Clark and A. Karch. Super Janus. *JHEP*, 0510:094, 2005.

[67] A.B. Clark, D.Z. Freedman, A. Karch, and M. Schnabl. Dual of the Janus solution: An interface conformal field theory. *Phys.Rev.*, D71:066003, 2005.

[68] Geoffrey Compere, Sophie de Buyl, Stephane Detournay, and Kentaroh Yoshida. Asymptotic symmetries of Schrodinger spacetimes. *JHEP*, 0910:032, 2009.

[69] Geoffrey Compere and Stephane Detournay. Centrally extended symmetry algebra of asymptotically Godel spacetimes. *JHEP*, 0703:098, 2007.

[70] Geoffrey Compere and Stephane Detournay. Boundary conditions for spacelike and timelike warped AdS_3 spaces in topologically massive gravity. *JHEP*, 0908:092, 2009.

[71] Geoffrey Compere and Stephane Detournay. Semi-classical central charge in topologically massive gravity. *Class.Quant.Grav.*, 26:012001, 2009.

[72] Geoffrey Compre, Wei Song, and Andrew Strominger. New Boundary Conditions for AdS_3. *JHEP*, 1305:152, 2013.

[73] Olivier Coussaert and Marc Henneaux. Selfdual solutions of (2+1) Einstein gravity with a negative cosmological constant. 1994.

[74] Ulf H. Danielsson and Larus Thorlacius. Black holes in asymptotically Lifshitz spacetime. *JHEP*, 0903:070, 2009.

[75] Justin R. David, Michael Ferlaino, and S. Prem Kumar. Thermodynamics of higher spin black holes in 3D. *JHEP*, 1211:135, 2012.

[76] Jan de Boer and Juan I. Jottar. Entanglement Entropy and Higher Spin Holography in AdS_3. 2013.

[77] Jan de Boer and Juan I. Jottar. Thermodynamics of Higher Spin Black Holes in AdS_3. 2013.

[78] Jan de Boer, Erik P. Verlinde, and Herman L. Verlinde. On the holographic renormalization group. *JHEP*, 0008:003, 2000.

[79] Sebastian de Haro, Sergey N. Solodukhin, and Kostas Skenderis. Holographic reconstruction of space-time and renormalization in the AdS / CFT correspondence. *Commun.Math.Phys.*, 217:595–622, 2001.

[80] Stephane Detournay, Thomas Hartman, and Diego M. Hofman. Warped Conformal Field Theory. *Phys.Rev.*, D86:124018, 2012.

[81] Stephane Detournay, Dan Israel, Joshua M. Lapan, and Mauricio Romo. String Theory on Warped AdS_3 and Virasoro Resonances. *JHEP*, 1101:030, 2011.

[82] O. DeWolfe, D.Z. Freedman, S.S. Gubser, and A. Karch. Modeling the fifth-dimension with scalars and gravity. *Phys.Rev.*, D62:046008, 2000.

[83] Eric D'Hoker, John Estes, and Michael Gutperle. Exact half-BPS Type IIB interface solutions. I. Local solution and supersymmetric Janus. *JHEP*, 0706:021, 2007.

[84] Eric D'Hoker, John Estes, and Michael Gutperle. Exact half-BPS Type IIB interface solutions. II. Flux solutions and multi-Janus. *JHEP*, 0706:022, 2007.

[85] Eric D'Hoker, John Estes, Michael Gutperle, and Darya Krym. Exact Half-BPS Flux Solutions in M-theory. I: Local Solutions. *JHEP*, 0808:028, 2008.

[86] Eric D'Hoker, John Estes, Michael Gutperle, and Darya Krym. Exact Half-BPS Flux Solutions in M-theory II: Global solutions asymptotic to AdS(7) x S**4. *JHEP*, 0812:044, 2008.

[87] Eric D'Hoker, John Estes, Michael Gutperle, and Darya Krym. Exact Half-BPS Flux Solutions in M-theory III: Existence and rigidity of global solutions asymptotic to AdS(4) x S**7. *JHEP*, 0909:067, 2009.

[88] Eric D'Hoker, John Estes, Michael Gutperle, and Darya Krym. Janus solutions in M-theory. *JHEP*, 0906:018, 2009.

[89] Xi Dong, Bart Horn, Eva Silverstein, and Gonzalo Torroba. Unitarity bounds and RG flows in time dependent quantum field theory. *Phys.Rev.*, D86:025013, 2012.

[90] Aristomenis Donos and Jerome P. Gauntlett. Supersymmetric solutions for non-relativistic holography. *JHEP*, 0903:138, 2009.

[91] Aristomenis Donos and Jerome P. Gauntlett. Lifshitz Solutions of D=10 and D=11 supergravity. *JHEP*, 1012:002, 2010.

[92] Nadav Drukker, David J. Gross, and Hirosi Ooguri. Wilson loops and minimal surfaces. *Phys.Rev.*, D60:125006, 1999.

[93] M.J. Duff, Hong Lu, and C.N. Pope. AdS(3) x S**3 (un)twisted and squashed, and an O(2,2,Z) multiplet of dyonic strings. *Nucl.Phys.*, B544:145–180, 1999.

[94] Sheer El-Showk and Monica Guica. Kerr/CFT, dipole theories and nonrelativistic CFTs. *JHEP*, 1212:009, 2012.

[95] Thomas Faulkner. The Entanglement Renyi Entropies of Disjoint Intervals in AdS/CFT. 2013.

[96] Thomas Faulkner, Aitor Lewkowycz, and Juan Maldacena. Quantum corrections to holographic entanglement entropy. *JHEP*, 1311:074, 2013.

[97] Charles Fefferman and C Robin Graham. Conformal invariants. *asterisque*, 95, 1985.

[98] Stefan Fredenhagen, Matthias R. Gaberdiel, and Cornelius Schmidt-Colinet. Bulk flows in Virasoro minimal models with boundaries. *J.Phys.*, A42:495403, 2009.

[99] D.Z. Freedman, S.S. Gubser, K. Pilch, and N.P. Warner. Renormalization group flows from holography supersymmetry and a c theorem. *Adv.Theor.Math.Phys.*, 3:363–417, 1999.

[100] D.Z. Freedman, S.S. Gubser, K. Pilch, and N.P. Warner. Continuous distributions of D3-branes and gauged supergravity. *JHEP*, 0007:038, 2000.

[101] Mitsutoshi Fujita, Tadashi Takayanagi, and Erik Tonni. Aspects of AdS/BCFT. *JHEP*, 1111:043, 2011.

[102] Dmitri V. Fursaev, Alexander Patrushev, and Sergey N. Solodukhin. Distributional Geometry of Squashed Cones. 2013.

[103] Matthias R. Gaberdiel and Rajesh Gopakumar. An AdS_3 Dual for Minimal Model CFTs. *Phys.Rev.*, D83:066007, 2011.

[104] Matthias R. Gaberdiel and Rajesh Gopakumar. Triality in Minimal Model Holography. *JHEP*, 1207:127, 2012.

[105] Matthias R. Gaberdiel, Rajesh Gopakumar, Thomas Hartman, and Suvrat Raju. Partition Functions of Holographic Minimal Models. *JHEP*, 1108:077, 2011.

[106] Matthias R. Gaberdiel and Thomas Hartman. Symmetries of Holographic Minimal Models. *JHEP*, 1105:031, 2011.

[107] Matthias R. Gaberdiel, Thomas Hartman, and Kewang Jin. Higher Spin Black Holes from CFT. *JHEP*, 1204:103, 2012.

[108] Matthias R. Gaberdiel, Kewang Jin, and Eric Perlmutter. Probing higher spin black holes from CFT. *JHEP*, 1310:045, 2013.

[109] Michael Gary, Daniel Grumiller, and Radoslav Rashkov. Towards non-AdS holography in 3-dimensional higher spin gravity. *JHEP*, 1203:022, 2012.

[110] G.W. Gibbons, M.J. Perry, and C.N. Pope. The First law of thermodynamics for Kerr-anti-de Sitter black holes. *Class.Quant.Grav.*, 22:1503–1526, 2005.

[111] L. Girardello, M. Petrini, M. Porrati, and A. Zaffaroni. The Supergravity dual of N=1 superYang-Mills theory. *Nucl.Phys.*, B569:451–469, 2000.

[112] Jaume Gomis and Filippo Passerini. Holographic Wilson Loops. *JHEP*, 0608:074, 2006.

[113] Jaume Gomis and Christian Romelsberger. Bubbling Defect CFT's. *JHEP*, 0608:050, 2006.

[114] Hernan A. Gonzalez, Javier Matulich, Miguel Pino, and Ricardo Troncoso. Asymptotically flat spacetimes in three-dimensional higher spin gravity. *JHEP*, 1309:016, 2013.

[115] Hernan A. Gonzalez, David Tempo, and Ricardo Troncoso. Field theories with anisotropic scaling in 2D, solitons and the microscopic entropy of asymptotically Lifshitz black holes. *JHEP*, 1111:066, 2011.

[116] Ruth Gregory, Susha L. Parameswaran, Gianmassimo Tasinato, and Ivonne Zavala. Lifshitz solutions in supergravity and string theory. *JHEP*, 1012:047, 2010.

[117] S.S. Gubser, Igor R. Klebanov, and Alexander M. Polyakov. Gauge theory correlators from noncritical string theory. *Phys.Lett.*, B428:105–114, 1998.

[118] Steven S. Gubser and Indrajit Mitra. The Evolution of unstable black holes in anti-de Sitter space. *JHEP*, 0108:018, 2001.

[119] Michael Gutperle, Eliot Hijano, and Joshua Samani. Lifshitz black holes in higher spin gravity. 2013.

[120] Michael Gutperle and Per Kraus. Higher Spin Black Holes. *JHEP*, 1105:022, 2011.

[121] Michael Gutperle and Joshua Samani. Holographic RG-flows and Boundary CFTs. *Phys.Rev.*, D86:106007, 2012.

[122] Thomas Hartman. Entanglement Entropy at Large Central Charge. 2013.

[123] Stephen W Hawking. Gravitational radiation from colliding black holes. *Physical Review Letters*, 26:1344–1346, 1971.

[124] Matthew Headrick. Entanglement Renyi entropies in holographic theories. *Phys.Rev.*, D82:126010, 2010.

[125] Marc Henneaux, Alfredo Perez, David Tempo, and Ricardo Troncoso. Chemical potentials in three-dimensional higher spin anti-de Sitter gravity. 2013.

[126] Marc Henneaux and Soo-Jong Rey. Nonlinear $W_{infinity}$ as Asymptotic Symmetry of Three-Dimensional Higher Spin Anti-de Sitter Gravity. *JHEP*, 1012:007, 2010.

[127] M. Henningson and K. Skenderis. The Holographic Weyl anomaly. *JHEP*, 9807:023, 1998.

[128] Eliot Hijano, Per Kraus, and Eric Perlmutter. Matching four-point functions in higher spin AdS_3/CFT_2. *JHEP*, 1305:163, 2013.

[129] Diego M. Hofman and Andrew Strominger. Chiral Scale and Conformal Invariance in 2D Quantum Field Theory. *Phys.Rev.Lett.*, 107:161601, 2011.

[130] Christoph Holzhey, Finn Larsen, and Frank Wilczek. Geometric and renormalized entropy in conformal field theory. *Nucl.Phys.*, B424:443–467, 1994.

[131] Petr Horava and Charles M. Melby-Thompson. Anisotropic Conformal Infinity. *Gen.Rel.Grav.*, 43:1391–1400, 2011.

[132] Gary T. Horowitz and Joseph Polchinski. Gauge/gravity duality. 2006.

[133] Veronika E. Hubeny, Henry Maxfield, Mukund Rangamani, and Erik Tonni. Holographic entanglement plateaux. *JHEP*, 1308:092, 2013.

[134] Veronika E. Hubeny, Mukund Rangamani, and Tadashi Takayanagi. A Covariant holographic entanglement entropy proposal. *JHEP*, 0707:062, 2007.

[135] Ling-Yan Hung, Robert C. Myers, and Michael Smolkin. On Holographic Entanglement Entropy and Higher Curvature Gravity. *JHEP*, 1104:025, 2011.

[136] Dan Israel, Costas Kounnas, Domenico Orlando, and P. Marios Petropoulos. Electric/magnetic deformations of S**3 and AdS(3), and geometric cosets. *Fortsch.Phys.*, 53:73–104, 2005.

[137] Shamit Kachru, Xiao Liu, and Michael Mulligan. Gravity Duals of Lifshitz-like Fixed Points. *Phys.Rev.*, D78:106005, 2008.

[138] Andreas Karch and Lisa Randall. Open and closed string interpretation of SUSY CFT's on branes with boundaries. *JHEP*, 0106:063, 2001.

[139] Parinya Karndumri and Eoin O Colgin. 3D Supergravity from wrapped D3-branes. *JHEP*, 1310:094, 2013.

[140] Igor R. Klebanov and Edward Witten. AdS / CFT correspondence and symmetry breaking. *Nucl.Phys.*, B556:89–114, 1999.

[141] I.R. Klebanov and A.M. Polyakov. AdS dual of the critical O(N) vector model. *Phys.Lett.*, B550:213–219, 2002.

[142] Yegor Korovin, Kostas Skenderis, and Marika Taylor. Lifshitz as a deformation of Anti-de Sitter. *JHEP*, 1308:026, 2013.

[143] Per Kraus. Lectures on black holes and the AdS(3) / CFT(2) correspondence. *Lect.Notes Phys.*, 755:193–247, 2008.

[144] Per Kraus, Finn Larsen, and Sandip P. Trivedi. The Coulomb branch of gauge theory from rotating branes. *JHEP*, 9903:003, 1999.

[145] Per Kraus and Eric Perlmutter. Partition functions of higher spin black holes and their CFT duals. *JHEP*, 1111:061, 2011.

[146] Per Kraus and Eric Perlmutter. Probing higher spin black holes. *JHEP*, 1302:096, 2013.

[147] Per Kraus and Tomonori Ugajin. An Entropy Formula for Higher Spin Black Holes via Conical Singularities. *JHEP*, 1305:160, 2013.

[148] Jason Kumar and Arvind Rajaraman. New supergravity solutions for branes in AdS(3) x S**3. *Phys.Rev.*, D67:125005, 2003.

[149] Jason Kumar and Arvind Rajaraman. Supergravity solutions for AdS(3) x S**3 branes. *Phys.Rev.*, D69:105023, 2004.

[150] Sangmin Lee, Shiraz Minwalla, Mukund Rangamani, and Nathan Seiberg. Three point functions of chiral operators in D = 4, N=4 SYM at large N. *Adv.Theor.Math.Phys.*, 2:697–718, 1998.

[151] Thomas S. Levi, Joris Raeymaekers, Dieter Van den Bleeken, Walter Van Herck, and Bert Vercnocke. Godel space from wrapped M2-branes. *JHEP*, 1001:082, 2010.

[152] Aitor Lewkowycz and Juan Maldacena. Generalized gravitational entropy. *JHEP*, 1308:090, 2013.

[153] Dao-Jun Liu, Bin Yang, Yong-Jia Zhai, and Xin-Zhou Li. Quasinormal modes for asymptotic safe black holes. *Class.Quant.Grav.*, 29:145009, 2012.

[154] Oleg Lunin. On gravitational description of Wilson lines. *JHEP*, 0606:026, 2006.

[155] Oleg Lunin. 1/2-BPS states in M theory and defects in the dual CFTs. *JHEP*, 0710:014, 2007.

[156] Oleg Lunin. Brane webs and 1/4-BPS geometries. *JHEP*, 0809:028, 2008.

[157] Juan Martin Maldacena. The Large N limit of superconformal field theories and supergravity. *Adv.Theor.Math.Phys.*, 2:231–252, 1998.

[158] Robert B. Mann. Lifshitz Topological Black Holes. *JHEP*, 0906:075, 2009.

[159] Ian A. Morrison and Matthew M. Roberts. Mutual information between thermo-field doubles and disconnected holographic boundaries. 2012.

[160] Karim Ait Moussa, Gerard Clement, and Cedric Leygnac. The Black holes of topologically massive gravity. *Class.Quant.Grav.*, 20:L277–L283, 2003.

[161] Y. Nutku. Exact solutions of topologically massive gravity with a cosmological constant. *Class.Quant.Grav.*, 10:2657–2661, 1993.

[162] Domenico Orlando and Linda I. Uruchurtu. Warped anti-de Sitter spaces from brane intersections in type II string theory. *JHEP*, 1006:049, 2010.

[163] Ioannis Papadimitriou and Kostas Skenderis. Correlation functions in holographic RG flows. *JHEP*, 0410:075, 2004.

[164] Alfredo Perez, David Tempo, and Ricardo Troncoso. Higher spin black hole entropy in three dimensions. *JHEP*, 1304:143, 2013.

[165] Alfredo Perez, David Tempo, and Ricardo Troncoso. Higher spin gravity in 3D: Black holes, global charges and thermodynamics. *Phys.Lett.*, B726:444–449, 2013.

[166] Eric Perlmutter, Tomas Prochazka, and Joris Raeymaekers. The semiclassical limit of W_N CFTs and Vasiliev theory. *JHEP*, 1305:007, 2013.

[167] Vasily Pestun. Localization of gauge theory on a four-sphere and supersymmetric Wilson loops. *Commun.Math.Phys.*, 313:71–129, 2012.

[168] C.N. Pope, L.J. Romans, and X. Shen. W(infinity) and the Racah-wigner Algebra. *Nucl.Phys.*, B339:191–221, 1990.

[169] S.F. Prokushkin and Mikhail A. Vasiliev. Higher spin gauge interactions for massive matter fields in 3-D AdS space-time. *Nucl.Phys.*, B545:385, 1999.

[170] Simon F. Ross. Holography for asymptotically locally Lifshitz spacetimes. *Class.Quant.Grav.*, 28:215019, 2011.

[171] Shinsei Ryu and Tadashi Takayanagi. Aspects of Holographic Entanglement Entropy. *JHEP*, 0608:045, 2006.

[172] Shinsei Ryu and Tadashi Takayanagi. Holographic derivation of entanglement entropy from AdS/CFT. *Phys.Rev.Lett.*, 96:181602, 2006.

[173] Subir Sachdev. What can gauge-gravity duality teach us about condensed matter physics? *Ann.Rev.Condensed Matter Phys.*, 3:9–33, 2012.

[174] Edgar Shaghoulian. Holographic Entanglement Entropy and Fermi Surfaces. *JHEP*, 1205:065, 2012.

[175] Kostas Skenderis. Lecture notes on holographic renormalization. *Class.Quant.Grav.*, 19:5849–5876, 2002.

[176] Wei Song and Andrew Strominger. Warped AdS3/Dipole-CFT Duality. *JHEP*, 1205:120, 2012.

[177] Jia-Rui Sun. Note on Chern-Simons Term Correction to Holographic Entanglement Entropy. *JHEP*, 0905:061, 2009.

[178] Leonard Susskind. The World as a hologram. *J.Math.Phys.*, 36:6377–6396, 1995.

[179] Leonard Susskind and Edward Witten. The Holographic bound in anti-de Sitter space. 1998.

[180] Gerard 't Hooft. Dimensional reduction in quantum gravity. 1993.

[181] Tadashi Takayanagi. Holographic Dual of BCFT. *Phys.Rev.Lett.*, 107:101602, 2011.

[182] Balt C. van Rees. Holographic renormalization for irrelevant operators and multi-trace counterterms. *JHEP*, 1108:093, 2011.

[183] Balt C. van Rees. Irrelevant deformations and the holographic Callan-Symanzik equation. *JHEP*, 1110:067, 2011.

[184] Mikhail A. Vasiliev. Higher Spin Algebras and Quantization on the Sphere and Hyperboloid. *Int.J.Mod.Phys.*, A6:1115–1135, 1991.

[185] Mikhail A. Vasiliev. Higher spin gauge theories in four-dimensions, three-dimensions, and two-dimensions. *Int.J.Mod.Phys.*, D5:763–797, 1996.

[186] Mikhail A. Vasiliev. Higher spin gauge theories: Star product and AdS space. 1999.

[187] Mikhail A. Vasiliev. Higher spin symmetries, star product and relativistic equations in AdS space. 2000.

[188] Aron C. Wall. Maximin Surfaces, and the Strong Subadditivity of the Covariant Holographic Entanglement Entropy. 2012.

[189] Edward Witten. (2+1)-Dimensional Gravity as an Exactly Soluble System. *Nucl.Phys.*, B311:46, 1988.

[190] Edward Witten. Anti-de Sitter space and holography. *Adv.Theor.Math.Phys.*, 2:253–291, 1998.

[191] Edward Witten. Anti-de Sitter space, thermal phase transition, and confinement in gauge theories. *Adv.Theor.Math.Phys.*, 2:505–532, 1998.

[192] Satoshi Yamaguchi. Bubbling geometries for half BPS Wilson lines. *Int.J.Mod.Phys.*, A22:1353–1374, 2007.